ADVANCES IN LIQUID CHROMATOGRAPHY AND LIQUID CHROMATOGRAPHY

MASS SPECTROMETRY FOR THE ANALYSIS OF BIOLOGICALLY

IMPORTANT PHARMACEUTICALS, GLYCOSAMINOGLYCANS

AND AMINO ACIDS

by

YADI WANG

Presented to the Faculty of the Graduate School of

The University of Texas at Arlington in Partial Fulfillment

of the Requirements

for the Degree of

DOCTOR OF PHILOSOPHY

THE UNIVERSITY OF TEXAS AT ARLINGTON

May 2019

Acknowledgements

Firstly, I would like to express my sincere gratitude to my advisor Prof. Daniel Armstrong, who gave me continuous support during the past five years. As my teacher and mentor, he has provided me extensive guidance on scientific research and stimulated my enthusiasm for exploring new knowledge. It is his enlightening suggestions and advice direct me whenever I get lost. I cannot finish this thesis and complete my study without his patience, encouragement and inspiration.

I want to say thanks to Prof. Kevin Schug for his support on my research and the efforts on bringing state-of-the-art mass spectrometry instrumentations to us. I would also like to express my appreciation to Prof. Krishnan Rajeshwar for his encouragement and advice during my study. I am truly thankful to Prof. Robin Macaluso for her support and help during my Ph.D program.

I also sincerely thank Dr. Farooq Wahab who led me into the word of chromatography when I joined Armstrong's group. It is an enjoyable experience working with him and I learned so much from him who is always innovative.

I would like to give my special thanks to my best friend Ms. Siqi Du. We've spent a lot of time for scientific discussion and idea exchanging. It is her who makes me never feel alone when working in the lab on weekends and late night. We shared a lot of happiness during of our study and everyday life.

I appreciated the help and assistance from our group members: Zach, Darshan, Chandan, Mohsen, Rahul, Rasangi, Garrett, Roy, Nimish, Durga, Beth, Abuid, Sam, Angel and Barbara. Special thanks should go to department stuff: Jill, Debbie and Roy.

I owe a lot of thanks to my beloved parents and husband. They have always loved me and supported my decision.

April 08, 2019

iii

Abstract

ADVANCES IN LIQUID CHROMATOGRAPHY AND LIQUID CHROMATOGRAPHY

MASS SPECTROMETRY FOR THE ANALYSIS OF BIOLOGICALLY

IMPORTANT PHARMACEUTICALS, GLYCOSAMINOGLYCANS

AND AMINO ACIDS

Yadi Wang, PhD

The University of Texas at Arlington, 2019

Supervising Professor: Daniel W. Armstrong

The use of high-performance liquid chromatography (HPLC) and liquid chromatography-mass spectrometry (LC-MS) is now commonplace among pharmaceutical laboratories. They are major analytical tools in the drug discovery process. They are used to check the identity and the purity of newly synthesized compounds as well as to follow the reaction processes. They are also utilized to monitor the concentration of a drug in different biological matrices. In this thesis, fundamental contributions to HPLC and LC-MS bioanalysis work are discussed.

The goal of the HPLC work is to develop a hydrolytically stable hydrophilic interaction liquid chromatography (HILIC) stationary phase. A carboxylate modified cyclofructan 6 was bonded onto superficially porous particles and was shown to have high hydrolytically stability. The stationary phase provided fast separation and unique selectivities compared to commercially available columns. The carboxylated CF6 simultaneously separated acidic, neutral and basic drugs and produced considerably

different retention and selectivity patterns for various classes of compounds including nucleic acid bases, β blockers, salicylic acid and its derivatives.

The goal of the remaining part of this thesis is to demonstrate the application of HPLC-MS for the analysis of glycosaminoglycan disaccharides and amino acids. For the analysis of glycosaminoglycan disaccharides, fast and sensitive methods were developed using two HILIC stationary phases for disaccharides following the enzymatic digestion of glycosaminoglycan. For the achiral analysis of amino acids, a sensitive detection method based on paired ion electrospray ionization was developed for the analysis of FMOC-amino acids in biological samples. This method showed improved detection sensitivity down to sub-pg level. A simple, rapid and sensitive method was developed by using HPLC-triple quadrupole mass spectrometry for the analysis of D and L-amino acid in various biological matrices, such as mouse brain tissue and cultured human breast cells. The levels of 22 amino acids and their enantiocompositions in the whole brain of wild-type ddY mice and ddY mice lacking DAO were compared. We describe, for the first time, the endogenous levels of free L- and D-amino acids in human breast cancer cells (MCF-7) and non-tumorigenic epithelial breast cells (MCF-10A).

Table of Contents

List of Illustrations

List of Tables

Chapter 1

Introduction

1.1 Hydrophilic interaction liquid chromatography

The term hydrophilic interaction liquid chromatography (HILIC) was coined by Alpert in 1990 [1], although this separation mode dates back a few decades. It is one of the most rapidly developing chromatography modes over the last few years. This technique uses polar stationary phases along with mobile phases containing a large portion of an aprotic polar solvent (typically acetonitrile) and a small portion of an aqueous buffer or water. It provides stronger retention of polar analytes and is a complementary chromatography method to reversed phase LC, where some of the polar and charged analytes elute at or near the dead volume. Conversely, hydrophobic compounds are mot retained well on HILIC stationary phases. HILIC also comes over the solubility problem which often is encountered in the normal phase chromatography mode when separating highly polar compounds.

1.1.1 Advantages of HILIC

HILIC is easily hyphenated to electrospray ionization mass spectrometry (ESI-MS) since the mobile phase used is acetonitrile and water with volatile salts and/or acids. Detection sensitivity is improved due to the higher percentage of organic solvent (typically 60%-95%) which allows for the efficient spraying and desolvation. In reversed phase chromatography, the mobile phase has greater amounts of aqueous solvent [2].

It is possible to use HILIC columns at higher flow rates owing to the lower viscosity of the high organic content mobile phase. Therefore longer columns can be used while maintaining the back pressure. Thus more theoretical plates can be obtained and better separations can be achieved.

1.1.2 Separation Mechanism of HILIC

The separation mechanism of HILIC is still under debate. However, it is commonly accepted that the separation of HILIC requires a stagnant water rich layer be formed on the surface of the stationary phase, into which polar/hydrophilic molecules can partition and hence be retained by the stationary phase [3]. Further, other interaction forces are usually involved, such as dipole-dipole, induced dipole, hydrogen bonding, ion-exchange and electrostatic interactions [4].

1.1.3 Hydrolytic Stability of HILIC

Most HPLC stationary phases employ silica as a support because of its mechanical strength and ease of chemical modification. However, attaching hydrophilic ligands on silica for HILIC purposes comes with a caveat – such phases are hydrolytically unstable. The silica has a finite solubility in water and can be hydrolized to silicic acid, especially at basic pHs.

1.1.4 Selectivity of HILIC Stationary Phase

HILIC stationary phases provide orthogonal selectivity to reversed phase separations. A selectivity plot with different HILIC stationary phases was constructed by Dinh et al.[5] and Ibrahim et al.[6] by choosing three analytes to probe the hydrophilicity and electrostatic characteristics of the stationary phases. The relative retention of cytosine/uracil categorizes the HILIC stationary phases according to their hydrophilicity. The higher the value, the more hydrophilic is the stationary phase. The retention of BTMA/uracil indicates the ion exchange character of the stationary phases. Stationary phases with a higher value show stronger cation exchange properties [6]. This approach provides an easy way for the evaluation of the selectivity characteristics of a new stationary phases. So far, silica particles are still the most frequently used stationary phase material for HILIC stationary phase. Various bonded phase chemistries are

available based on silica, such as amide-, cyano-, cyclodextrin, diol-, polyethylene glycol-, poly(succinimide)-, sulfoalkylbetaine-, pentafluorophenylpropyl, polyvinylalcohol, polypeptide, and others [7]. Other materials were also introduced for use as HILIC stationary phase. Porous graphic carbon (PGC) [8-10], organic polymer monoliths like (poly)methacrylate diol- or (poly)hydroxymethacrylate) [11], aluminosilicates based geopolymer particles [12] are examples.

1.2 HPLC-MS analysis of Glycosaminoglycan Disaccharides

Glycosaminoglycan disaccharides are an important group of long unbranched polysaccharides constructed of repeating disaccharide units. They are highly sulfated, complex, polydisperse and have various important biological roles including cell signaling and migration, inflammation, angiogenesis, homeostasis, anticoagulation, and cancer progression [13-15]. Each disaccharide unit contains an amino sugar (N-acetyl-D-galactosamine (GlaNAc) or N-acetylglucosamine (GlcNAc) alternating with a uronic acid (either D-glucuronic acid and/or L-iduronic acid) [16]. They can be categorized into four classes based on their composition: 1) chondroitin sulfates (CS)/dermatan sulfates (DS), 2) heparin (HP)/ heparan sulfates(HS), 3) keratan sulfates (KS), and 4) hyaluronic acid (HA) which contributes to their different biological functions [17]. Considering the complexity of the glycosaminoglycans, they are usually enzymetically digested and the resulting disaccharides are separated and quantified by HPLC or capillary electrophoresis. In order to increase the spectroscopic absorbance, various derivatization reagents have been reported, such as 2-aminoacridone (AMAC) [18], 2-aminobenzamide (2-AB) [19], and 4,4-difluoro-5,7-dimethyl-4-bora-3a,4a-diaza-s-indacene-3-propionic acid (BODIPY) [20]. Such derivatization methods improve the retention of disaccharides on C18 stationary phases and enable sensitive fluorescence detection. The development of LC-MS/MS technology

3

provides alternative methods for direct and sensitive analysis of disaccharides. However,

challenges still remain, such as the effective separation of structural isomeric

disaccharides, and separating homologues and isomers produced by different degrees of

sulfation. Separation of CS/DS disaccharides were reported by using a graphite porous

carbon (Hypercarb) stationary phase [21], but the peak shapes were poor. An amide based

HILIC stationary phase also was used. However, some isomers were not well separated

by this method [22,23].

1.3 HPLC-MS Analysis of Amino Acids

Amino acids are the essential building blocks of proteins and also are

intermediates in metabolism. They are among the most important group of compounds in

nature. They contain both amino groups ($-NH_3^+$) and carboxylate groups ($-COO^-$). There

are proteinogenic amino acid which are incorporated biosynthetically into proteins. Non-

proteinogenic amino acids are also found in nature. Though they are not incorporated

into proteins, they are still crucial compounds to maintain many cellular functions. It has

been noted that abnormal concentrations of amino acid are associated with some

diseases and metabolic disorders [24].

1.3.1 Analysis of Amino Acids by LC-MS

Analysis of amino acids is a fundamental biochemical technique for the

determination of free amino acid concentrations or amino acid compositions of peptides,

proteins, glycoproteins and different pharmaceutical samples. These can be done in

biological matrices, such as plasma, urine and blood. Proteins and peptides, must first be

hydrolyzed prior to the amino acid detection and quantitation [25]. HPLC is the prevalent

method for analyzing amino acids. In most cases, amino acids can be detected by UV

detection due to the absorption of the carboxyl group (-COOH) in the 200 to 210 nm

range, while some amino acids with aromatic rings can also be detected in the 250 to 280 nm range. However, in general, native amino acids do not have sufficient UV absorption for sensitive and accurate quantitation especially from biological matrices. As a result, amino acids are often derivatized in order to achieve better sensitivity. Derivatization involves introducing a bulk, typically fluorescent moiety at the α-amine group and leaving the carboxyl group free. Typical derivatization agents are fluorenylmethyloxycarbonyl chloride (FMOC-Cl) [26], o-phthalaldehyde (OPA) [27,28], and 7-fluoro-4-nitrobenzoxadiazole (NBD-F) [29,30]. Not only can the detection sensitivity be enhanced when either using a UV or fluorescence detector, but the polarity of compound is decreased hence retention in the reversed phase HPLC is increased.

Amino acids are polar compounds and it has been reported that underivatized AAs are well retained and easily separated using HILIC stationary phases [31,32]. This method has the advantage that complex derivatization procedures are no longer necessary, which overcomes the potential drawbacks such as derivative instability and insufficient reproducibility of the derivative yield [33]. In addition, the work flow involving sample pretreatment is simplified and more rapid sample analyses can be achieved. However, one major limitation of this method is the need of highly sensitive MS detector since native AAs have low molecular weights and are detected at low m/z range where more inherent instrumental background noise can occur.

1.3.2 LC and LC-MS Analysis of D-amino acids

All protein amino acids exist in either L- or D-forms, except for glycine due to its lack of a chiral center. Initially it was believed that only L-amino acids were relevant in higher organisms, while D-amino acids were thought to be absent. In the mid-20th century, D-Ala and D-Glu were found to be present in the bacterial peptidoglycan, which

5

is a major component of the bacterial cell wall. Subsequently, D-amino acids were detected in plants, invertebrates, and mammals.

No comprehensive study of all free proteinogenic L- and D-amino acid levels in the mammals has been done. Chiral amino acid analysis is rather challenging especially in cases involving complex biological samples. Our previous method for analyzing D-amino acids in biological samples involved heart-cutting 2D-HPLC with precolumn FMOC derivatization [34]. In the first dimension, an achiral separation of all the amino acids was obtained in a C18 column. Then a specific segment of sample was selected and switched to the second dimension where the enantioseparation of amino acids was achieved on a teicoplanin-based stationary phase. With this method, we successfully separated and quantified D-amino acids in Swiss mouse brain tissue and blood. Although adequate selectivity and sensitivity was achieved with this method, the analysis time was quite long for each sample. Therefore, it is necessary to develop a rapid, sensitive and selective method that simultaneously detects D and L amino acids.

Triple quadrupole mass spectrometry (QqQ-MS) coupled with HPLC is a selective and highly sensitive platform for the quantitative analysis of small molecule mixtures from complex matrices. Samples are typically analyzed and quantified using multiple reaction monitoring (MRM) mode following the chromatographic separation. The "triple quad" has three consecutive quadrupoles, the first acting as a mass filter to transmit a certain precursor ion to the next quadrupole. The second quadrupole is a collision chamber, where molecular ions collide with an inert gas and are broken into fragments. The third quadrupole also acts as a mass filter, to transmit a unique product ion to the detector. By monitoring different transitions, mixtures of compounds can be analyzed simultaneously. The LC-QqQ-MS provides a robust platform for the sensitive detection of trace levels of compounds.

In 1994, teicoplanin was first introduced as a chiral stationary phases. It showed good chiral selectivity for various classes of compounds, especially for acidic compounds [35]. The teicoplanin stationary phase can be used under normal phase, reversed phase and polar organic mode conditions. Consequently the optimal mobile phase for mass spectrometry compatible separation methods can be used. Quinine based stationary phase also show enantiodiscrimination capabilities for acidic compounds, particularly native and derivatized amino acids. Interesting, the two stationary phases provide complementary selectivity for the enantioseparation of amino acids, with the teicoplanin stationary phase, all the L-amino acids (except for proline) elute earlier than the D enantiomers, while with the quinine stationary phase, all the D-amino acids (except for the proline) elute first, followed by their L isomers. The use of the two stationary phase help to provide more accurate and robust peak identification as well as quantitation. The stationary phases used in the D-amino acid studies are shown in Figure 1-1.
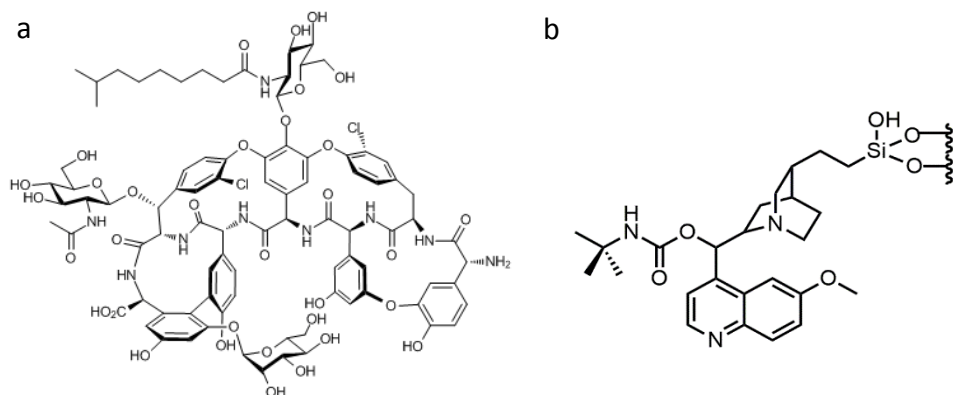
Figure 1-1 Structure of the chiral stationary phase used (a) teicoplanin (b) quinine

1.4 Research Objectives and Organization of the Thesis

This dissertation focuses on advancing HPLC and LC-MS techniques and applying them to pharmaceutical analysis and bioanalysis. Chapter 2 address the synthesis of a hydrolytically stable high efficiency stationary phase based on cyclofructan

6 which provides unique selectivity. Chapter 3 describes the development of a rapid and sensitive method for glycosaminoglycan disaccharide analysis by HPLC-MS/MS. Chapter 4 focuses on the evaluation and application of paired ion electrospray ionization (PIESI) for the sensitive analysis of FMOC-amino acids from biological samples. Chapters 5 and 6 demonstrate the application of HPLC-MS for the analysis of D and L amino acids in biological systems. Chapter 5 examines the altered D and L amino acids profiles in whole mouse brain of wild-type and mutant mice lacking D-amino acid oxidase activity. Baseline concentrations of D and L amino acids in cultured human breast cancer cells and non-tumorigenic human breast epithelial cells and their potential as a biomarkers is addressed in Chapter 6.

Chapter 2

Carboxylated Cyclofructan 6 As a Hydrolytically Stable High Efficiency Stationary Phase

for Hydrophilic Interaction Iiquid Chromatography and Mixed Mode Separations

Abstract

Stationary phases composed of native cyclofructan 6 (CF6) and benzoic acid modified CF6 were synthesized and evaluated for hydrophilic interaction liquid chromatography (HILIC). The ligands were bonded onto 2.7 mm core–shell silica using multipoint attachment technology. These cyclofructan 6 based columns exhibited excellent hydrolytic stability and efficiency (205, 000 N m^{-1}). The new column chemistry was compared for stability with core–shell silica (the starting material) using neutral, positive and a negatively charged probes. Additionally, the advantage of the use of a pre-saturating column in HILIC mode is shown. The HILIC selectivity chart shows that the benzoic acid modified cyclofructan-6 column shows strong hydrophilicity as well as cation exchange properties. A variety of hydrophilic/ionizable compounds were examined, and based on the selectivity chart, it was found that the new column chemistry is different from 33 commercial columns. The benzoic acid CF6 column can simultaneously separate acidic, neutral and basic drugs and produced considerably different retention and selectivity patterns for various classes of compounds including nucleic acid bases, β-blockers, salicylic acid and its analogues. The newly developed column chemistry also shows a potential to work in the reverse phase mode.

2.1 Introduction

Hydrophilic interaction liquid chromatography (HILIC) is one of the fastest growing chromatographic modes over the last few years. Because of the stronger interaction between the polar analytes and hydrophilic stationary phases, HILIC provides a superior method to separate polar and hydrophilic molecules over reversed phase liquid chromatography (RPLC). Stronger retention and selectivity can be gained with HILIC for a wide variety of compounds such as carbohydrates, peptides, proteins, oligosaccharides, pharmaceutical products and metabolites [36].

The term HILIC was first coined in 1990 [1], although this separation mode previously had been utilized for a long time for separating sugars and other polar molecules [37-40]. The polar analytes interact with the stationary phases via hydrogen boding, dipole–dipole interaction, charge dipole interaction and ion-exchange mechanism [36]. A typical mobile phase contains a large portion of acetonitrile with a smaller portion of aqueous buffer (usually 5–40%). Mobile phases with high organic content generate less column back pressure which make high flow rates possible and thus shortened analysis times [41]. Typical HILIC mobile phases also improves sensitivity for compounds analyzed by electrospray ionization mass spectrometry (ESI-MS) [42-46]. Amide-, cyano-, diol-, polyethylene glycol-, poly(succinimide)-,sulfoalkylbetaine-, cyclodextrin, pentafluorophenylpropyl, polyvinyl alcohol, polypeptide and other polar chemically bonded stationary phases as well as unmodified silica stationary phases have been available for HILIC separations [7]. Most of these HPLC stationary phases employ silica as a support because of its high efficiency and ease of chemical modification. However, attaching hydrophilic ligands on silica for HILIC purposes comes with a challenge – such phases are hydrolytically unstable. There are two different degradation mechanisms for bonded-phase columns *viz.* acid induced ligand hydrolysis

from the silica support and base induced silica skeleton dissolution [47,48]. The hydrophilic ligand promotes adsorption of a water layer, which in turn accelerates silica surface damage. Several successful strategies have been reported to ensure the stability and reproducibility of the silica based HILIC columns bonded phases. The majority of HILIC columns available today, are based on cross-linked polymers which resist leaching and the hydrolysis problems (*vide supra*). The potential drawback of such columns is lower efficiency than conventional bonded phases. Other approaches include: protective bulky groups which "hide" the siloxane bond from water, acids or bases [49]; densely-bonded, end-capped, longer-chain alkyl stationary phases; buffers with concentrations lower than 50 mM and operation temperatures lower than 40 °C [50-54]. The use of pre-column ('pre-saturators') has been suggested as an effective approach to increase the lifetime of a column in RPLC [55]. Cyclofructans and derivatives were first employed by Armstrong et al. in the development of chiral selectors for capillary electrophoresis (CE), [56] gas chromatography (GC) [57] as well as high performance liquid chromatography (HPLC) [58-62]. Given the hydrophilic nature of native CF6 and the ease of introducing polar functional groups into the molecule, we introduced a weak cation exchange functionality in the native CF6. Benzoic acid moieties were covalently attached to impart ionizable character to the CF6. The modified CF6 molecule was bonded to silica by reacting the hydroxyl groups of the sugar with a silane containing isocyanate groups. The large bonded bulky CF6 molecule protects the silica surface from hydrolytic attack while maintaining the high efficiency of bonded phases. We demonstrate that using multiple attachment technology results in a hydrolytically stable stationary phase. The performance of new bonding chemistry is also compared with core–shell silica, CF6 bonded core–shell silica, along with 33 other commercial phases.

2.2 Experimental

2.2.1 Chemicals

Anhydrous toluene, acetone, acetonitrile (ACN), methanol (MeOH), N,N-Dimethylformamide (DMF), heptane, pyridine, ammonium acetate, acetic acid, formic acid, methyl 4-(bromomethyl)benzoate, 3-(triethoxysilyl)propyl isocyanate, sodium hydride (NaH) and all analytes tested in this study were obtained from Sigma Aldrich (St. Louis, MO, USA). Sodium hydroxide was purchased from EMD (Gibbstown, NJ, USA). All solvents for chromatographic purposes were HPLC grade. Distilled water was further purified with Milli-Q water purification system to 18 MΩ (Millipore, Billerica, MA). Superficially porous silica (Poroshell 120 SIL, L.N. PSIL142718, 2.7 µm spherical diameter with 120 Å pore size) was utilized as the chromatographic support material.

2.2.2 Synthesis of stationary phases

In this work, 4.2 g of dry CF6 was dissolved in 200 mL of anhydrous DMF at 75 °C and 2.12 g of NaH was added and the mixture was stirred for 45 minutes. A solution of methyl 4-(bromomethyl)benzoate (2.0 g dissolved in 50 mL anhydrous DMF) was added into the above CF6/NaH solution slowly. The mixture was heated at 75 °C for 20 hours. After cooling to room temperature, the solid was filtrated off. Then the filtrate was rotovaped and the crude material was further purified by washing with 2 portions of 750 mL of deionized water. The product was vacuum dried overnight. Then the CF6-bezoate ester (8.5192 g) was hydrolysed with 6.0 g of sodium hydroxide (6.0 g dissolved at 50 mL of water) containing 200 mL of methanol. The mixture was heated to reflux for 5 hours. After cooling to room temperature, the pH of the mixture was adjusted to 3 with formic acid to precipitate the CF6-benzoic acid. The precipitate was washed with D.I. water. After filtration, the product was dried under reduced pressure at 40 °C. Mass spectrum showed that the major CF6 product has a benzoic acid degree of substitution 1:4.

A slurry of 6.0 g superficially porous silica gel in 150 mL of anhydrous toluene was refluxed for 30 minutes and 22 mL toluene with the residual water was azeotropically removed using a Dean-Stark trap. In another flask, 3-(triethoxysilyl)propyl isocyanate (2.1 mL) dissolved in 20 mL of pyridine was added drop by drop to a solution of CF6-benzoic acid (3 g) in 100 mL anhydrous DMF over 30 min. The reaction was carried out with continuous stirring under argon atmosphere at 90 °C for 5 h. After cooling to room temperature, the product was mixed with the dried silica gel slurry in toluene. This slurry was heated at 110 °C for 24 h under argon to yield the stationary phases. The elemental analysis showed that the stationary phase has a carbon loading of 9.48%, H of 0.87% and N of 0.82%. The stationary phases were packed into 15 cm x 0.46 cm and 5 cm x 0.46 cm columns from IDEX. The slurry was pressurized using Haskel (DSTV-122) pump using a dispersed slurry system. The columns were conditioned with several solvents phase prior to use for > 24 hours. Once the baseline was stable, the columns were ready for use.

2.2.3 Chromatographic conditions

All experiments were conducted on an Agilent HPLC series 1260 system (Agilent Technologies, Palo Alto, CA), equipped with a quaternary pump, an autosampler, and a multi-wavelength UV–Vis detector, sampling frequency of 80 Hz and 0.063 s response time. Extra-column effects were minimized by using 0.075 mm i.d. connection nanoViper tubings (Thermo Scientific, Waltham, MA). Separations were carried out at room temperature if not otherwise specified. Each sample was analyzed in duplicate. The mobile phase consists of a mixture of ACN and aqueous buffer stated as volume ratios. The buffer solution was prepared by dissolving ammonium acetate in deionized water and adjusted to the desired pH with acetic acid. Appropriate volumes of ACN and the buffer solution were mixed manually or by the pump and degassed by ultrasonication

under vacuum before use. All the chromatograms were obtained with a silica pre-column installed between the pump and the injector unless stated otherwise.

2.2.4 Tested columns and test probes

Uracil, cytosine and benzyltrimethylammonium chloride (BTMA) were used to evaluate the hydrophilicity and ion exchange behavior of the stationary phases [6]. Specifically: selectivity of cytosine/uracil was used to probe the hydrophobic/hydrophilic characteristics of the column; selectivity of BTMA/cytosine is used to probe the column ion exchange character. Toluene was used as the unretained dead time marker (t_0) for the silica phase, and acetone was used as the dead time marker for the CF6 and benzoic CF6 stationary phases.

Nicotinic acid, adenine and BTMA were used to examine the stability of the stationary phases with or without the silica pre-column by measuring their change in retention times. Nicotinic acid, adenine and BTMA mixture was injected every one hour and the total duration for a test was 30 hours.

A bare silica and a CF6 stationary phases were selected for the comparison to the newly developed stationary phases in the HILIC mode. Several types of analytes such as nucleic acids and bases, salicylic acid and its analogues and β-blockers were chosen for this purpose. A series of acidic, neutral and basic drugs were also selected for the applicability for pharmaceutical compounds.

2.3 Results and discussion

HILIC phases offer orthogonal selectivity to reversed phase separations and hence there is considerable interest in developing new and hydrolytically stable chemistries for HILIC. The aim of this work is to develop a hydrolytically stable high efficiency core–shell based HILIC column with cation exchange properties along with a different selectivity than existing chemistries. Unfortunately, the very nature of HILIC

14

mode requires that a water rich layer be formed on the "silica surface" into which polar/hydrophilic molecules can partition and hence be retarded by the stationary phase. Although Alpert had postulated this mechanism, the direct evidence of water uptake by HILIC stationary phases came from Karl Fisher titrations [63]. Silica is still widely used and sold by many manufacturers as a HILIC stationary phase. As is well known, silica has a finite solubility of 0.01 to 0.012% in water [64] and the Si–O–Si linkage is very susceptible to hydrolysis at moderate to high pHs with basic conditions significantly more deleterious than acidic conditions. HILIC phases are more prone to hydrolytic attack and silica dissolution than reversed phases, since the hydrophobic chains of C-18 phases help prevent water "seeing" the siloxane linkage. There are several approaches which make stable HILIC phases such as extensive cross-linking of polymers [65,66], usage of bidentate silanes [67,68], sterically hindered silanes [49] and the use of other pH stable oxides such as titania [69,70] and bonded porous graphitic carbon [10].

2.3.1 Hydrolytic Stability of the Stationary Phase

It is well known in the field of adhesion technology that using dipodal silanes increase the durability of bonded coating on surfaces by a factor of 10,000 times greater resistance to hydrolysis than i.e. silanes which can form only one siloxane bond with the surface [71]. The enhanced hydrolytic stability of dipodal silanes is associated with an increased cross-link density of the silane and the inherent resistance to hydrolysis, as they can potentially form five or six, rather than three siloxane bonds. In this work, we adapted a facile bonding approach which is similar to dipodal silane chemistry yet potentially stronger than dipodal silanes. Essentially, by employing four triethoxysilane units for every cyclofructan unit, we "ideally" have 12 possible linkages to the silica particle as compared to 6 (Figure 2-1).
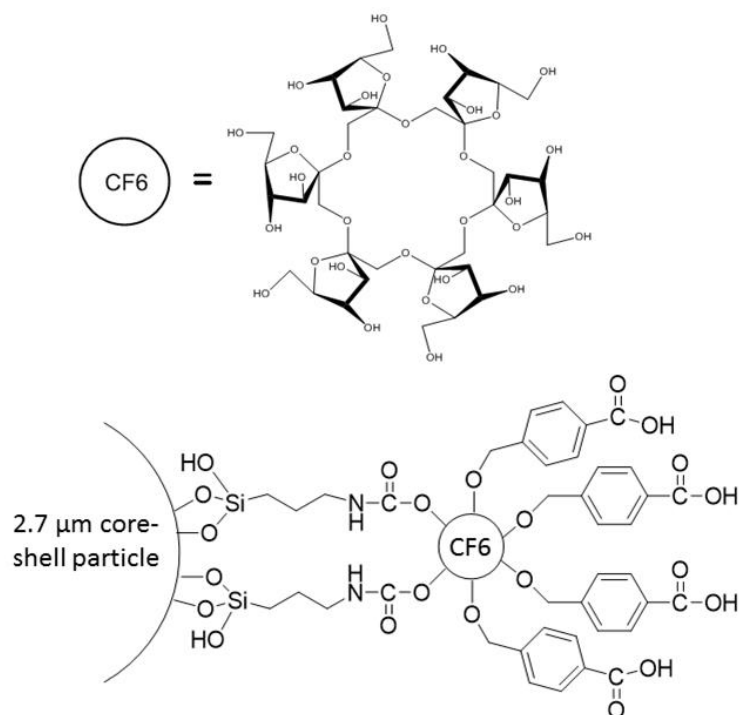
Figure 2-1 Representation of the CF6-benzoic bonded stationary phase.

(Up to four triethoxysilane units for each modified cyclofructan unit).

Previous studies have shown that high pH mobile phases result in deterioration of the silica support by dissolving silica into silicates [51-54]. A pre-saturating column can help to reduce or eliminate the dissolution of the silica in the analytical column by saturating the incoming mobile phase with silicate [54]. The pre-saturating column is simply a short column (3 cm) filled with large porous silica particles. The pre-column is placed after pump and prior to the injection valve and thus does not affect the separation and retention of the analytes, nor the peak band broadening. In our research, we design an experimental approach to test the stability of the stationary phases and the protective effect of the pre-saturating column. A neutral pH ammonium aqueous buffer (pH 6.8) was

chosen and when combined with acetonitrile the apparent pH of the mobile phase is above 7.0. Adenine, BTMA and nicotinic acid were used as test probes. Adenine is a neutral probe to test the hydrophilic character. BTMA is a positively charged quaternary amine which indicates the silanol and/or carboxyl group activity. Nicotinic acid acts as a negatively charged probe under the chosen conditions. The mixture was injected every one hour and all columns were continuously flushed at 1 mL/min for 30 hours without recycling the mobile phase to study column stability. Figure 2-2 represents the retention change of the analytes on the stationary phases with or without pre-column. Figure 2-2a shows the results of silica phase without attaching the pre-column. The retention of BTMA increased continuously which indicated that the silanol concentration on silica surface was increasing as a result of breaking the siloxane bonds of the silica, generating more silanols. On the other hand, the retention of nicotinic acid continuously decreased and this confirmed an increase in the number of negatively charged silanol groups. Interestingly, since adenine is neutral, its retention does not change much. We propose this mixture as a good HILIC column stability marker. Figure 2-2b shows the protective effect of the pre-saturating column to the silica support (one freshly packed silica column). As a result, retention times for both BTMA and nicotinic acid drift very slowly as compared with those in Figure 2-2a. The stability of the benzoic acid CF6 phase was also studied without and with a pre-column as shown in Figure 2-2c and 2-2d (same column was used) respectively. Even without the pre-column, the benzoic acid CF6 phase exhibited better stability than the pre-column protected silica column. The results clearly demonstrate the pre-column is useful in maintaining the column stability and reproducibility in the HILIC mode. In addition, the bulky cyclofructan molecules sterically protect the silica surface by preventing water to access the Si–O–Si bonds. The improved stability is also achieved by multiple linkages of the cyclofructan with the silanes.

17
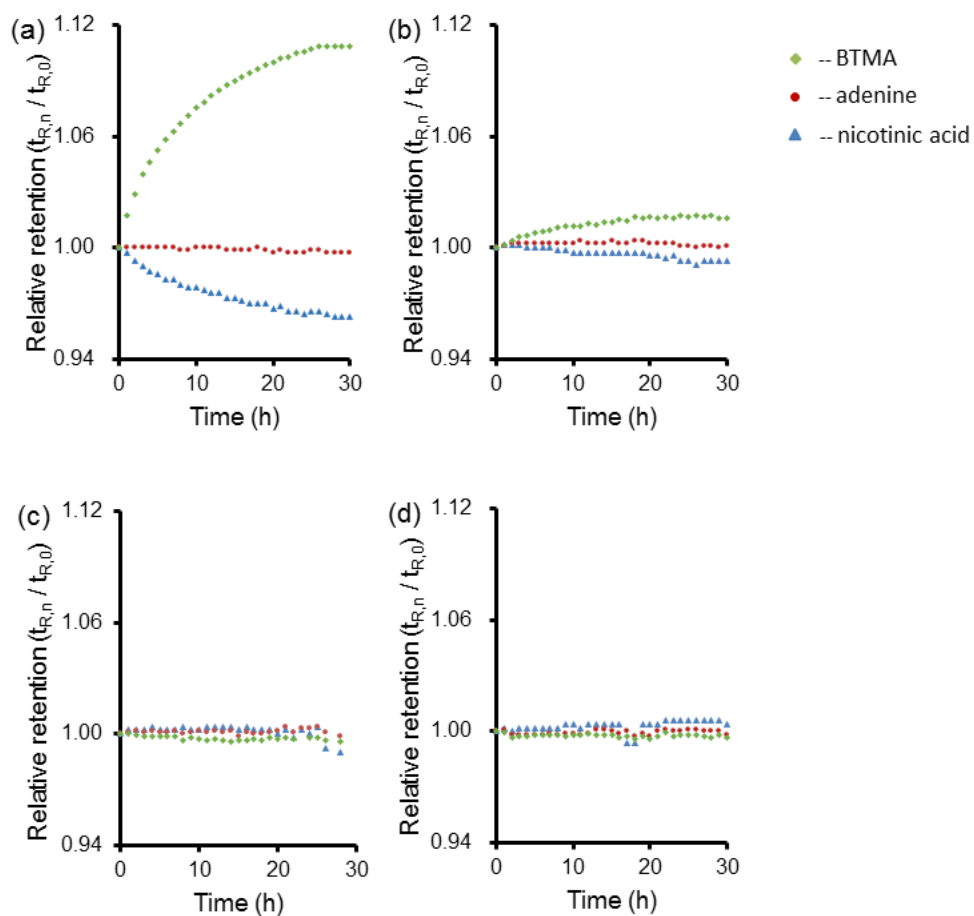
Figure 2-2 Hydrolytic stability of columns. Conditions: column, (a) silica core–shell (50 mm x 4.6 mm i.d.), without pre-column, (b) silica core–shell (50 mm x 4.6 mm i.d.), with pre-column, (c) benzoic acid CF6 core–shell (50 mm x 4.6 mm i.d.), without pre-column, (d) benzoic acid CF6 core–shell (50 mm x 4.6 mm i.d.), with pre-column; flow rate, 1.0 mL min^{-1}; eluent: acetonitrile/25 mM NH4OAc pH 6.8, 75/25 (v/v); UV detection at 220 nm. $t_{R,0}$ indicates the initial retention time at the beginning of the test; $t_{R,n}$ represents the retention time at any given hour.

2.3.2 Selectivity

Any newly designed stationary phase should have a different selectivity than the existing phases to be a useful addition to existing plethora of HPLC columns. Figure 2-3 represents a selectivity plot of different HILIC stationary phases (33 of them were previously studied and 3 additional phases tested in this research; details are shown in Appendix A). According to the literature [5], three analytes were chosen to probe the hydrophilicity and electrostatic characteristics of the stationary phases. The x-axis categorizes the HILIC stationary phases according to their hydrophilicity by plotting relative retention factors of cytosine/uracil. The higher the value, the more hydrophilic the stationary phase. Relative retention factor of BTMA/cytosine is plotted on the y-axis and it indicates the electrostatic character of the stationary phase. Stationary phases at the top show stronger cation exchange properties. Underivatized core–shell silica phase studied in this research settled in the silica phase region and exhibited hydrophilicity and cation exchange character due to its negatively charged and polar silanol groups. The core-shell CF6 and benzoic acid CF6 stationary phases appear at the right hand side of the selectivity plot, which indicate that the two stationary phases are strongly hydrophilic. The CF6 showed weaker cation exchange interaction with the analytes than the underivatized silica phase since a large portion of the silanol groups were bonded with the neutral CF6 molecules. The plot also indicated that the benzoic acid CF6 had stronger cation exchange property than the native CF6 since the attached carboxyl groups were negatively charged and therefore strongly retained BTMA. The plot clearly reveals that the benzoic acid CF6 stationary phase has a unique hydrophilic characteristic and ion exchange behavior compared to existing HILIC phases and other commercial HPLC columns.
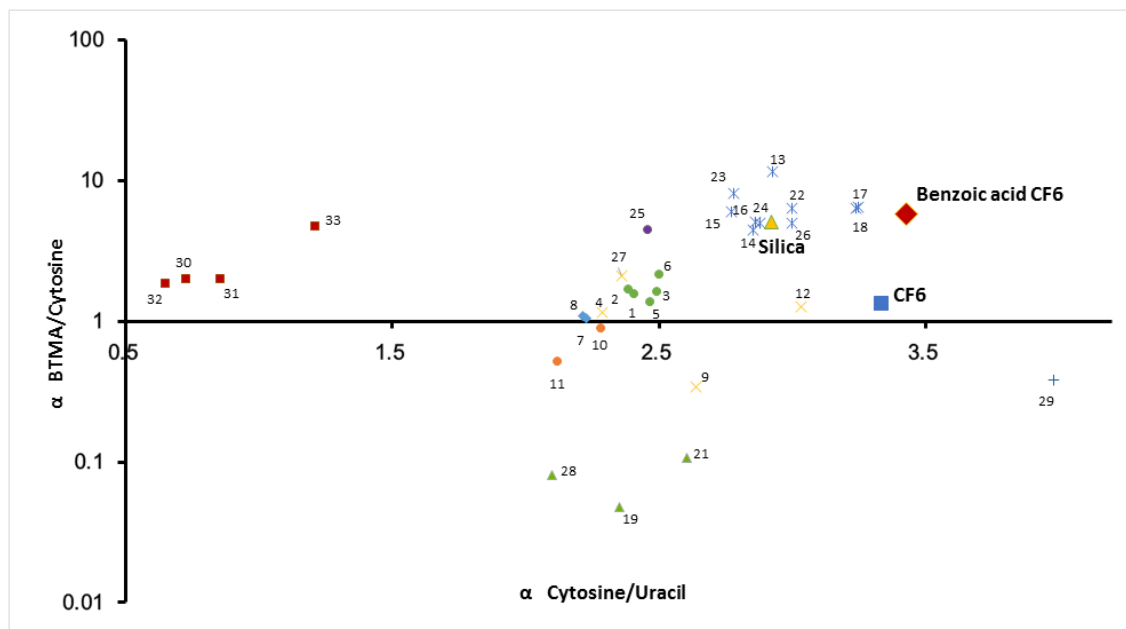
Figure 2-3 Plot of electrostatic character vs. hydrophilicity character for the evaluated HILIC phases: Amide (◆), diol (●), amine and/or triazole (▲), poly (×), silica (✳), zwitterionic (●), proprietary polar phase (+), RPLC (■), Latex coated silica (●).The numbered markers are for Irgum's columns and for Lucy's columns as defined in Supporting information 1.* The newly evaluated columns are Benzoic acid CF6 (◆), CF6 (■), Bare silica (▲). The experimental conditions: eluent, ACN/25 mM ammonium acetate, pH 6.8, 80/20 (v/v); flow rate, 1.0 mL/min; UV detection at 254 nm. *Column (20) is not plotted in the chart since it gave (BTMA/cytosine) ratio out of scale at −0.0026.

2.3.3 Changing the chromatography mode

Weak retention of hydrophobic compounds is a drawback of HILIC due to the low hydrophobicity of most HILIC stationary phases. However, the benzoic acid CF6 stationary phase can work under both HILIC and RP modes. Under HILIC mobile phase conditions (90% ACN in Figure 2-4b), the retention order of toluene and uracil is consistent with the polarity of analytes. When the % ACN is decreased to 30% (Figure 2-4a), retention of toluene and uracil is reversed indicating that the column can also be used under reversed phase condition, similar to other mixed-mode stationary phases. [72,73] Compared with the previously reported benzoic acid PGC column, the core–shell silica based column shows higher efficiencies and better peak shapes than PGC.
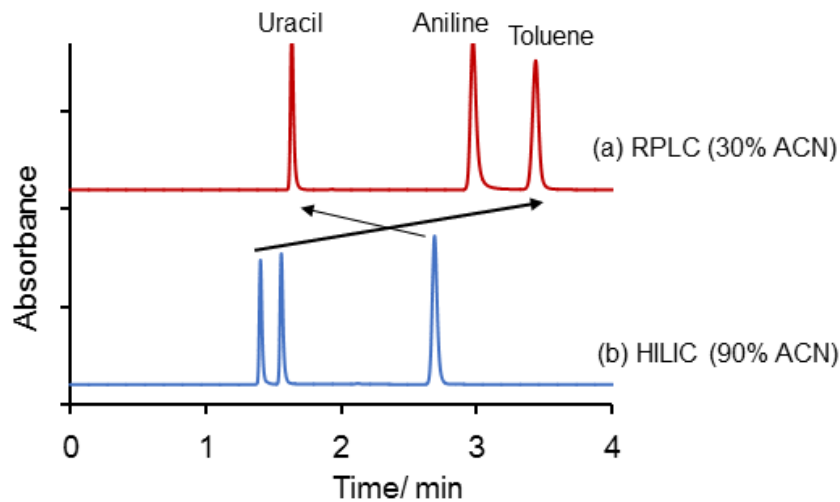
Figure 2-4 HILIC/RPLC mixed-mode retention behaviour of the benzoic acid CF6 phase. Conditions: column, Benzoic CF6 core-shell (150 × 4.6 mm i.d.); flow rate, 1.0 mL/min; eluent, (A) RPLC mode: Acetonitrile/ 20 mM ammonium acetate pH 4.2 30/70 (v/v), (B) HILIC mode: Acetonitrile/ 20 mM ammonium acetate pH 4.2 90/10 (v/v); UV detection at 254 nm.

2.3.4 Optimized separation of polar analytes

In this study, test mixtures of drugs, nucleic acid bases, salicylic acids and analogues, β-blockers and phenols were used to characterize the stationary phase. In general, the newly prepared core–shell benzoic acid CF6 stationary phase shows different selectivity, excellent Gaussian peak shapes and higher efficiencies than the previously reported carboxylated HILIC phases [10,73]. Figure 2-5 to 2-8 compare the performance of the newly prepared benzoic CF6 core–shell stationary phase with CF6 core–shell and silica core–shell columns.

Figure 2-5 shows chromatograms of acidic, neutral, basic drugs obtained on the three columns under the same mobile phase acetonitrile/20 mM ammonium acetate pH 4.2 90/10 (v/v). There are seven pharmaceutical drugs: where maleic acid and ibuprofen are acidic, dexamethasone and hydrocortisone are neutral drugs, and the remaining ones are basic drugs. These seven drugs were separated within 5 minutes on the columns. As expected from the selectivity chart, the elution orders are different on all three columns. The benzoic acid CF6 column provided the best performance in separating those drugs where all the seven analytes were separated simultaneously and all the adjacent peaks have desired resolutions. On the CF6 core–shell column, except for ibuprofen and theophylline, the other adjacent peaks were baseline separated. On silica core–shell column, two pairs of compounds ibuprofen and caffeine, caffeine and theophylline were partially separated. The benzoic acid CF6 stationary phase showed electrostatic repulsion to the acidic analytes, which is the main reason for early elution of maleic acid and ibuprofen. Also, the retention times of theophylline and dyphylline are significantly longer on the benzoic acid CF6 phase than the other two stationary phases which reveals that the benzoic acid CF6 stationary phase has cation exchange properties. The two neutral drugs dexamethasone and hydrocortisone eluted a little later in benzoic CF6

22

indicating that the new benzoic CF6 phase is more hydrophilic as expected from the selectivity plot (Figure 2-3).
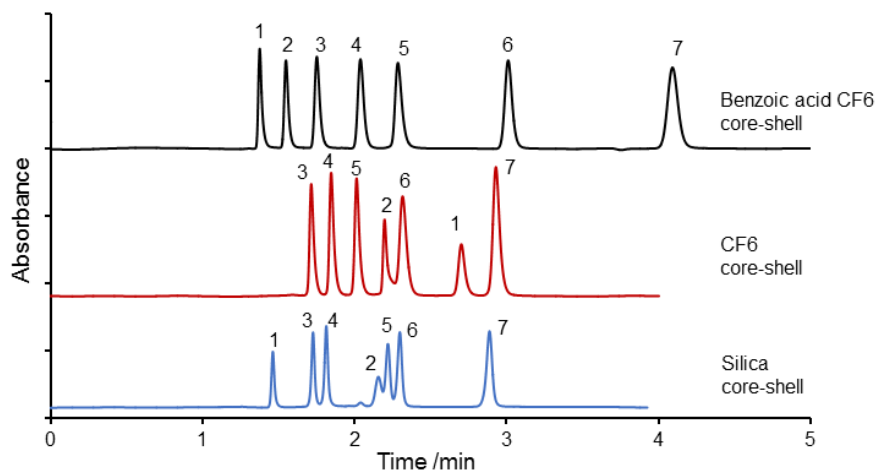
Figure 2-5 Separation of basic, neutral, acidic drugs. (1) maleic acid; (2) ibuprofen; (3) dexamethasone; (4) hydrocortisone; (5) caffeine; (6) theophylline; (7) dyphylline. Condition: eluent, acetonitrile/ 20 mM ammonium acetate pH 4.2 90/10 (v/v), 1.0 mL/min; UV detection at 254 nm.

Salicylic acid and its analogues were all separated with these three columns as shown in Figure 2-6. Gaussian peak shapes and efficiencies were observed for all the analytes. Most of the analytes eluted earlier on the benzoic acid CF6 phase than the other two tested columns due to the stronger electrostatic repulsion of the negatively charged analytes. Salicylic acid and salicylamide reversed their elution order on the CF6 column. In comparison, the silica phase showed the same elution order but greater retention than the benzoic acid CF6 phase.
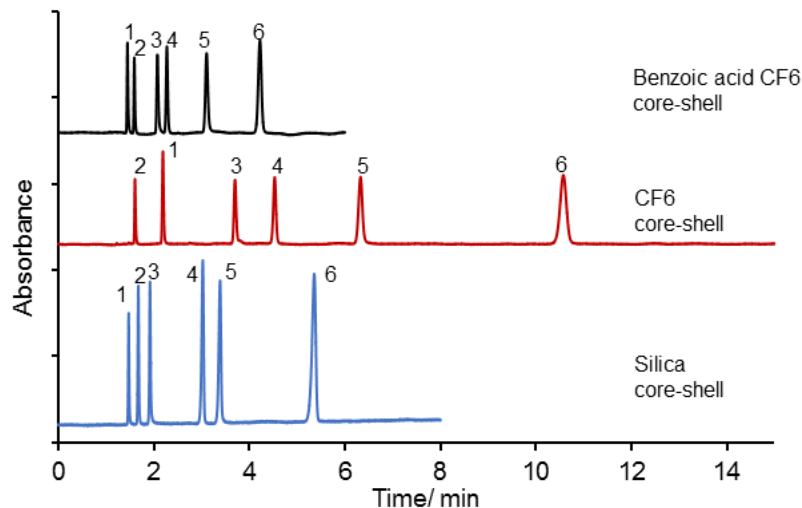
Figure 2-6 Separation of salicylic acid and derivatives. (1) salicylic acid; (2) salicylamide;

(3) 4-aminosalicylic acid; (4) acetylsalicylic acid; (5) salicyluric acid; (6) hippuric acid.

Condition: eluent, acetonitrile/20 mM ammonium acetate pH 4.2 90/10 (v/v), 1.0 mL/min;

UV detection at 254 nm.

In the case of β-blockers, the benzoic acid CF6 stationary phase was the most

retentive column as expected for a negatively charged stationary phase. The pKas of β-

blockers are in the range of 7.8–9.8 and they are positively charged under the studied

conditions. The mobile phase composition was adjusted for the benzoic acid CF6

stationary phase in order to separate all the selected β-blockers. Figure 2-7 shows the

HILIC separation of the seven b-blocker mixture. When the mobile phase is

acetonitrile/20 mM ammonium acetate pH 4.2 75/25 (v/v), the separation window of the

β-blockers is around 25 minutes on benzoic acid CF6, which is considerably longer than

the separation on CF6 (3 minutes) and silica stationary phases (5 minutes). All these

compounds are in their protonated form with this mobile phase, so longer retention times

are expected when there are strong cation exchange interactions between the analytes

and carboxylated stationary phase. This electrostatic interaction also seems to play an indispensable role in separating the sample mixture. These three stationary phases showed different elution orders because of their different functionalities, and benzoic acid CF6 gave the best separation in terms of selectivity and resolution. At this optimized mobile phase condition for the benzoic acid CF6 stationary phase described above, all the seven β-blockers were separated. But metoprolol and pindolol were partially separated on the CF6 column while metoprolol and sotalol were partially resolved on the silica column. Compared with previously reported sulfonated cyclofructan 6 stationary phase which is another negatively charged phase [74], these analytes have much shorter retention time and two pairs of analytes (esmolol and metoprolol & pindolol and sotalol) reversed their elution orders on the benzoic acid CF6 phase. Unfortunately, the synthesis of sulfonated CF6 is very challenging and further studies were not done as this phase.
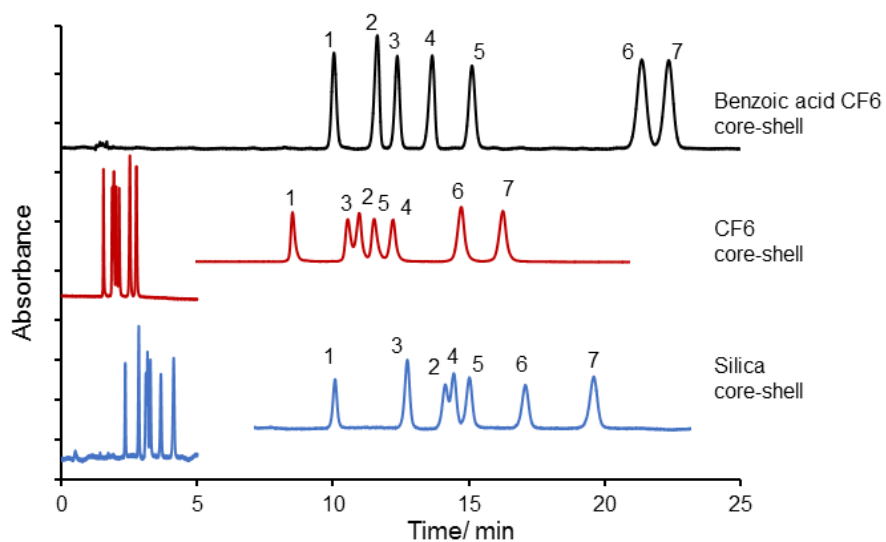
Figure 2-7. Separation of β-blockers. (1) carvedilol; (2) metoprolol; (3) pindolol; (4) sotalol; (5) acebutolol; (6) nadolol; (7) atenolol. Condition: eluent, acetonitrile/ 20 mM ammonium acetate pH 4.2 75/25 (v/v), 1.0 mL/min; UV detection at 220 nm.

Figure 2-8 shows the separation for nucleic acids and their bases. All three columns separated the nucleic acids and bases with symmetric peak shapes and good efficiencies. The separation window for this group of analytes using the benzoic acid CF6 is about 10 minutes. These analytes elute much earlier on CF6 and on the silica stationary phases because the carboxylate groups on benzoic acid CF6 phase could contribute to stronger cation exchange as well as hydrophilic interaction between the analytes and the stationary phase. Under this mobile phase condition, all the analytes were separated by the benzoic acid CF6 stationary phase, but cytidine and guanosine co-eluted on the CF6 column. On the silica column, guanosine and cytosine were partially separated and reversed elution order was also observed for guanosine and cytosine/cytidine. Other published reports also compared the selectivity of HILIC stationary phases on the separation of nucleic acid bases. [75] Although the elution pattern is similar on those phases, such as the amide phase, aspartamide phase, sulfobetaine phase, diol phase, cross-linked diol phase, polyhydroxy phase, polyvinyl alcohol phase, amino phase as well as imidazole phase except for adenosine and uridine is reversed on these reported HILIC stationary phases. Uridine and adenosine co-eluted on the amide phase. Cytidine and guanosine were partially separated by diol phase and polyvinyl alcohol phase.
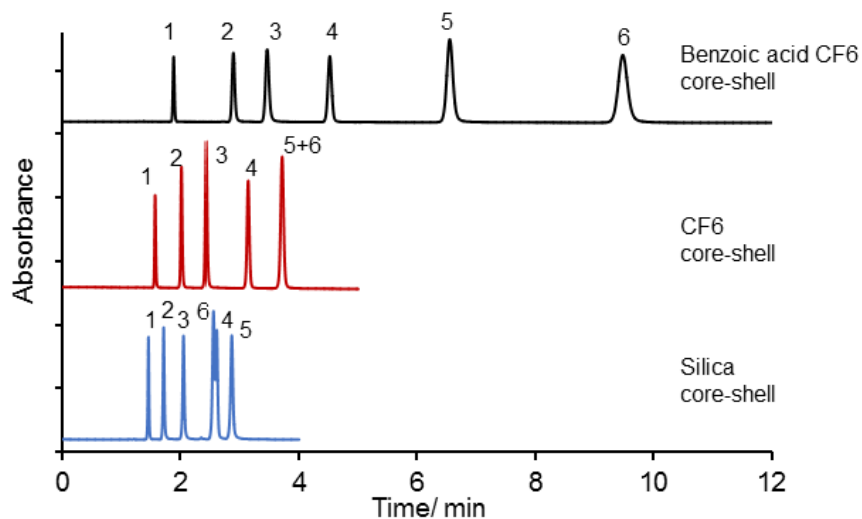
Figure 2-8 Separation of nucleic acid bases. (1) uracil; (2) uridine; (3) adenosine; (4) cytosine; (5) cytidine; (6) guanosine. Condition: eluent, acetonitrile/water 85/15 (v/v) containing 10 mM ammonium acetate, 1.5 mL/min; UV detection at 254 nm.

2.4 Conclusions

In this work, core–shell silica particles bonded with CF6 benzoic acid stationary phase were successfully synthesized and characterized chromatographically. The stationary phase showed improved hydrolytic stability compared to the silica column. The advantage of using silica pre-column was evaluated and proven to be an effective method to maintain the reproducibility of the column and increase the column lifetime. The benzoic acid CF6 appears to be an exceptional HILIC stationary phase for the separation of polar pharmaceutical drugs, salicylic acid analogues, β-blockers as well as nucleic acids and their bases. Additionally, the benzoic acid CF6 stationary phase showed different hydrophilicity and electrostatic character compared with all the existing HILIC phases included in this study.

Chapter 3

Analysis of Chondroitin Sulfate (CS)/Dermatan Sulfate (DS) Disaccharides by Using

Hydrophilic Interaction Liquid Chromatography Mass Spectrometry

Abstract

Glycosaminoglycans are an important group of biopolymers. This research describes a rapid and sensitive method for the analysis of chondroitin sulfate/dermatan sulfate disaccharides using HILIC stationary phases and triple quadrupole mass spectrometry detection. Glycosaminoglycans were first depolymerized by Chondroitinases ABC and reduced with an ammonia borane complex. The resulting disaccharides were separated using two different HILIC stationary phases: cyclofructan 6 and teicoplanin, and quantified. Mobile phase pHs and buffer concentrations were evaluated and optimized in order to obtain the best separation while maintaining sensitive mass spectrometric detection. Separation of the disaccharides including the isomeric compounds was achieved on cyclofructan 6 stationary phase within 12 minutes. The teicoplanin stationary phase provided a faster separation than the cyclofructan 6 stationary phase, where all analytes were separated within 8 mins. The disaccharides were simultaneously quantified with a detection range from 1.5- 80 ng/mL. The method that used a teicoplanin stationary phase showed slightly higher detection limit for the compounds. The two methods were applied to profile and quantify the disaccharides component of the glycosaminoglycans from porcine intestinal mucosa, bovine trachea, whale cartilage and shark cartilage. The results of the two methods are comparable thus supporting the validity of the HILIC-MS method for the analysis of glycosaminoglycans.

3.1 Introduction

Glycosaminoglycans (GAGs) are a family of long, unbranched polysaccharides that consist of repeating disaccharide units. Each disaccharide unit contains a uronic acid moiety (D-glucuronic acid or L-iduronic acid) alternating with an amino sugar (N-acetyl-D-galactosamine or N-acetylglucosamine (GlcNAc) [16]. Chondroitin sulfate (CS)/dermatan sulfate (DS) is one of the most important groups of GAGs. They are attached covalently to serine residues of the core protein via a tetrasaccharide linkage to form proteoglycans. CS contains the N-acetylgalactosamine (GalNAc) linked to D-glucuronic acid in the core disaccharide structures. DS is the modified form of CS, where the D-glucuronic acid is epimerized to L-iduronic acid [76]. The disaccharide structures of CS/DS are highly heterogenous because O-sulfation can occur at multiple positions, such as the C2 of the uronic acid and the C4 or C6 of GalNAc, resulting in highly diverse and negatively charged GAG species [77,78]. As an important component of cell surface and extracellular matrices, CS/DS play critical roles in various biological process including cell migration and signaling [79,80], inhibition of blood coagulation [81,82], cancer metastasis [83,84], brain development [85] and as crucial environmental modulators in the central nervous system (CNS) [86-88].

Due to the complexity and high dispersity of the CS/DS structure, the direct structure characterization of CS/DS is challenging. Usually GAGs are depolymerized to disaccharides, and the resulting disaccharides are analyzed and quantified to obtain the GAG structural information [89]. The enzymes used for CS/DS depolymerization is the chondroitinases (ABC and ACII) which cleave glycosidic linkages between the hexosamine and uronic acid residues, forming a deoxy-α-L-threo-hex-4-enopyranosyluronic acid (ΔUA) residue at the nonreducing end [89]. The native disaccharides are not retained on the stationary phase in RPLC because they are highly

negative charged and polar. In order to improve their chromatographic retention as well as to enhance the detection sensitivity, derivatization of the disaccharide by introducing a hydrophobic fluorophore is accomplished through reductive amination with 2-aminoacridone (AMAC) [18], 2-aminobenzamide (2-AB) [19], and 4,4-difluoro-5,7-dimethyl-4-bora-3a,4a-diaza-s-indacene-3-propionic acid (BODIPY) [20]. These strategies were applied for sensitive analysis of disaccharides extracted from various biologic matrices, such as liver tissue, CHO cells and urine [90,91]. However, these methods typically involved the use of excess derivatization reagent which introduced chromatographic interferences and the sample preparation procedure was more labor intensive and time consuming.

Separation methods using hydrophilic interaction (HILIC) stationary phase with mass spectrometric detection were developed. An amide-HILIC prototype column was used for separation of CS/DS disaccharides, but the two structural isomers, ∆CS–4S and ∆CS–6S, could not be fully separated under any of the conditions tested in those studies [22,23]. A separation of CS/DS disaccharides also was reported by using a graphitic porous carbon (Hypercarb) stationary phase [21]. Though isomeric compounds were separated by this column, the peak shapes were poor and contributed to poor separation efficiency as well as low sensitivity. The recent availability of HILIC stationary phases based on superficially porous particles (SPP) demonstrated the potential to improve chromatographic speed and efficiency [92,93]. The use of higher solvent percentages of acetonitrile in the HILIC mode greatly enhances the electrospray ionization efficiency and desolvation when hyphenated with mass spectrometry. In this article, we report a rapid and sensitive LC-MS approach for separating and quantifying CS/DS disaccharides using two different HILIC stationary phases.

3.2 Materials and Methods

3.2.1 Materials and chemicals

Chondroitin sulfate A (bovine trachea, whale cartilage) and chondroitin sulfate B sodium salt (porcine intestinal mucosa) and chondroitin sulfate C (shark cartilage), chondroitinase ABC, ammonia-borane complex, acetic acid and ammonium acetate were purchased from Sigma-Aldrich (St. Louis, MO). Acetonitrile hypergrade for LC-MS was purchase from EMD Millipore (Burlington, MA) and LC-MS water were purchased from Honeywell (Charlotte, NC). The CS/DS disaccharide standards ΔUA – GalNAc, ΔUA – GalNAc, 4S, ΔUA – GalNAc, 6S, ΔUA, 2S – GalNAc, ΔUA, 2S – GalNAc, 4S, ΔUA, 2S – GalNAc, 6S, ΔUA – GalNAc, 4S, 6S, ΔUA, 2S – GalNAc, 4S, 6S were purchased from Galen Lab Supplies (North Haven, CT).

3.2.2 Reduction of disaccharides

The reduction of disaccharides was adopted from a previously reported method for analysis of glycans with a slight modification [94]. A solution 50 µg/µL of ammonia-borane complex was prepared by dissolving 10 mg of ammonia-borane into 200 µL of H_2O. An aliquot of 40 µL of the solution was added into 40 µL of the disaccharide standard solutions or the digested GAG samples. The mixture was incubated at 60 °C for 2 hours. The remaining ammonia-borane complex was destroyed by adding acetic acid. The borane salt was removed by vacuum drying after adding methanol to the mixture. The resulting sample was dissolved with 100 µL of a 90/10 ACN/H_2O mixture. The reaction is shown in Figure 3-1.
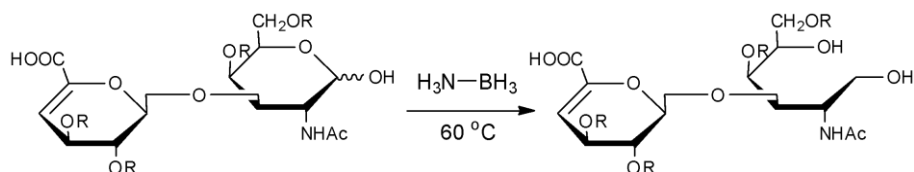
Figure 3-1. Reaction between disaccharide and ammonia-borane complex, R=-SO$_3$H.

3.2.3 Depolymerization of CS/DS

The GAG samples (20 µg) were incubated with Chondroitinases ABC (20 mU) in 50 mM NH$_4$OAc (pH adjusted to 8) with 0.01% BSA at 37 ^{o}C for 16 hours. The chondroitinase enzymes were inactivated by boiling to 100 ^{o}C for 2 min. After cooling to room temperature, the samples were centrifuged, and the supernatants were collected for reduction are described above.

3.2.4 LC-MS/MS Conditions

HPLC-MS/MS analysis was performed on LCMS-8040 (Shimadzu Scientific Instruments, Columbia, MD, USA), a triple quadrupole spectrometer with electrospray ionization (ESI) source. The HPLC-MS/MS was operated in the negative ion multiple reaction monitoring (MRM) mode. The drying gas and nebulizing gas flow rate were 15 L/min and 2 L/min, respectively; the desolvation line temperature and heat block temperature were 275 °C and 400 °C, respectively. Collision energies (CV) and MRM transitions were optimized for each GAG disaccharide by infusion of each standard analyte directly to the mass spectrometer.

Two HILIC columns (10 cm x 4.6 mm i.d.), cyclofructan 6 (FructoShell-N) and teicoplanin (TeicoShell) bonded to superficially porous particles (2.7 µm) were provided by AZYP, LLC (Arlington, TX). The optimized separation condition by using CF6 stationary phase was ACN/20 mM NH$_4$OAc in water pH 6.8 (80/20, v/v) with flow rate at 1 mL/min. The optimized condition by using teicoplanin stationary phase was ACN/50 mM NH4OAc in water pH 4, (83/17, v/v) with flow rate at 0.85 mL/min. The flow was split and half (50%) was sent to the ESI-QqQ-MS.

3.2.5 Calibration

Disaccharide stock solutions were prepared at 1 mg/mL in water and stored at -20 ^{o}C. An intermediate solution of the disaccharide mixture was prepared by mixing an

appropriate volume of each stock solution: 100 µL of ∆CS–0S and ∆CS–4S6S; 10 µL of ∆CS–2S; 20 µL of ∆CS–4S ; 50 µL of ∆CS–6S, ∆CS–2S6S, and ∆CS–2S4S; 200 µL of ∆CS–tS, and adjusting the final volume to 1 mL with deionized water. Calibration standards were prepared by serial dilution of the intermediate mixture solution and the calibration curves were constructed within the following dynamic ranges: 0.1-50 µg/mL for ∆CS–0S and ∆CS–4S6S; 0.01-5 µg/mL for ∆CS–2S; 0.02-10 µg/mL for ∆CS–4S; 0.05-25 µg/mL for ∆CS–6S, ∆CS–2S6S, and ∆CS–2S4S; 0.2-100 µg/mL for ∆CS–tS. All analyses were performed in triplicate. Standard calibration curves were generated by plotting the analyte peak area against the concentration for each standard. The linearity of the method was evaluated by the correlation coefficient (r) for all the analytes. The limits of detection were determined at the concentrations when signal-to-noise ratios were at 3.

3.2.6 Precision and Accuracy

Intra-day precision and accuracy were evaluated by analyzing QC sample at three different concentrations: low, 0.03 µg/mL (0.3 µg/mL for ∆CS–tS); medium, 1 µg/mL; and high, 10 µg/mL (80 µg/mL for ∆CS–tS) with five replicates on the same day. Inter-day precision was determined using the same solutions of five replicates on three successive days.

3.3 Results and Discussion

The separation of CS/DS disaccharides is an essential step for the analysis of GAGs. The structure and mass of the studied disaccharides and the assignment of the precursor ion scan mass to charge are shown in Table 3-1. Note that ∆CS–2S, ∆CS–6S and ∆CS–4S are structural isomers and ∆CS–2S6S, ∆CS–2S4S and ∆CS–4S6S are structural isomers. By monitoring each transition, one can identify and quantify the molecules simultaneously within a single injection. However, in the LC-MS analysis of

GAG disaccharides, one major challenge is the loss of sulfate groups during electrospray ionization due to in-source fragmentation. As a result, the desulfated ions of high-sulfated disaccharides will interfere the transitions of the less-sulfated disaccharides if they produce the same product ions. Therefore, not only do the structural isomers need to be separated, but it is also important to separate all other analytes even they have different molecular weights.

Table 3-1 Structure, nomenclature and mass of the unsaturated CS/DS disaccharides studied

DS disaccharide structure	Abbreviation	Theoritical mol weight	Mw-Reduced	Observed m/z after reduction (Charge)	Assignment
	ΔCS–0S	379.1	381.1	380.00 (-1)	[M-1]$^{-1}$
	ΔCS–2S	459.1	461.1	459.95 (-1)	[M-1]$^{-1}$
	ΔCS–4S	459.1	461.1	459.95 (-1)	[M-1]$^{-1}$
	ΔCS–6S	459.1	461.1	459.95 (-1)	[M-1]$^{-1}$
	ΔCS–2S4S	539.0	541.0	539.90 (-1)	[M-1]$^{-1}$
				269.45 (-2)	[M-2]$^{-2}$
	ΔCS–2S6S	539.0	541.0	539.90 (-1)	[M-1]$^{-1}$
				269.45 (-2)	[M-2]$^{-2}$

Table 3-1—*Continued*

Structure	Name				
	ΔCS–4S6S	539.0	541.0	539.90 (-1)	[M-1]$^{-1}$
				269.45 (-2)	[M-2]$^{-2}$
	ΔCS–tS	619.0	621.0	309.45 (-2)	[M-2]$^{-2}$

3.3.1 Choice of stationary phase

In this experiment, two different HILIC stationary phases were examined to separate the CS/DS disaccharides. The structures of the stationary phases are shown in Figure 3-2. The cyclofructan 6 (FructoShell-N) stationary phase was reported to be a hydrolytically stable stationary phase with unique selectivity for highly polar and hydrophilic compounds [61,95]. Teicoplanin, a macrocyclic glycopeptide (TeicoShell), which was first introduced as a hydrolytically stable chiral stationary phase, has been widely applied for chiral amino acids and peptide epimers [35,96]. It showed extraordinary selectivity for enantioseparation of different type of compounds under normal phase, reversed phase, polar ionic mode, especially for anionic compound [35,97]. Besides its enantiomeric selectivity, the sugar moieties on the teicoplanin provide hydrophilic properties to the stationary phase and it can also be used in the HILIC mode. Teicoplanin stationary phases have been used to separate a variety of analytes in the HILIC mode, including cyclosporin, gonadotropin-releasing hormones, low molecular weight cyclic hormones and peptides [62]. Considering the good selectivity of these two stationary phases in the HILIC mode, the separation of disaccharides by these columns were explored.
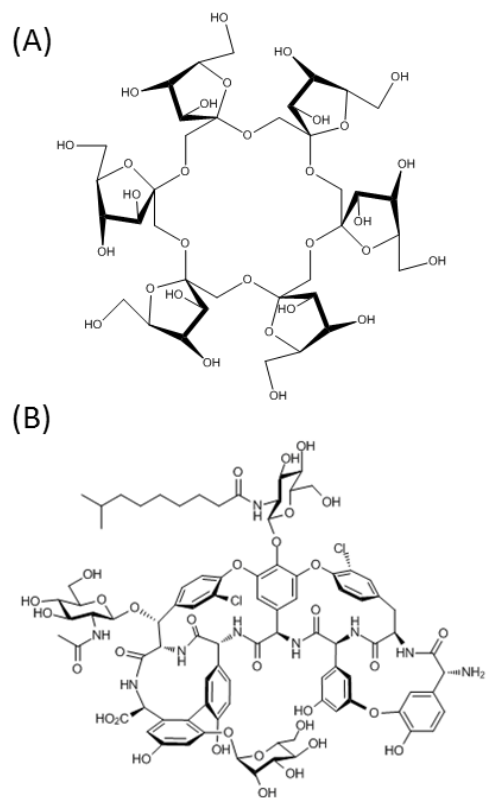
Figure 3-2. Structure of stationary phase used in this study. (A) FructoShell-N;

(B) TeicoShell.

3.3.2 Optimization of Mobile Phase

3.3.2.1 Separation of CS/DS disaccharides with FructoShell-N

The initial separation method tested with the FructoShell-N column was ACN/20 mM ammonium acetate in water, 80/20 (v/v). The isocratic separation was achieved at room temperature at a flow rate of 1 mL/min. Figure 3-3 shows the overlaid MRM chromatograms of each transitions. Under these separation conditions, the two groups of isomeric compounds (mono-sulfated including ΔCS–2S, ΔCS–6S and ΔCS–4S, and di-sulfated including ΔCS–2S6S, ΔCS–2S4S and ΔCS–4S6S) were well separated. Mono-sulfated disaccharide ΔCS–2S eluted earlier than its structural isomers ΔCS–6S and

ΔCS–4S. Also, the di- sulfated disaccharides were well separated with ΔCS–2S6S eluting

first followed by ΔCS–2S4S and then ΔCS–4S6S. The tri-sulfated disaccharide ΔCS–tS

had longer retention times than other analytes due to its high hydrophilicity. As shown in

Figure 3-3A, by increasing the concentration of the ammonium acetate in the aqueous

solution, the retention time of all the analytes increased. The di-sulfated disaccharides

showed greater shifts in retention time when changing the NH_4OAc concentration. For

example, at lower concentrations of ammonium acetate (20 mM of ammonium acetate),

ΔCS–2S6S eluted right after the mono-sulfated disaccharide ΔCS–2S. While with 30 mM

of ammonium acetate, ΔCS–2S6S started to coelute with ΔCS–6S. When the

concentration of NH_4OAc increased to 50 mM in the aqueous phase, ΔCS–2S6S showed

longer retention than ΔCS–6S. The pH of the mobile phase usually plays critical role in

the retention time. The pH effect was investigated as well by evaluating the retention of

the CS/DS disaccharides using the 20 mM ammonium acetate with different pH value

(Figure 3-3B). Decreased pH resulted in the greater retention of these disaccharides.
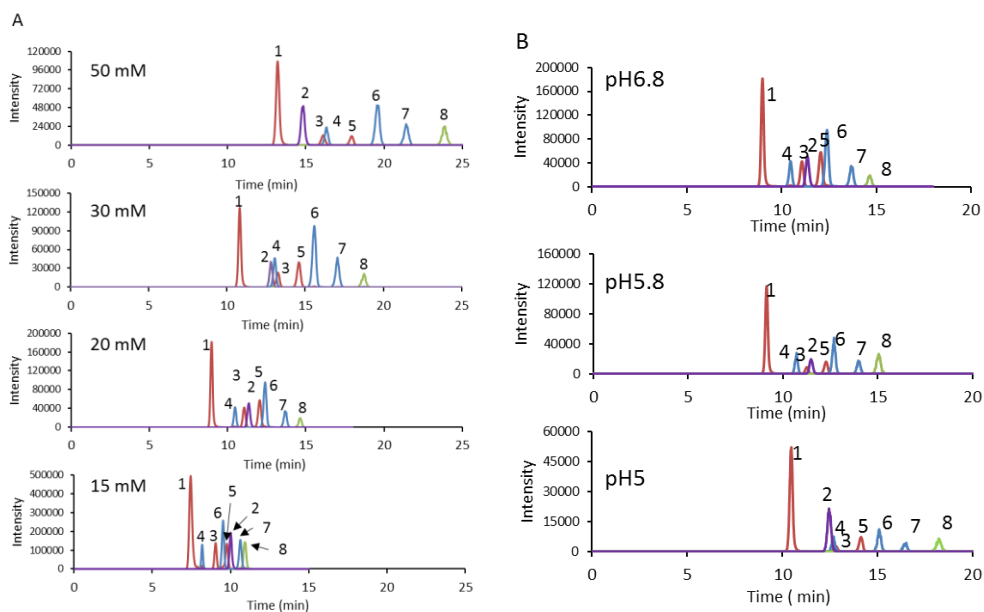
Figure 3-3 Effect of ammonium acetate concentration (A) and pH (B) on the separation of CS/DS disaccharides by using CF6 stationary phase. MRM chromatogram for each transition are overlaid. (A) Mobile phase: ACN/ NH$_4$OAc in water, 80/20 (v/v) with different concentration (15 mM, 20 mM, 30 mM, 50 mM). (B)Mobile phase: ACN/20 mM NH$_4$OAc in water, 80/20 (v/v) with different pH (5.0, 5.8, 6.8). The disaccharide peaks are: 1, ΔCS–2S; 2, ΔCS–0S; 3, ΔCS–6S; 4, ΔCS–2S6S; 5, ΔCS–4S; 6, ΔCS–2S4S; 7, ΔCS–4S6S; 8, ΔCS–4S6S.

3.3.2.2 Separation of CS/DS disaccharides with TeicoShell

The separation of CS/DS disaccharides also was investigated and optimized on the teicoplanin stationary phase. It is not surprising that the elution order of the compounds was different from what was achieved on the CF6 stationary phase (Figure 3-4). In the working pH range (pH 4-7), the teicoplanin exists in the zwitterionic form, where the amine groups are in the positively charged form (-NH$_3^+$) and the carboxyl group are in

38

the anionic form (-COO⁻) [98]. Under all the mobile phase conditions tried, the ΔCS–0S was retained longer than the other analytes. This may because the anionic sites of the stationary phase tend to repel the disaccharides contain more sulfated groups but have relatively stronger retention to ΔCS–0S which contains only one carboxyl group. Aqueous solutions with various concentration of ammonium acetate were evaluated (Figure 3-4A). The higher the concentration of salt in the mobile phase, the greater was the retention for all the analytes. The retention of the disaccharides was tremendously affected by the percentage of organic solvent in the mobile phase. As shown in Figure 3-4B, a 3% decrease of ACN shortened the analysis time from 14 minutes to 7 minutes. The disaccharides were well separated under this condition. To further optimize the separation, the pH of the aqueous buffer was decreased to 4, the analytes showed slightly longer retention times and were all baseline separated from each other (Figure 3-4C). Consequently, an aqueous solvent of pH 4 was used in the following study.
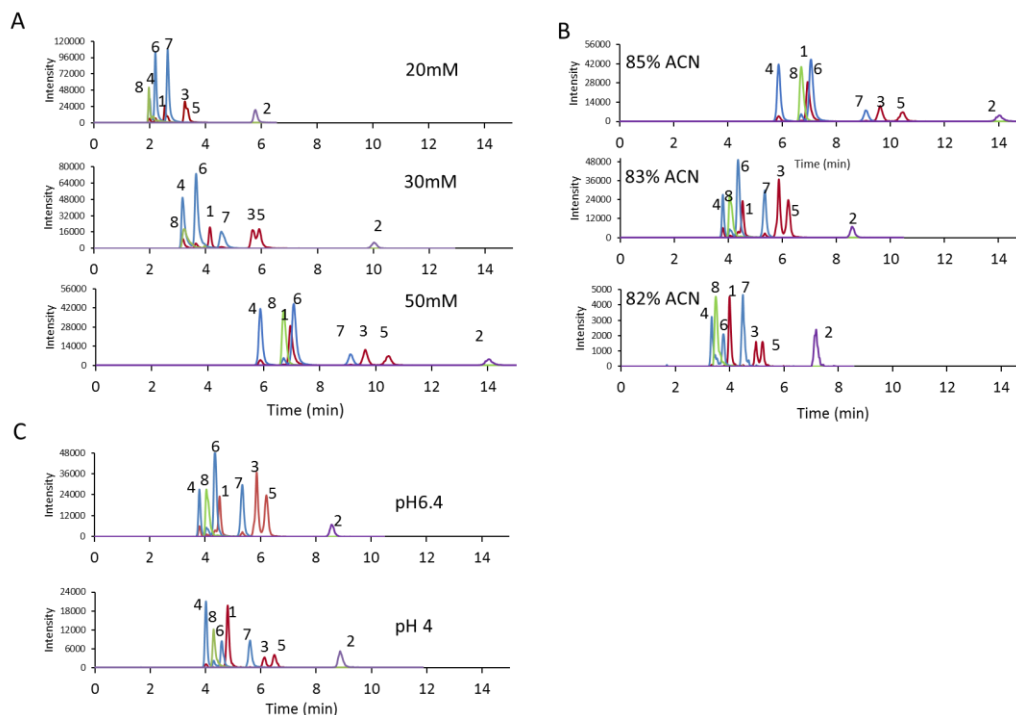
Figure 3-4 Effect of ammonium acetate concentration (A), % of ACN (B) and pH (C) on the separation of CS/DS disaccharides by using teicoplanin stationary phase. MRM chromatogram for each transition are overlaid. (A) Mobile phase: ACN/ NH₄OAc in water, 85/15 (v/v), pH 6.4 with different concentration of NH₄OAC (20 mM, 30 mM, 50 mM); (B) Mobile phase: 50 mM NH4OAc pH 6.4 with different percentage of ACN (85%, 83%, 82%); (C) Mobile phase: ACN/ 50 mM NH₄OAc in water, 83/17 (v/v) with different pH (4.0 and 6.4). The disaccharide peaks are: 1, ΔCS–2S; 2, ΔCS–0S; 3, ΔCS–6S; 4, ΔCS–2S6S; 5, ΔCS–4S; 6, ΔCS–2S4S; 7, ΔCS–4S6S; 8, ΔCS–4S6S.

3.3.3 Identification of CS/DS Disaccharides by Multiple Reaction Monitoring

Optimized MRM transitions obtained for each disaccharide are listed in Table 3-2. The fragmentation patterns were determined and shown in Figure 3-5. The non-sulfated and mono-sulfated disaccharides show the highest intensity precursor ion as [M-

H]⁻. The dominate di-sulfated and tri-sulfated disaccharide molecular ions were [M-2H]$^{2-}$.

From the product ion spectra of the disaccharides, the major fragment was produced

from the dissociation of the labile sulfate group ([HSO4]⁻), which is one of the major

product ions for the sulfated disaccharides except for ΔCS–4S6S and ΔCS–tS. The

glycosylic bond between the uronic acid and the GalNAc is easily broken as well. A

desulfated B ion (m/z 157) was observed by MS analysis of ΔCS–0S, ΔCS–2S, ΔCS–6S

and ΔCS–2S4S. Two mono-sulfated disaccharides ΔCS– 4S and ΔCS– 6S as well as di-

sulfated disaccharides, ΔCS–2S6S, ΔCS–4S6S and ΔCS–tS produce the desulfated Y

ion (m/z 302). Intra-ring fragmentation also occurred for ΔCS–0S, ΔCS–2S, ΔCS–4S,

ΔCS–6S and ΔCS–4S6S.

41
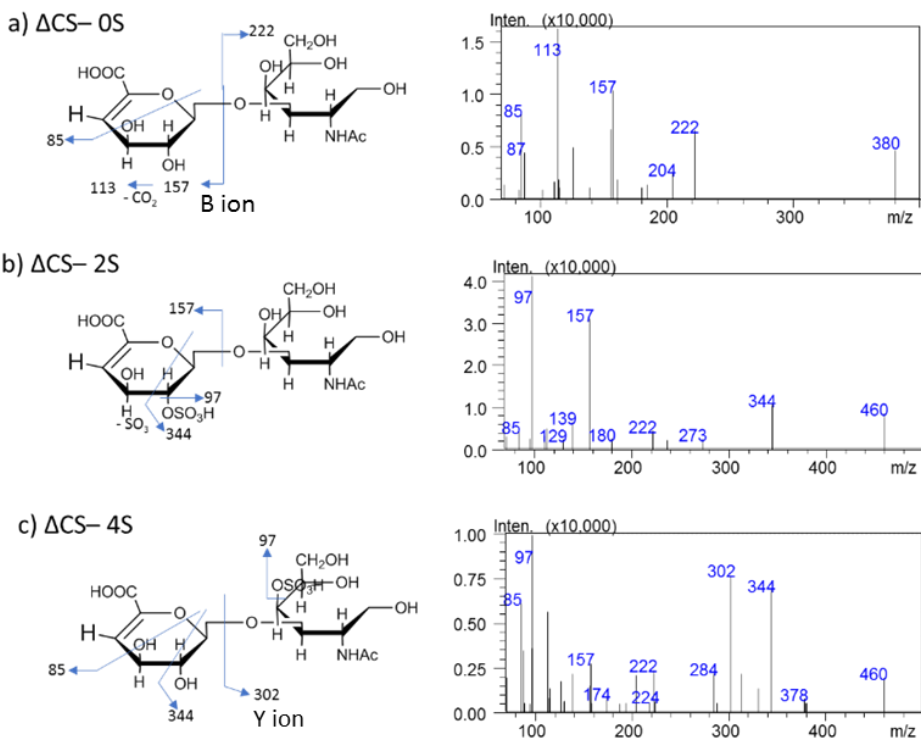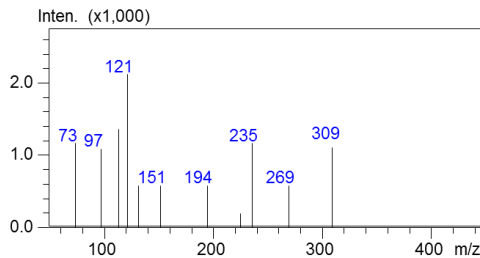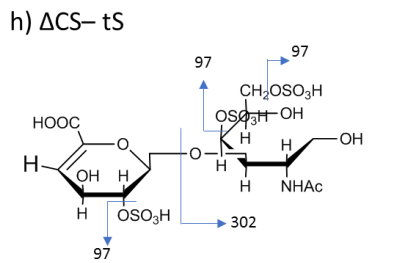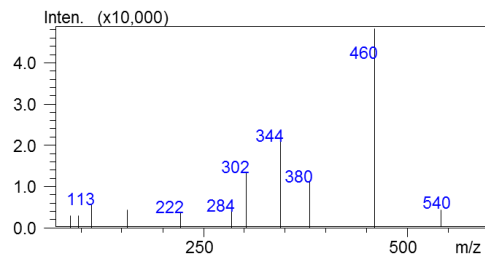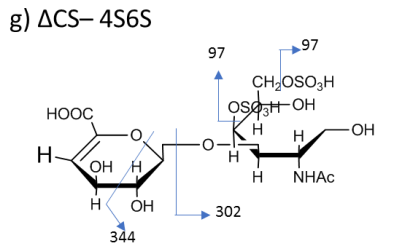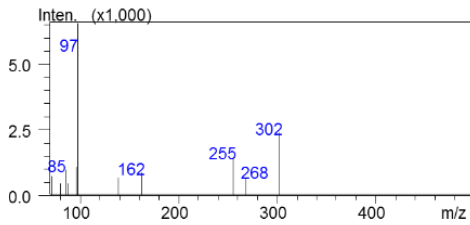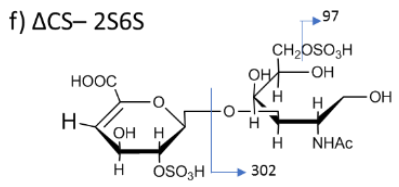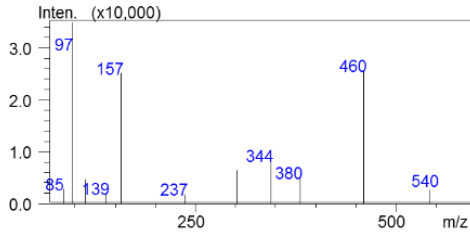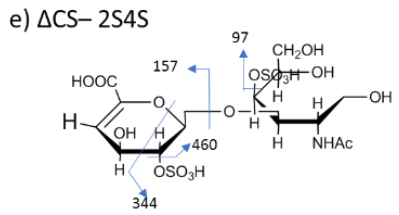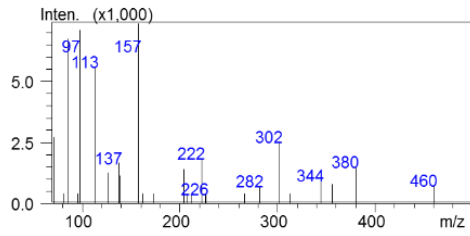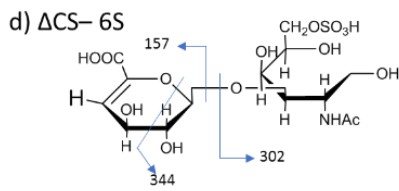
Figure 3-5 Product ion mass spectra of reduced disaccharides.

Table 3-2 Optimized MRM transition for each disaccharide

	Precursor (m/z)	Product (m/z)	CE	Q1 (V)	Q3 (V)
ΔCS–0S	380.00	157.00	17.0	19.0	13.0
ΔCS–2S	459.95	96.95	40.0	17.0	15.0
ΔCS–4S	459.95	344.00	27.0	17.0	20.0
ΔCS–6S	459.95	96.90	40.0	17.0	15.0
ΔCS–2S4S	539.90	460.05	19.0	20.0	29.0
ΔCS–2S6S	269.45	96.95	29.0	13.0	18.0
ΔCS–4S6S	539.90	460.05	19.0	20.0	29.0
ΔCS–tS	309.45	269.45	10.0	16.0	25.0

3.3.4 Limits of detection, Calibration curve and Precision

The chromatographic peak intensities are somewhat different for the two stationary phases, at least in part due to the different mobile phases. In general, the methods using the FructoShell-N column show greater peak intensities than methods using Teicoshell column. Increased concentrations of ammonium acetate produced a deleterious effect on signal strength due to the builtup of salt on the mass spectrometer ionization source as well as the less efficient droplet desolvation. For example, as the ammonium acetate increased from 20 mM to 50 mM, the signal intensity was suppressed by 75%. The tri-sulfated disaccharide ΔCS–tS showed highest LOD values among all the analytes and its LOD was 30 ng/mL and 80 ng/mL when using CF6 and teicoplanin stationary phase respectively. The detection for the non-sulfated disaccharide ΔCS–0S was the second lowest among all the disaccharides, which has an LOD of 10 ng/mL on the FructoShell and 30 ng/mL on TeicoShell column. The LOD, calibration range and coefficient correlation of the calibration curve for each disaccharide is listed in Table 3-3. Repeatability of analysis was determined as well by evaluating the relative standard deviation of the peak areas at low, medium and high concentrations within the same day

(intra-day) and over three different days (inter-day). The results are shown in Table 3-4 and all the %RSD values are within 18%.

Table 3-3 Calibration range, linearity, LOD for the disaccharide standards

| | Range (µg/mL) | CF6 | | Teicoplanin | |
		r	LOD [a] (ng/mL)	r	LOD [a] (ng/mL)
ΔCS–0S	0.1-50	0.998	10	0.996	30
ΔCS–2S	0.01-5	0.996	2	0.997	3
ΔCS–4S	0.02-10	0.998	1.5	0.999	5
ΔCS–6S	0.05-25	0.999	5	0.997	15
ΔCS–2S4S	0.05-25	0.996	5	0.994	20
ΔCS–2S6S	0.05-25	0.998	5	0.997	15
ΔCS–4S6S	0.1-50	0.999	8	0.993	30
ΔCS–tS	0.2-100	0.999	30	0.999	80

Table 3-4 Intra-day and inter-day relative standard deviation of peak areas for the

reduced DS/CS disaccharides.

| | Intra-day RSD peak area % | | | | | |
| DS disaccharides | CF6 | | | Teicoplanin | | |
	Low	Medium	High	Low	Medium	High
ΔCS–0S	6.0	4.8	1.7	1.4	1.8	0.5
ΔCS–2S	0.3	3.0	4.9	1.4	0.9	0.8
ΔCS–4S	3.9	3.8	3.7	5.0	3.3	1.1
ΔCS–6S	9.5	1.9	1.4	6.2	6.6	1.7
ΔCS–2S4S	1.7	4.8	2.5	12.9	2.8	1.5
ΔCS–2S6S	9.8	4.1	0.2	4.2	3.5	2.2
ΔCS–4S6S	6.4	2.7	0.5	0.5	8.9	1.3
ΔCS–tS	17.8	2.7	0.8	5.5	2.1	0.9
	Inter-day RSD peak area %					
DS disaccharides	CF6			Teicoplanin		
	Low	Medium	High	Low	Medium	High
ΔCS– 0S	10.5	5.2	6.6	12.2	4.8	3.5
ΔCS– 2S	7.8	5.6	3.1	6.0	4.2	10.2
ΔCS– 4S	10.4	4.1	4.6	11.2	8.9	7.8
ΔCS– 6S	5.8	4.9	6.3	10.3	8.0	6.5

Table 3-4 —*Continued*

ΔCS– 2S4S	6.7	4.3	4.0	8.2	7.5	7.9
ΔCS– 2S6S	6.9	7.6	7.1	9.0	9.1	8.5
ΔCS– 4S6S	15.2	10.3	8.4	7.1	8.8	6.5
ΔCS– tS	9.1	6.5	7.2	5.9	7.7	7.3

3.3.5 Quantitation of CS/DS Disaccharides in Different Biological Samples

Relative components of disaccharides of GAGs from four animal resources were analyzed using the optimized methods of this study. A comparison between the results obtained from the two stationary phases are shown in Figure 3-6. As shown in Figure 3-6, the two methods based on the different stationary phases produced comparable quantitative results for percentages of the disaccharide components. Although the TeicoShell column method produced faster separation times for the disaccharides, one disadvantage is that higher detection limits were obtained with it and the compounds with low abundance cannot be detected. For example, the ΔCS–tS could not be detected from chondroitin sulfate of whale cartilage using the TeicoShell column since it was below the detection limit, but it was detected as 0.2% using FructoShell-N method. The mono-sulfated disaccharides were quite prevalent in the GAGs of the animal resources studied here. Bovine trachea and porcine intestinal mucosa had the highest percentage of ΔCS–4S which was over 50% of the overall composition. The cartilage of the marine animals shark and whale contained ΔCS–6S as the most abundant disaccharide component, which was about 50% of the total [99]. The lowest component in the bovine trachea was the ΔCS–tS, but ΔCS–2S was the lowest in the porcine intestinal mucosa, shark and whale cartilage.
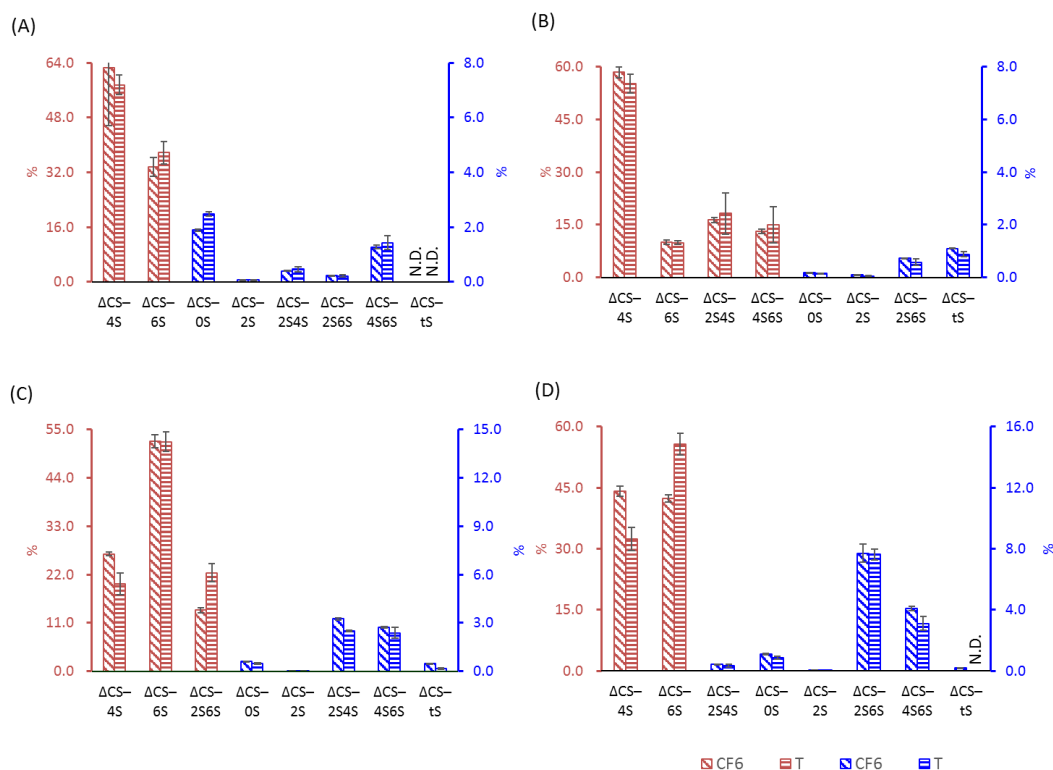
Figure 3-6 Comparison of the relative abundance of CS/DS disaccharides from different animal sources analyzed by two methods with CF6 and teicoplanin. Disaccharides were from (A) bovine trachea; (B) porcine intestinal mucosa; (C)shark cartilage; (D) whale cartilage. Axial values are shown as the percentage of each disaccharide in the total of ΔCS. N.D.- Not detected.

3.4 Conclusion

We have demonstrated a simple and rapid LC-MS/MS method for the analysis of CS/DS disaccharides by using two HILIC columns: FructoShell-N and TeicoShell. These HILIC stationary phases easily separated isomeric disaccharides and provided good peak shapes. Though faster separations could be obtained with the TeicoShell column,

the detection limits were 2 to 3 times lower when the FructoShell-N column approach. The use of high organic solvent in the mobile phase enhanced ionization efficiency and enable sensitive detection in the negative ion mode. The quantitation methods were well validated. Thus, it is possible to efficiently quantify the disaccharide components of GAGs from animal resources by using these methods.

Chapter 4

Sensitive Analysis of N-blocked Amino Acids Using High-Performance Liquid

Chromatography with Paired Ion Electrospray Ionization Mass Spectrometry

Abstract

In this study, a paired ion electrospray ionization (PIESI) mass spectrometry method was developed for sensitive detection of 9-fluorenylmethyl chloroformate (Fmoc)-derivatized amino acids. The structure-optimized ion-pairing reagent was introduced post column to form positively charged complexes which can be detected in the positive ion mode. These complexes are more surface-active than the original analytes, and meanwhile, the intensity of sodium adducts was significantly reduced. The limit of detection of the amino acids obtained with the optimal ion-pairing reagent was 0.5 to 20 pg which was 5 - 100 times lower than the negative mode. In addition, two mass spectrometry platforms - linear ion trap and triple quadrupole - were used to compare the PIESI improvements. Eventually, the method was applied to successfully detect the level of amino acids in human urine samples with high accuracy and the added benefit of minimizing matrix effects.

4.1 Introduction

Amino acids are one of the most important classes of compounds in nature since they play essential roles as building blocks in proteins as well as metabolic intermediates. [100] They are also involved in other biological pathways, such as transport and storage of nutrients, oxidation protection and regulation of gene expression, and neurotransmission [101,102]. Abnormal amino acid concentrations can indicate metabolic disorder and can be used as indicators to diagnose disease [103]. Consequently, the sensitive and accurate detection of amino acids are essential in different fields, especially in clinical diagnostics.

Amino acids have been analyzed with gas chromatography (GC), liquid chromatography (LC), and capillary electrophoresis (CE). Enantioseparation of amino acids was also achieved by chiral GC/LC stationary phases or introducing chiral selectors in CE [96,104-109]. To achieve improved separation and detection, amino acids were analyzed using MS detection and/or derivatized before analysis [34,96,110,111]. Different derivatization reagents have been introduced for amino acids, while the most commonly used ones, such as fluorenylmethyloxycarbonyl chloride (Fmoc-Cl) [26], o-phthalaldehyde (OPA) [27,28], and 7-fluoro-4-nitrobenzoxadiazole (NBD-F) [29,30], react with the amino group and leave the carboxyl group free. OPA derivatization is fast but can only react with primary amines, and some of the products were labile and must be analyzed right after derivatization [112]. Fmoc-Cl can react with both primary and secondary amines in a short time with high yield, and the product is quite stable for at least 3 days [26,113]. In addition to providing a chromophore for UV or fluorescence detection, Fmoc derivatization is also suitable for MS analysis. Fmoc-derivatized amino acids (Fmoc-AAs) and short-chain peptides show 2 orders of magnitude higher ionization efficiency compared to their underivatized analogues in LC-MS analysis [114].

To further enhance the detection sensitivity of Fmoc-AAs with LC-MS, a method based on paired ion electrospray ionization (PIESI) mass spectrometry was developed in this study. PIESI was found to provide ultra-trace level detection sensitivity for anions and some zwitterions (often ≤ parts per trillion (ppt) levels) [115-124]. This simple approach introduces low levels of designed synthetic ion-pairing reagents (IPRs) into the sample stream just prior to ESI (Fmoc-AA− + IPR2+ → [Fmoc-AA + IPR]+) [125,126]. The gas-phase paired ions are then detected in the more sensitive positive ion mode rather than the negative ion mode. The adducts of IPRs and analytes are more surface-active as compared to the original anions and thus show better ionization efficiency with ESI. Furthermore, especially for anions with small molecular weights, the analytes were detected in a higher m/z range with less inherent chemical noise.

In this work, we examined the sensitivity enhancement of 22 (20 proteinogenic and 2 non-proteinogenic) amino acids by using PIESI-MS in both selected ion monitoring (SIM) and selected reaction monitoring (SRM) modes. Different IPRs (symmetrical and unsymmetrical dicationic, tricationic, tetracationic) were examined and compared. Moreover, the optimized PIESI approach was then hyphenated to HPLC for the analysis of amino acids in urine samples.
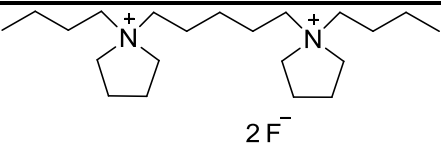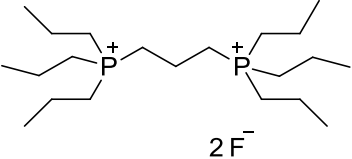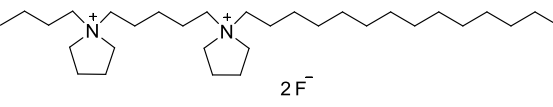
4.2 Experimental

4.2.1 Reagents and materials

The abbreviations and chemical structures of the ion-pairing reagents used in this study are shown in Table 4-1. 1,5-Pentanediyl-bis(1-butylpyrrolidinium) difluoride solution, 1,3-propanediyl-bis(tripropylphosphonium) difluoride solution, 1-butyl-1-[5-(1-tetradecyl-1-pyrrolidiniumyl)pentyl]pyrrolidinium difluoride, 1,3,5-tris[(tripropylphosphonium)methyl]benzene trifluoride solution, and 1,4-butanediyl-

bis[diphenylphosphomium-(1'-4'-butyl-triphenylphosphonium)] tetrafluoride solution were

originally developed in our laboratory, and some of them are also commercially available

from AZYP, LLC (Arlington, TX, USA). These ion-pairing reagents were initially

synthesized in bromide salt form and then ion exchanged to their fluoride form. The

amino acid standards [alanine (Ala), γ-aminobutyric acid (GABA), arginine (Arg),

asparagine (Asn), aspartic acid (Asp), cysteine (Cys), glutamic acid (Glu), glutamine

(Gln), glycine (Gly), histidine (His), isoleucine (Ile), leucine (Leu), lysine (Lys), methionine

(Met), phenylalanine (Phe), proline (Pro), serine (Ser), taurine (Tau), threonine (Thr),

tryptophan (Trp), tyrosine (Tyr), valine (Val)] and their Fmoc derivatives (9-

fluorenylmethyl chloroformate (Fmoc-Cl)), HPLC-MS grade acetonitrile (ACN), and formic

acid were purchased from Sigma-Aldrich (St. Louis, MO, USA). Borate buffer was from

Waters Corporation (Milford, MA, USA). HPLC-MS water was from Honeywell Burdick

and Jackson (Morristown, NJ, USA).

Table 4-1 Abbreviation, exact mass and structure of the ion pairing reagent used in this

study

Ion pairing reagent	Abbreviation Exact mass	Structure
1,5-Pentanediyl-bis(1-butylpyrrolidinium) difluoride	C$_5$(bpyr)$_2$, 324.4	
1,3-Propanediyl-bis(tripropylphosphonium) difluoride	C$_3$(triprp)$_2$, 362.3	
1-Butyl-1-[5-(1-tetradecyl-1-pyrrolidiniumyl)pentyl] pyrrolidinium difluoride	UDC, 464.5	

| 1,3,5-Tris[(tripropylphosphonium)methyl]benzene trifluoride solution | Tristriprp, 597.5 | |
| 1,4-Butanediyl-bis[diphenylphosphonium-(1'-4'-butyl-triphenylphosphonium] tetrafluoride | Tetpp4+, 1062.6 | |
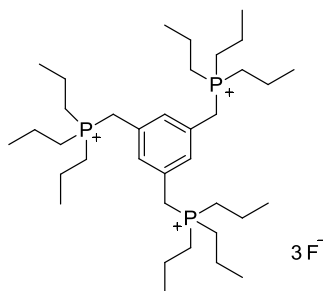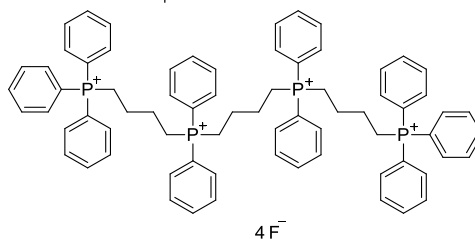
4.2.2 Paired Ion ESI Analysis

A scheme of the instrumental setup for the PIESI-MS detection is shown in Figure 4-1. Briefly, a carrier flow consisting of acetonitrile and water (67:33, v/v) was delivered by the binary LC pump at 300 µL/min, while a 40 µM aqueous solution of ion-pairing reagent was introduced by another pump (Shimadzu LC-6A; Shimadzu, Columbia, MD, USA) at a flow rate of 100 µL/min. The two streams were combined in a low dead volume mixing tee (Thermo Scientific, San Jose, CA, USA). A total flow of acetonitrile/water (50:50, v/v) with 10 µM of ion-pairing reagent was introduced into the MS at a flow rate of 400 µL/min. The continuous use of the non-volatile ion-pairing reagent can result in the contamination of the ion source. To ensure the producibility and accuracy of the analysis results and maintain the optimum performance of the ion source, a mobile phase of 50:50 methanol/water was pumped at a flow rate of 200–400 µL/min through the sample transfer line, sample tube, and ESI probe for 1 h at the end of each working day until the ion-pairing reagent memory peaks were no longer detected. The spray cone and ion transfer capillary were cleaned weekly according to the

52

manufacturer's instruction. Fmoc amino acids were injected into the HPLC system through a six-port injection valve. As the consequence, positively charged analyte/ion-pairing reagent complexes could be detected by the MS in the positive ion mode. An analytical column was inserted between the mixing device and the injection valve (see Figure 4-1) for the chromatographic separations and sample analysis.
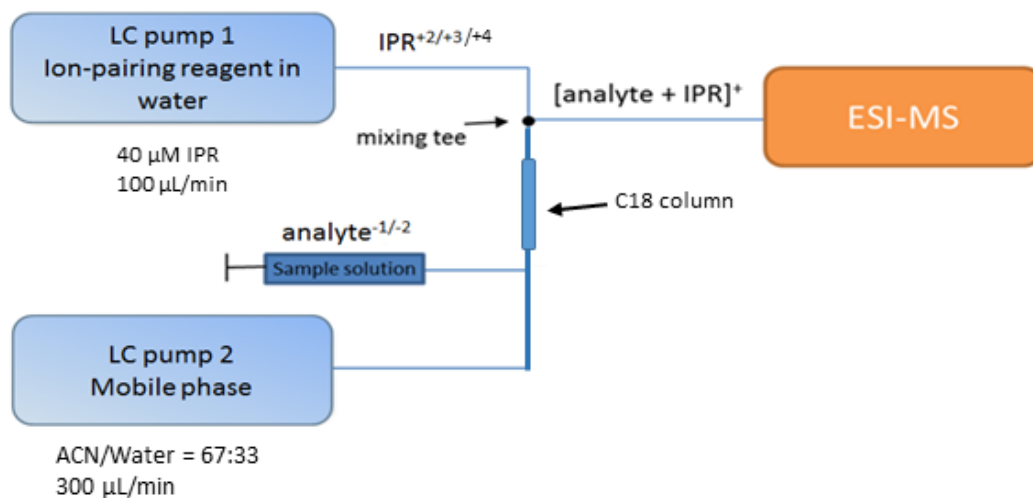
Figure 4-1 The instrument set up of HPLE-PIESI-MS.

4.2.3 Linear ion trap and triple-quadrupole mass spectrometer conditions

The HPLC-MS system used in the study is a Thermo Finnigan LXQ linear ion trap mass spectrometer with an off-axis (45°) Ion Max ESI source, (Thermo Fishier Scientific, San Jose, CA, USA). The MS parameters for the LXQ in the positive ion mode were set as follows: spray voltage (3 kV), capillary voltage (11 V), capillary temperature (350 °C), sheath gas flow (37 arbitrary units (AU)), and the auxiliary gas flow (6 AU). In the SRM mode, the normalized collision energy, the Q value, and the activation time were set at 30, 0.25, and 30 ms, respectively. A Shimadzu LCMS-8040 triple-quadrupole mass spectrometer (Shimadzu, Kyoto, Japan) equipped with an orthogonal ESI source

was compared. Operating conditions of the source were performed as follows: ionization voltage (3.5 kV), temperature of desolvation line (250 °C), temperature of heating block (400 °C), nebulizing gas (3 L/min; N2), and drying gas (15 L/min; N2), respectively. The voltages at Q1 prebias, collision energies, or Q3 prebias were optimized for each analyte individually.

The signal-to-noise (S/N) ratio was calculated with Xcalibur 2.0 software for the LXQ MS or a LabSolutions system for triple-quadrupole MS. The limit of detection (LOD) was determined at the concentration with a S/N ratio of 3 in five replicated injections for each sample. The PIESI-MS detection was performed in both the SIM mode and SRM mode. In the SIM mode, the m/z of the analyte/ion-pairing reagent complex ion was monitored, while in the SRM mode, the most abundant MS/MS fragment ion from the collision-induced dissociation (CID) was monitored. The injection volume was kept at 5 µL for all the experiments. The LODs obtained in the negative ion mode was used for comparison to the PIESI results. The MS parameters in this mode were optimized also. To have comparable LC conditions, a carrier flow consisting of acetonitrile and water (50:50, v/v) at 400 µL/min was introduced into the MS directly without using ion-pairing reagent.

4.2.4 Preparation and Separation of Calibration Standards

An internal standard method was used for calibration. The standard stock solution contained 1 µmol/mL of each amino acid and was further diluted to the desired concentrations: 1, 2, 5, 10, 20, 50, 100, and 200 nmol/mL. To each concentration, 400 µL of amino acid solutions was mixed with 100 µL of 50 nmol/mL norvaline as internal standard (IS). The resulted mixture was derivatized by using the following procedures: 50 µL of borate buffer and 20 µL of sample were added into an autosampler vial, and an aliquot of 5 µL of 0.1 M Fmoc-Cl was added and the mixture was incubated at room

temperature for 20 min. Then, 5 µL of 0.8 M 1-aminoadamantane (ADAM) solution was added to quench the reaction. A scheme of the Fmoc derivatization reaction and the structures of each amino acid studied are shown in Figure 4-2. The separation of Fmoc-AA standards was achieved using a gradient method with a C18 stationary phase (Ascentis® Express C18 2.7 µm SPP, 10 cm × 2.1 mm I.D.). Mobile phase A was acetonitrile, and mobile phase B was 0.1% formic acid in H_2O, respectively. The flow rate was 0.25 mL/min; the gradient was 30–60% A, 0–19.5 min; 60–95% A, 19.5–20.0 min; and 95% A, 20.0–21.0 min; and the mobile phase went back to 30% A for re-equilibrium of the column for another 10 min. MS data acquisition started with a time delay of 2.5 min.
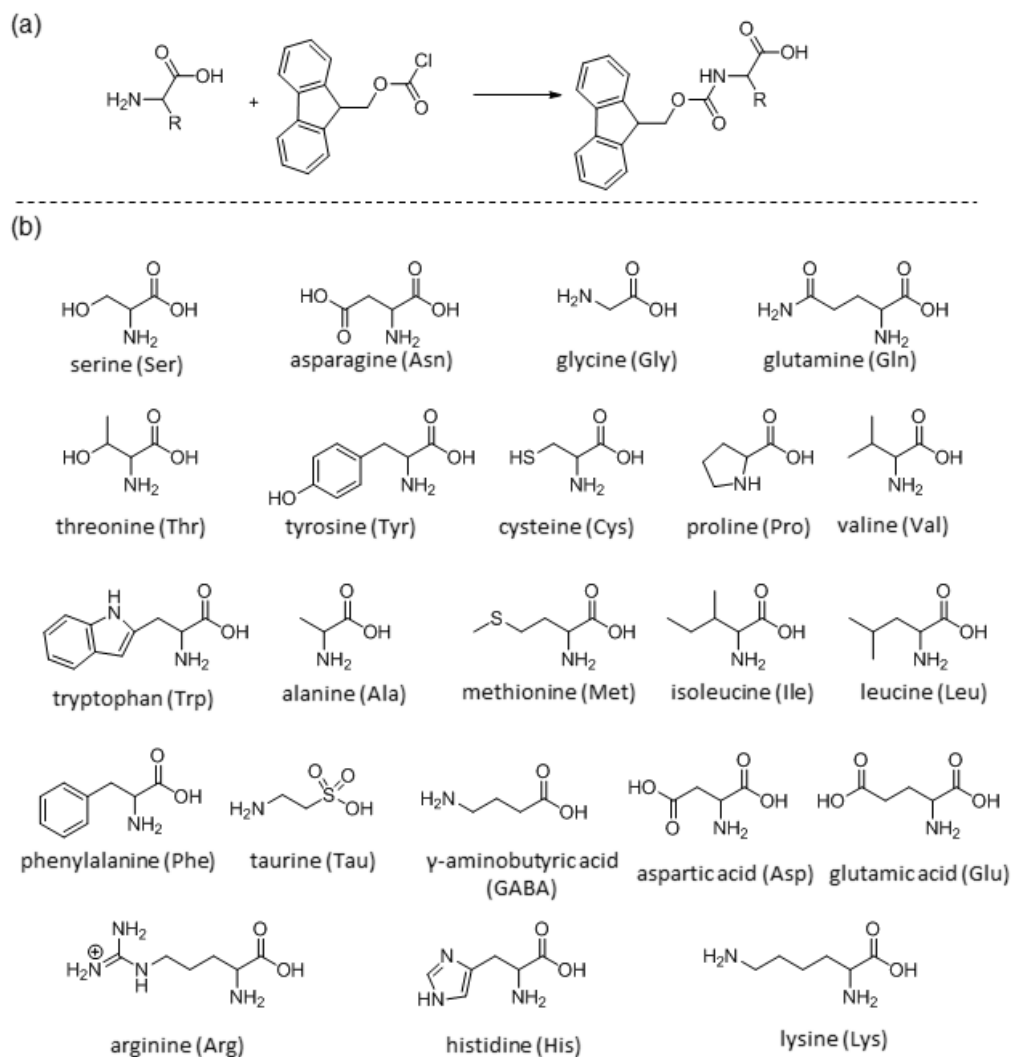
Figure 4-2 (a) Fmoc-derivatization reaction. (b) Structure of all the amino acids studied in this paper.

4.2.5 Urine sample preparation and analysis

Urine samples were obtained from healthy volunteers. For the recovery studies, urine samples were 2 or 10 times diluted with 0.5% formic acid in water. Three aliquots of urine sample were prepared at each dilution factor. One of the samples was non-spiked

and used for the analysis of the amino acid content in the urine. The other two samples were spiked with amino acid standards with a final concentration of 2 and 25 nmol/mL. An aliquot of 400 µL of urine sample was mixed with 100 µL of IS (three per experimental condition). The mixture was then centrifuged at 13,000 rpm at 4 °C for 15 min to precipitate any protein. The supernatant was collected and filtrated through a filter and stored at − 80 °C until analysis. The resulting samples were processed according to the derivatization protocol described in section "Preparation and separation of calibration standards." The use of solvent and derivatization reagent dilutes the sample fourfold, so the final dilution factors for the urine are 8 and 40 times. The quantification of the urine sample was accomplished in the PIESI-SIM mode using an internal standard calibration ($R2 > 0.99$, see section "Preparation and separation of calibration standards").

4.3 Results and Discussion

4.3.1 Mechanism for the Improved Performance of Ion-pairing Reagents for Fmoc Amino Acids

Fmoc-AAs were screened in both the positive and negative ion modes for an initial study. In the positive ion mode, sodium adducts rather than the protonated molecules were detected as the base peaks for the amino acids except for His, Arg, and Lys (an example MS spectrum of Fmoc-Ile is shown in Figure 4-3a). When the sodium adducts were fragmented as precursor ions at MS/MS, insufficient fragmentations were observed. In the negative ion mode, other than the base peak $[M-H]^-$, a significant deprotonated dimer $[2M-H]^-$ was observed, as shown in Figure 4-3b. As a consequence, in both the positive and negative ion modes, the formation of adducts significantly decreases the intensity of $[Fmoc-AA+H]^+$ or $[Fmoc-AA-H]^-$. ESI conditions could be optimized in order to minimize the formation of the sodium adducts or dimers, but they

57

could not be eliminated. Although these non-covalent adducts can provide information for qualitative analysis, the poor reproducibility of the adducts makes the sensitive and accurate quantitation of low-abundance amino acids highly restricted [127,128]. It has been reported previously that the ion-pairing reagents used in PIESI shown superior competition versus protons and other small metal cations for anionic sites [129]. So, as expected, when the IPR was infused post column, stable positive charged complexes were formed between the IPR and deprotonated Fmoc-AA anions (pKa $\approx$ 2), as shown in Figure 4-3c. It should be pointed out that the Fmoc-His, Fmoc-Arg, and Fmoc-Lys were detected as [M+H]+ even with the presence of the IPRs, which means there was little association between the basic amino acids and IPR. In this way, all the Fmoc amino acids can be detected simultaneously at the more sensitive positive ion mode. When the Fmoc-Ile complex ion [C5(bpyr)$_2^{2+}$ + Fmoc-Ile$^-$]$^+$ was fragmented subsequently, structurally specific product ions were produced (see Figure 4-3d). The mass spectra for each amino acid are shown in Fig. S3 (see ESM). In summary, the utilization of PIESI for Fmoc amino acids overcomes the shortage of common MS approaches in regard to their ionization and fragmentation.

Figure 4-4 shows an example of the S/N improvement when the C$_5$(bpyr)$_2$ is used as the IPR for the detection of 100 ng/mL of Fmoc-Ile. In the negative SIM mode, no peak was detectable. In the positive SIM mode, only sodium adducts were detected and the S/N was less than 3. In the PIESI-SIM mode, a significant response with S/N 67 was detected, and the detection at the PIESI-SRM mode further enhanced the detection sensitivity (Figure 4-4).
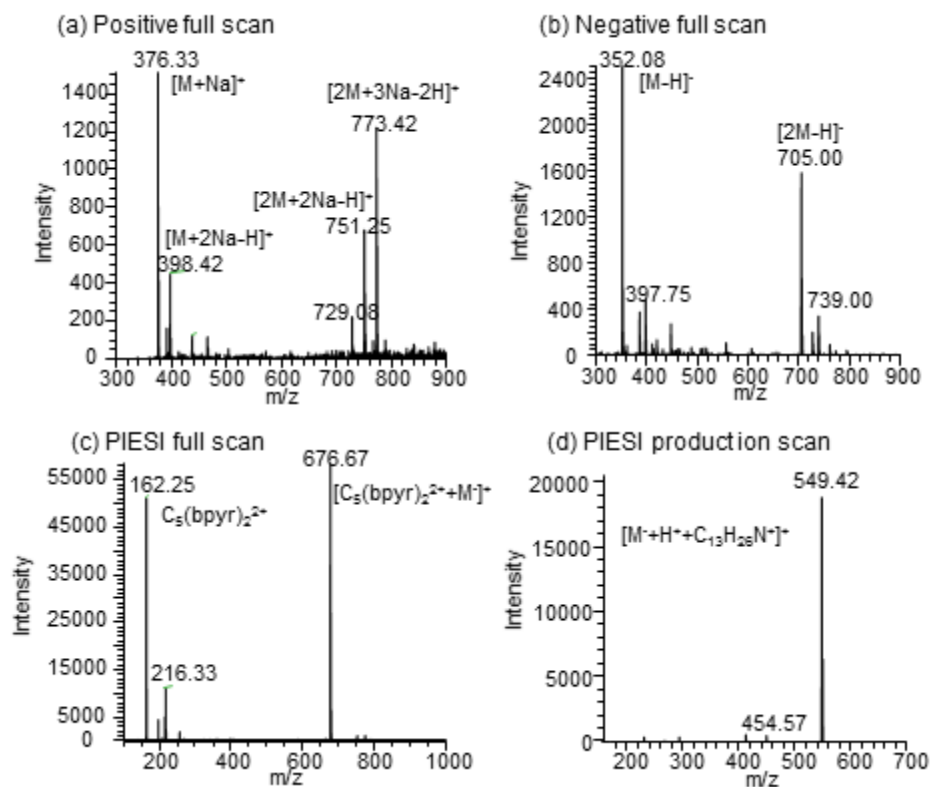
Figure 4-3 Representative full-scan MS spectra of Fmoc-Ile with and without ion-pairing reagent (IPR). (a) Positive full scan without IPR. (b) Negative full scan without IPR. (c) PIESI full scan. (d) PIESI product ion scan when using the m/z 676.7 as precursor. Molecular weight of Fmoc-Ile = 353. The IPR used in this experiment is 40 μM $C_5(bpyr)_2$.
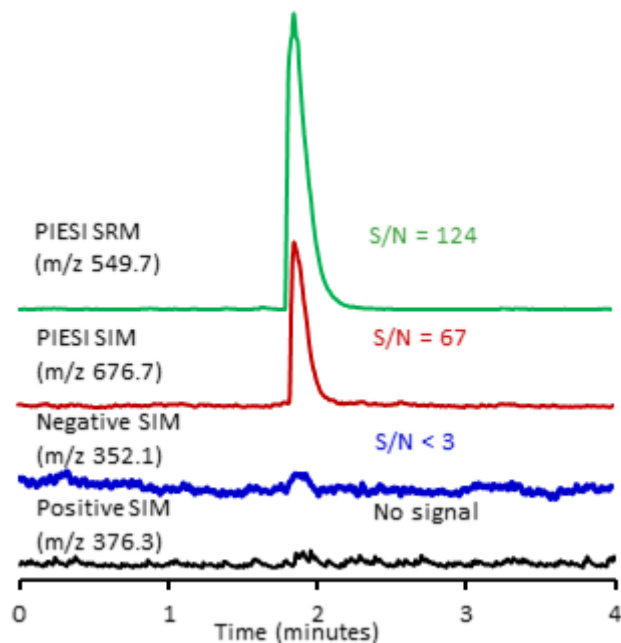
Figure 4-4 Chromatographic profile of signal-to-noise ratio at positive SIM mode, negative

SIM mode, PIESI-SIM mode, and PIESI-SRM mode. Sample injected: 100 ng/mL of

Fmoc-Ile. The dicationic ion-pairing reagent used in the PIESI analysis is 40 μM

$C_5(bpyr)_2$.

4.3.2 Selection of the ion-pairing reagent

The overall structure and the nature of the charged moieties of the IPR reagents

play essential roles in the selectivity and sensitivity of the PIESI method. In previous

studies, the dicationic IPRs provided the best performance for singly charged anions

[122,130]. The tricationic IPRs were shown to have the capability to improve the detection

sensitivity for divalent anions [116,120]. Tetracationic IPRs showed versatility and sensitivity

not only to trivalent anions but also to divalent ions and some zwitterions [117-119,131]. In this

work, three dicationic IPRs: $C_5(bpyr)_2$, $C_3(triprp)_2$, plus the unsymmetrical IPR (UDC); one

tricationic IPR (Tristriprp); and one tetracationic IPR (Tetpp4+) were chosen as potential

IPRs for Fmoc-AA analysis. The structures for all the tested ion-pairing reagents are shown in Table 1. UDC was specifically designed to have a long alkyl chain on one end, contract to its symmetrical analogue. This surface-active IPR provided superior performance to its symmetrical IPR for small inorganic and organic ions owing to enhanced ionization efficiencies [126].

The ESI S/N improvement factor for each individual Fmoc-AA was calculated using the value of the negative SIM mode over the PIESI-SIM/SRM mode. Positive SIM mode was not included in this comparison since the quantitation based on sodium adduct was shown to be much less reproducible and sensitive. To test the sensitivity enhancement for different PIESI reagents, three Fmoc-AAs were evaluated as the test analytes: Fmoc-Leu, Fmoc-Phe, and Fmoc-Glu, because they are aliphatic, aromatic, and acidic amino acids, respectively. No basic amino acid was tested in this study since they did not form a complex as with similarly charged IPRs as verified by the screening results (see section "4.3.1"). As shown in Figure 4-5, the S/N improvement is more substantial for the Fmoc-Leu and Fmoc-Phe than the Fmoc-Glu with the dicationic IPRs. This could be explained by the fact that the Fmoc-Leu and Fmoc-Phe contain one free carboxyl group while the Fmoc-Glu contains two, so the majority of Fmoc-Glu + $C_5(bpyr)_2$ complexes are uncharged. The tetracationic IPR (Tetpp4+) was superior to the other IPRs for Fmoc-Glu. In contrast, it showed less enhancement than $C_5(bpyr)_2$ for Fmoc-Leu and Fmoc-Phe because they can form + 3 and + 2 complexes. The UDC did not show better performance than the $C_5(bpyr)_2$, which may be due to the fact that Fmoc amino acids already have some surface activity. As a result, the $C_5(bpyr)_2$ and Tetpp4+ performed best for monovalent anionic Fmoc-AA and divalent anionic Fmoc-AA, respectively, so these two IPRs were used for all subsequent studies.
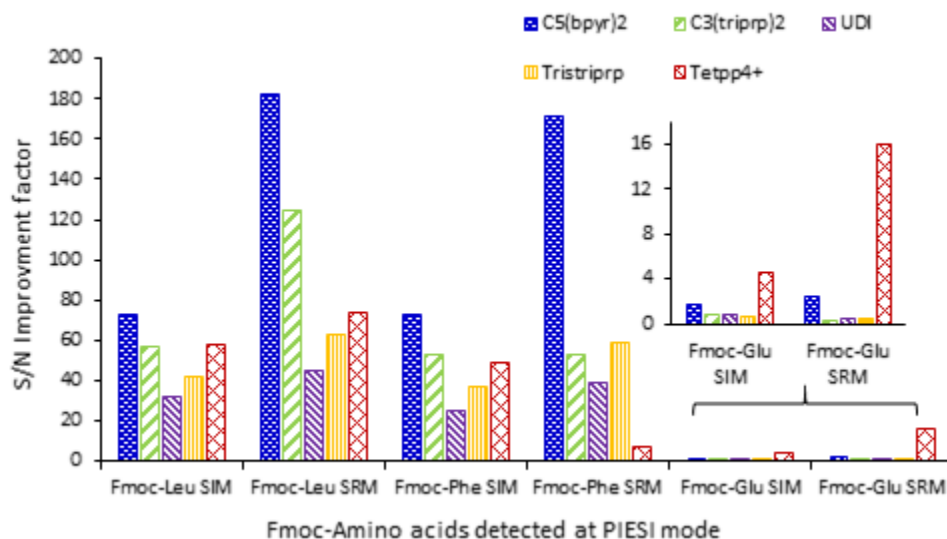
Figure 4-5 The ESI signal-to-noise (S/N) improvement factor for each amino acid is calculated as the S/N value at the PIESI mode over the negative SIM mode. Concentration of sample = 1 μg/mL. Concentration of IPR = 40 μM; except for UDI with 4 μM. Obtained with the linear ion trap MS analyzer. Refer to Table 1 for the structure of each ion-pairing reagent.

4.3.3 Limit of Detection of Fmoc Amino Acids

Table 2 shows the comparison of the absolute limits of detection for a total of 22 Fmoc amino acids obtained in PIESI modes and the negative ion mode on a linear ion trap mass spectrometer (see "Experimental"). All 22 Fmoc amino acids were detected with LODs from the nanogram to picogram levels in the PIESI mode, which were 10–500 times lower than the LODs obtained in the negative mode. Fmoc-Gly had the lowest LOD value among all the amino acids. This may due to the smaller size and hydrophilicity of glycine. The SRM of negative mode cannot be conducted because no fragmented signal was detected. The LODs in the SRM mode were evaluated by using the IPR/Fmoc-AA

complex ion as the precursor ion and the most abundant fragment as the daughter ion

(Table 2). The SRM mode shows improved sensitivity over the SIM mode due to the

reduction of background noise.

Table 4-2 Limit of detection values of Fmoc-AAs at negative mode and PIESI SIM/SRM

mode obtained with linear ion trap mass analyzer.

	Negative SIM		PIESI SIM		PIESI SRM	
Sample	LOD (pg)	m/z	LOD (pg)	m/z	LOD (pg)	m/z
Ser	250	326	30	650	6.5	523
Asn	450	353	50	677	8.2	550
Gly	800	296	7.5	620	0.8	493
Gln	500	367	50	691	10.0	564
Thr	300	340	25	664	15.0	537
Tyr	500	402	100	726	20.0	599
Cys	700	683	25	1007	7.5	880
Pro	1200	336	15	660	5.0	533
Val	200	338	15	662	2.5	535
Trp	1000	425	20	749	5.0	622
Ala	800	311	12.5	635	5.0	508
Met	250	370	17.5	694	15.0	567
Ile	750	352	12.5	676	2.5	549
Leu	750	352	12.5	676	2.5	549
Phe	400	386	12.5	710	2.5	583
Tau	1200	346	12.5	670	1.0	543
GABA	1000	324	20	648	4.5	521
Asp	125	354	25	473[a]	12.5	354[a]
Glu	100	367	25	715[a]	5.0	604[a]
Arg[b]			5	397[c]	1.0	336
His[b]			12.5	378[c]	2.0	156
Lys[b]			15	600[c]	2.0	556

a LOD was obtained with the tetracationic ion pairing reagent: 40 μM Tetpp4+.

b Basic amino acids were not detected at negative mode.

c Detected at [M+H]+

63

4.3.4 Comparison of the performance of PIESI on linear ion trap versus triple-quadrupole mass spectrometer

Linear ion trap MS (LIT-MS) and triple-quadrupole MS (qQq-MS) are the most prevalent tandem mass spectrometer technologies. The fragmentation process (collision-induced dissociation) of analytes can vary considerably between these instruments [132], and the design of the ionization interface and sample introduction system can result in different detection sensitivities. In this study, we have compared the detection limits of these two mass spectrometers for Fmoc-AAs in the PIESI mode (see "Experimental"). Table 3 presents the LOD values of each Fmoc amino acid with qQq-MS in negative SIM, PIESI-SIM, and PIESI-SRM mode. The PIESI-SRM and PIESI-SIM generally improve the detection limits 2–10 times compared to the negative mode in qQq-MS for most of the analytes. When comparing the LOD values obtained in the negative SIM mode, the qQq device provides at least an order of magnitude better LODs (Table 3) compared to the ion trap (Table 2). This might be due to the improved design of the Shimadzu LC-MS 8040 instrument, which suffers less from corona discharge and background noise in the negative mode. Although the LOD values are instrumentally dependent in the PIESI-SIM/SRM mode, LIT and qQq instruments achieved LODs in the same magnitude which indicates that PIESI-MS is a powerful method in improving the detection sensitivity on both instruments, especially for the cost-effective system LIT-MS.

Table 4-3 Limit of detection values of Fmoc-AAs at negative mode and PIESI SIM/SRM

mode obtained with triple quadrupole MS analyzer

Sample	Negative SIM		PIESI SIM		PIESI SRM	
	LOD (pg)	m/z	LOD (pg)	m/z	LOD (pg)	m/z
Ser	15	326	40	650	10	523
Asn	30	353	50	677	2.5	550
Gly	80	296	30	620	7	493
Gln	25	367	50	691	5	564
Thr	30	340	5	664	25	537
Tyr	25	402	5	726	2.5	599
Cys	25	683	5	1007	2.5	880
Pro	50	336	5	660	1	533
Val	30	338	5	662	2.5	535
Trp	27	425	35	749	2.5	622
Ala	50	311	2.5	635	25	508
Met	50	370	5	694	2.5	567
Ile	25	352	10	676	2.5	549
Leu	25	352	12.5	676	2.5	549
Phe	50	386	10	710	30	583
Tau	75	346	22.5	670	5	543
GABA	50	324	25	648	2.5	521
Asp	40	354	5	473[a]	12	354[a]
Glu	25	367	20	715[a]	7.5	604[a]
Arg[b]			5	397[c]	1	336
His[b]			30	378[c]	7.5	156
Lys[b]			15	600[c]	2	556

[a] LOD was obtained with the tetracationic ion pairing reagent: 40 µM Tetpp4+.

[b] Basic amino acids were not detected at negative mode.

[c] Detected at [M+H]+

4.4 Application

The test of amino acid in urine is used for diagnosis and monitoring of renal function. For example, general elevated levels of amino acids in urine can indicate a disorder in the amino acid transport system resulting from cystinuria and proximal renal tubular dysfunction [133]. In this study, amino acid levels in urine were analyzed using the sensitive PIESI-MS method.

4.4.1 Chromatographic separation of amino acids

A gradient method was developed to simultaneously separate all the 22 Fmoc amino acids using a reversed phase C18 stationary phase. All the amino acids were separated within 22 min (Figure 4-6). The detection was performed in the PIESI mode with the use of $C_5(bpyr)_2$ as an IPR (including Fmoc-Asp and Fmoc-Glu) at full scan mode within the entire run. The total ion chromatogram (TIC) is shown in Figure 4-6, as is the extracted ion chromatogram (EIC) for each amino acid. The presence of each amino acid in urine samples was confirmed in the TIC and EIC according to the identical retention time and its mass spectrum profile as compared to the standard solutions (as shown in Figure 4-7).
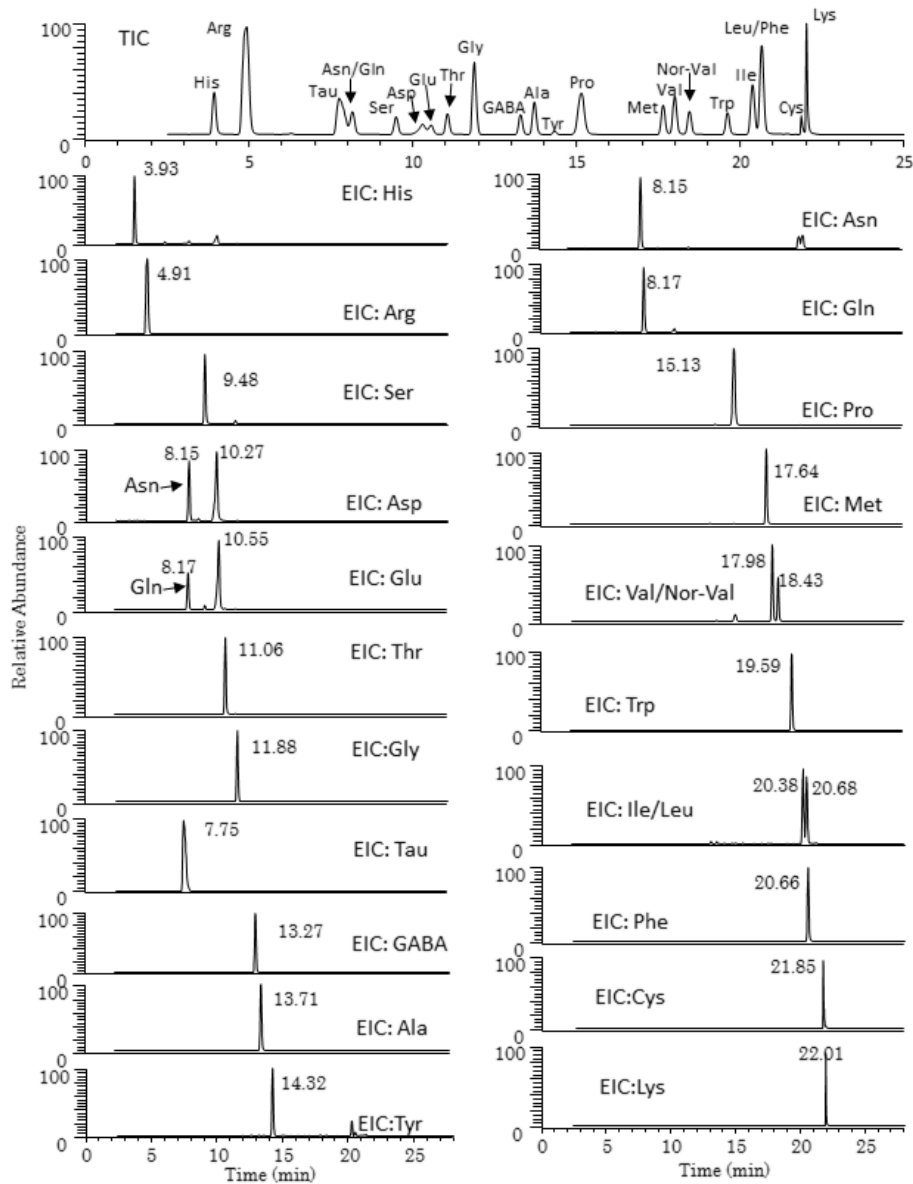
Figure 4-6 Total ion chromatogram (EIC) and extracted ion chromatogram (TIC) of the separation of 22 Fmoc-AAs with HPLC-PIESI-MS. Column: Ascentis® Express C18 2.7 µm SPP, 10 cm × 2.1 mm I.D. Mobile phase A is acetonitrile, and mobile phase B is 0.1% formic acid in H_2O, respectively. Gradient: 30–60% A, 0–19.5 min; 60–95% A, 19.5–20.0 min; 95% A, 20.0–21.0 min. Flow rate = 0.25 mL/min. MS start delay = 2.5 min
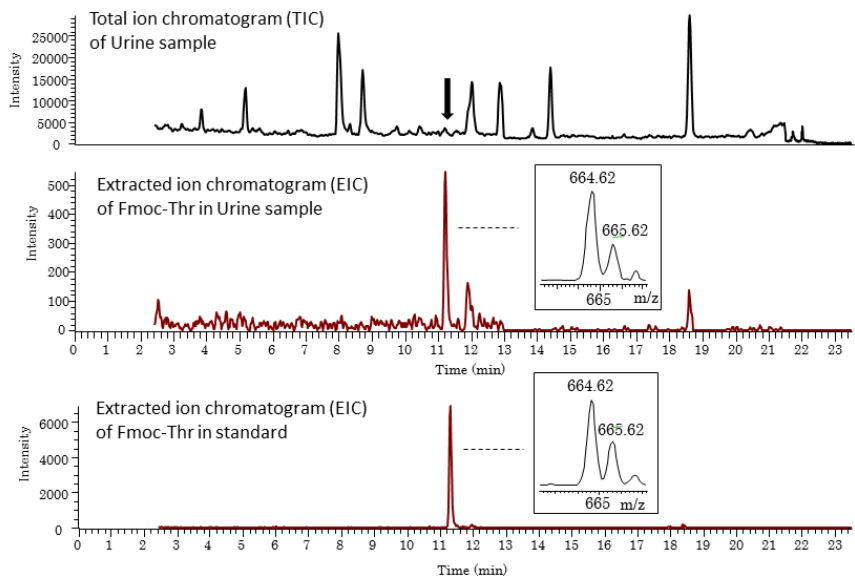
Figure 4-7 HPLC-PIESI-MS analysis of urine sample. The present of threonine in urine sample (top and middle) was confirmed according to the identical retention time and mass spectrum profile in the EIC of the standard solution (bottom).

4.4.2 Recovery Studies

Our previous study showed that a particular advantage of PIESI-MS over the negative mode is the ease with which it can reduce matrix effects with minimal dilution in different types of matrices, like groundwater and urine [129]. In this study, dilution factors of 2 and 10 for urine were tested to evaluate the influence of matrix effects. The results are given in Table 4-4 for the low (2 nmol/mL) and high (25 nmol/mL) spiked concentrations with each dilution factor. The best recovery value ranges from 75 to 116% and from 80 to 109% were obtained at low and high spiked concentrations with a dilution factor of 10. Nevertheless, the low accuracy of the sample with a dilution factor of 2 could be

attributed to significant matrix effects. Therefore, a dilution factor of 10 was selected to minimize the matrix effect for further quantitative analysis.

4.4.3 Determination of Free Amino Acids in Human Urine

The proposed method based on sample dilution and HPLC-PIESI-MS was used to analyze urine samples, and the concentration of each amino acid is shown in Figure 4-8. The results showed that the glycine is the most concentrated amino acid in the urine samples at about 1130 μmol/L. Other than that, the urine sample contains a higher level of Lys, Trp, Tyr, Tau, and Ala than the other amino acids (Figure 4-8a). Concerning the profile of the amino acids in the urine sample, most of the values are consistent with the reported concentrations in the literature [134]. The lower concentration of histidine and glutamic acid than the literature value may be due to the age and regional difference of the studied individuals.

Table 4-4 Recovery values at urine sample with different dilution factor. Values are expressed as percent (%) for each amino acid as a function of the dilution factor and the spiked concentration.

Spiked conc.	Dilution factor							
	2				10			
	Low (2 nmol/mL)		High (25 nmol/mL)		Low (2 nmol/mL)		High (25 nmol/mL)	
Sample [a]	recovery (%)	RSD [b] (%)	recovery (%)	RSD [b] (%)	recovery (%)	RSD [b] (%)	recovery (%)	RSD [b] (%)
Ser	51	6	73	5	83	5	88	5
Asn	83	4	88	5	85	5	92	4
Gly	77	6	86	2	83	4	94	3
Gln	82	7	85	7	80	4	87	2
Thr	77	9	83	2	90	4	92	4
Tyr	51	9	73	4	93	4	85	2
Cys	70	6	71	6	86	6	83	3
Pro	63	5	61	3	82	2	86	2
Val	54	5	71	3	88	3	99	1

Trp	52	8	69	5		113	6	90	4
Ala	77	7	72	4		94	6	91	2
Met	53	3	61	4		84	5	92	2
Ile	48	8	66	4		109	9	109	3
Leu	47	9	72	3		84	7	105	4
Phe	57	8	71	5		84	5	102	2
Tau	82	2	86	1		80	2	87	5
GABA	– [b]	–	–	–		–	–	–	–
Asp	61	4	66	3		–	–	–	–
Glu	55	5	68	5		–	–	–	–
Arg	62	8	65	6		84	3	82	4
His	55	3	64	4		75	4	80	2
Lys	79	4	79	5		116	4	92	4

[a] n=3 at each spiked leave

[b] Intra-day RSD value

[c] Not detectable
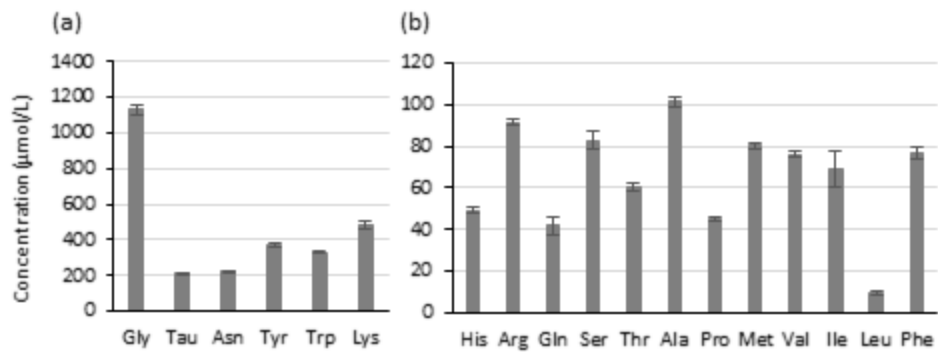
Figure 4-8 Analysis of amino acid concentrations in the urine sample with HPLC-PIESI-MS. Asp and Glu were not detected. (a) High-concentration amino acids. (b) Low-concentration amino acids

4.5 Conclusions

The proposed PIESI-MS method for detection of Fmoc-derivatized amino acids shows improved detection sensitivity compared to the direct MS positive and negative mode approaches. After testing with different PIESI reagents, it was found that the dicationic IPR produces the best sensitivity enhancements for the neutral amino acids while the tetracationic IPR works best with the two acidic amino acids (Asp and Glu). By applying the optimized ion-pairing reagent, the absolute LOD values in the low picogram levels were obtained with both linear ion trap and triple-quadrupole MS instruments. Simple urine sample preparation consisting of dilution was studied, and good results were obtained with a dilution factor of 10 for both low-level and high-level spiked concentrations. With this methodology, basic, natural, and acidic amino acid concentrations were determined simultaneously with a small volume of human urine. The technique should be applicable for the detection of other anionic metabolites in biological fluids, and further investigation of ultra-trace level of D-amino acid is in progress.

Chapter 5

Variations of L- and D-Amino Acid Levels in the Brain of Wild-Type and Mutant Mice

Lacking D-Amino Acid Oxidase Activity

Abstract

D-amino acids are now recognized to be widely present in organisms and play essential roles in biological processes. Some D-amino acids are metabolized by D-amino acid oxidase (DAO), while D-Asp and D-Glu are metabolized by D-aspartate oxidase (DDO). In this study, levels of 22 amino acids and the enantiomeric compositions of the 19 chiral proteogenic entities have been determined in the whole brain of wild-type ddY mice (ddY/DAO+/+), mutant mice lacking DAO activity (ddY/DAO-/-), and the heterozygous mice (ddY/DAO+/-) using high performance liquid chromatography-tandem mass spectrometry (HPLC-MS/MS). No significant differences were observed for L-amino acid levels among the three strains except for L-Trp which was markedly elevated in the DAO+/- and DAO-/- mice. The question arises as to whether this is an unknown effect of DAO inactivity. The three highest levels of L-amino acids were L-Glu, L-Asp, and L-Gln in all three strains. The lowest L-amino acid level was L-Cys in ddY/DAO+/- and ddY/DAO-/- mice, while L-Trp showed the lowest level in ddY/DAO+/+mice. The highest concentration of D-amino acid was found to be D-Ser, which also had the highest % D value (~ 30%). D-Glu had the lowest % D value (~ 0.1%) in all three strains. Significant differences of D-Leu, D-Ala, D-Ser, D-Arg, and D-Ile were observed in ddY/DAO+/- and ddY/DAO-/- mice compared to ddY/DAO+/+ mice. This work provides the most complete baseline analysis of L- and D-amino acids in the brains of ddY/DAO+/+, ddY/DAO+/-, and ddY/DAO-/- mice yet reported. It also provides the most effective and efficient analytical approach for measuring these analytes in biological samples. This study provides

fundamental information on the role of DAO in the brain and maybe relevant for future development involving novel drugs for DAO regulation.

5.1 Introduction

Amino acids are essential building blocks of proteins in all living organisms. All proteinogenic amino acids can exist in either L- or D-form, except glycine. Only a few decades ago scientists believed L-amino acids were solely relevant in higher organisms, while D-amino acids were thought to be inessential. However, by the mid-20th century, D-Ala was discovered in animal tissue, specifically milkweed bug blood [135]. Additionally, D-Ala and D-Glu were found in the bacterial peptidoglycan components of cell walls [136]. Subsequently, free D-amino acids were detected in plants, invertebrates, vertebrates, and mammals in significant amounts [105,137-140]. Moreover, peptides and proteins containing D-amino acids were discovered in various animal tissues [141,142], and D-pipecolic acid, a non-proteinogenic amino acid, was found in human urine and plasma [143].

Thus, questions arise about to the production, regulation, and function of D-amino acids in biological systems. Several free D-amino acids have been found to participate in neurological processes. D-Ser is a co-agonist of the N-methyl-D-aspartate (NMDA) receptor and activates the NMDA receptor together with glutamate [144,145]. Low D-Ser levels in serum and cerebrospinal fluid have been reported in schizophrenia patients [146]. Also, increased D-amino acid oxidase (DAO) activity has been found in the brain of schizophrenia patients [147]. DAO oxidizes D-Ser to its corresponding imino acid, and this could explain the decreased levels of D-Ser in schizophrenia patients. However, hypofunction of NMDA receptors due to decreased D-Ser levels and its consequence needs further study and evaluation [148]. In addition to D-Ser, D-Ala and D-Asp have been

73

reported to act as co-agonists of NMDA receptors [149,150]. NMDA receptor has been shown to be involved in learning and memory processes and decreased D-Asp levels in the brain were suggested to contribute to memory loss in patients with Alzheimer's disease [151,152]. D-Ser has been found to serve another function as a biomarker for patients with treatment-resistant depression (TRD) who were treated with ketamine. It was found that plasma D-Ser levels were significantly lower in TRD patients who responded to ketamine treatment in comparison to the patients who did not respond to ketamine treatment [153]. Also, it has been found that D-Leu, but not L-Leu, can serve as a unique treatment for terminating ongoing seizures in mice [154]. Additionally, mice lacking Tas1R2/R3, which is a D-amino acid receptor, have been found to be protected against seizures [155]. Recently, it was reported that in NIH Swiss mice the levels of all D-amino acids, except D-Glu, were orders of magnitude higher in the hippocampus and cortex than in blood [156]. The low levels of only D-Glu were in stark contrast to all other proteinogenic amino acids and indicated a specific or unique removal/control mechanism. This further suggests that they can have diverse effects: some essential and others deleterious.

Some endogenous D-amino acid levels in microorganisms, plants, and invertebrates are currently known to be controlled via DAO and D-amino acid racemases. D-amino acid racemases can convert L-amino acids to their corresponding D-amino acids [157]. To date, serine racemase and aspartate racemase have been found in mammalian tissues [158,159]. DAO, which was first discovered by Krebs in pig kidneys in 1935, is an important enzyme that regulates certain D-amino acid levels in mammals [160]. DAO is a flavoprotein and catalyzes the oxidation of neutral and basic D-amino acids to give α-keto acids and ammonia. Kinetic studies of DAO from yeast, pigs, and humans have determined D-amino acids' specificity for DAO [161,162]. As expected, increased levels of D-Ser, D-Pro, D-Ala, and D-Leu have been reported in ddY/DAO$^{-/-}$ mice, which is a

naturally-occurring mutant mouse strain [163,164]. The single point mutation (G541A) in the DAO gene resulted in a non-conservative change in the DAO enzyme, causing the inactivity of DAO in ddY/DAO$^{-/-}$ mice. [165].

Growing evidence indicates that D-amino acids are involved in various diseases. D-amino acid regulating enzymes, *e.g.,* racemases and DAO, could be promising targets for novel drug development. Consequently, a fundamental baseline study of all free proteinogenic L- and D-amino acids is needed to clarify the natural variation and levels of intrinsic L- and D-amino acids following the alteration of DAO activity. This study reports a comprehensive high performance liquid chromatography-tandem mass spectrometry (HPLC-MS/MS) analysis of all free proteinogenic L- and D-amino acids in the brain of wild-type ddY mice (ddY/DAO$^{+/+}$), mutant mice lacking DAO activity (ddY/DAO$^{-/-}$), and the heterozygous mice (ddY/DAO$^{+/-}$). Although they are not chiral, taurine and gamma-amino butyric acid (GABA) also were investigated due to their neurotransmitter activity in the central nervous system (CNS) [166-168].

5.2 Materials and Methods

5.2.1 Chemicals

Amino acid standards, perchloric acid, and ammonium formate were obtained from Sigma-Aldrich (St. Louis, MO). The AccQ·Tag Ultra derivatization kit (AccQ·Tag Ultra reagent powder, AccQ·Tag Ultra borate buffer, and AccQ·Tag Ultra reagent diluent) was purchased from Waters Corporation (Milford, MA, USA). HPLC-MS grade methanol and water were purchased from Sigma-Aldrich, and ultrapure water was obtained from a Milli-Q water system (Millipore, Bedford, MA, USA).

75

5.2.2 Animals

Male and female ddY mice (a gift from T. Seyfried, Boston College) were housed under a 14 hr light/10 hr dark cycle in a vivarium and were given food and water freely. Successive generations were bred and maintained. Mice lacking D-amino acid oxidase activity were identified by genotyping and were maintained by heterozygote-heterozygote crosses. Male ddY/DAO$^{+/+}$, ddY/DAO$^{+/-}$, and ddY/DAO$^{-/-}$ mice were sacrificed at 2-4 months of age by CO_2 exposure in a closed container in the vivarium, followed by decapitation. Detailed procedures for mouse brain dissection and perfusion were described in our previous study [156]. All procedures were approved by the Johns Hopkins Institutional Animal Care and Use Committee. Samples were all stored at -80 °C until analyzed.

5.2.3 Stock solutions and standards

Stock solutions were prepared by dissolving standard amino acids in ultra-pure water. The concentrations of D- and L-amino acid stock solutions were 2 mM and 1 M, respectively. D-norvaline was used as an internal standard (IS) with a concentration of 100 μM. The concentration of the calibration solutions ranged from 0.05 to 20 μM for D-amino acids and 5 to 1000 μM for L-amino acids. Each 1 mL of the calibration solution was mixed with 50 μL of IS. Low, medium and high concentration of quality control (QC) samples were prepared by spiking different amounts of standard solutions including the IS into the matrix (**Table S3 & S4,** see Electronic Supplemental Material).

5.2.4 Sample preparation and derivatization procedure

AccQ·Tag Ultra derivatization kit was used in all derivatization procedure. Following the protocol provided by the manufacturer, 10 μL of the amino acid solution was mixed with 70 μL of borate buffer and 20 μL of reconstituted AccQ·Tag Ultra reagent (6-aminoquinolyl-*N*-hydroxysysuccinimidyl carbamate (AQC), 3 mg/mL in acetonitrile).

The sample was vortexed followed by incubation for 10 min at 55 °C, and 3 µL of the reaction mixture was injected into the HPLC-MS/MS system for analysis. Enantiomers of AQC-amino acids are easily separated and can be detected in the positive mode of LC-MS [169].

Mouse whole brain tissues were homogenized in 1 mL of 0.3 M perchloric acid and 50 µL of IS on ice for 30 s (three 10 s pulses) with a Q-Sonica CL-18 probe (Newtown, CT, USA). The homogenates were incubated on ice for 15 min and centrifuged at 4 °C for 20 min at 13,000 rpm. The supernatant was collected, filtered, and derivatized following the procedure described above.

5.2.5 Instrumentation and Chromatographic Conditions

HPLC-MS/MS analysis was performed on a LCMS-8040 (Shimadzu Scientific Instruments, Columbia, MD, USA), triple quadrupole spectrometer with electrospray ionization (ESI). Two different chiral stationary phases with opposite enantioselectivity were used for all analyses. A quinine based chiral stationary phase was utilized for the separation and quantification of amino acids. It was prepared in-house utilizing quinine covalently bonded to superficially porous particles (SPP) and slurry packed into a 4.6 x 50 mm i.d. stainless steel column (IDEX Health and Science, Oak Harbor, WA) [170]. A gradient method was used for the chiral separation of amino acids on the quinine column. Mobile phase A was 100 mM ammonium formate and methanol (v:v 10:90; adjust to the apparent pH of 6), and mobile phase B was 50 mM ammonium formate and methanol (v:v 10:90; adjust to the apparent pH of 5). The following gradient was applied: 0 - 4 min, 0 to 100% B; 4 - 15 min, 100% B; 15 - 16 min, 100 – 0% B. The column was re-equilibrated for 9 min before another injection. A TeicoShell column (4.6 x 150 mm, AZYP, LLC) also was used to confirm the peak identity of the amino acids due to its opposite enantioselectivity compared to the quinine column. This chiral stationary phase

is based on macrocyclic glycopeptides [35,171,172]. Mobile phase A was 5 mM ammonium formate (pH 4), and mobile phase B was acetonitrile. A gradient method for TeicoShell column was applied as following: 0-2 min, 30% to 40% B; 2-15 min, 40% to 50% B; 15-16 min, 50% to 30% B; 16-30 min, 30% B. The flow rate was 0.65 mL/min for both columns, and a splitter was used before the MS. The flow rate directed to the MS was 0.325 mL/min. HPLC-MS/MS was operated in multiple reaction monitoring (MRM) mode using positive electrospray ionization source. The drying gas and nebulizing gas flow rate were 15 L/min and 2 L/min, respectively. The desolvation line and heat block temperatures were 275 °C and 400 °C, respectively. Collision energies and MRM transitions were optimized for each amino acid. Shimadzu LabSolution software was used for data acquisition.

The method was evaluated for linearity, sensitivity, precision, accuracy, and matrix effect according to US Food and Drug Administration (FDA) document for bioanalytical method validation [173]. Detailed method validation procedures and results are shown in the supplementary material (See Electronic Supplementary Material Table S1-S5). To evaluate the statistical significance of differences among the three strains, data was analyzed by one-way analysis of variance (ANOVA). The student's t-test was performed to compare the difference for ddY/DAO$^{+/-}$ *vs* ddY/DAO$^{+/+}$, and ddY/DAO$^{-/-}$ vs ddY/DAO$^{+/+}$. All statistical analyses were carried out using XLSTAT add-on package to Microsoft Excel. *P* values less than 0.05 were considered to have significant differences compared to the wild-type. Literature data for the only six amino acid levels reported in the same mouse strain were found to be comparable to those in this study and were included in **Tables 5-1 & 5-2** [163,174,175].

Table 5-1 L-Amino Acid Levels in Mice Whole Brain (ng/mg wet tissue)

	ddY/DAO$^{+/+}$			ddY/DAO$^{+/-}$			ddY/DAO$^{-/-}$		
	Range		Average	Range		Average	Range		Average
Asn	21.3 – 81.8		51.5	40.3 – 65.8		47.6	29.6 – 62.2		37.8
Asp[b]	410.7 – 1723.8		815.4	364.7 – 1871.6		749.2	345.0 – 1627.4		738.2
Glu	1315.8 – 2062.4		1689.1	1159.1 – 1633.9		1444.1	1267.2 – 1606.9		1411.2
Gln	442.0 – 734.5		588.2	501.5 – 694.8		595.3	492.7 – 657.1		579.3
Gly	52.6 – 73.8		63.2	60.6 – 79.9		68.3	60.9 – 76.0		69.5
Leu[b]	5.8 – 16.2		10.5	5.0 – 13.6		9.0	5.9 – 15.9		10.1
Ile	11.7 – 28.3		20.0	14.8 – 27.9		20.7	14.8 – 23.7		19.3
Met	4.0 – 18.1		11.1	11.5 – 18.3		15.0	11.4 – 20.9		15.4
Phe	41.9 – 91.4		66.6	59.4 – 100.6		75.9	54.6 – 94.0		74.3
Pro[b]	7.7 – 19.5		11.2	5.5 – 17.0		11.0	5.4 – 12.7		7.7
Thr	109.7 – 195.1		152.4	114.2 – 151.2		133.7	96.4 – 143.3		131.0
Trp[b]	1.0 – 5.1		3.8	18.0 – 24.6		21.0	19.7 – 25.5		22.4
Val	19.1 – 37.6		28.4	21.6 – 34.6		25.9	23.9 – 32.5		28.0
Tyr	10.4 – 19.8		15.1	13.8 – 17.8		15.4	11.0 – 19.2		14.9
Ser[b]	68.7 – 113.6		88.1	63.3 – 127.4		91.4	70.8 – 119.3		91.1
Ala[b]	54.8 – 278.9		113.5	59.8 – 183.1		107.9	88.5 – 169.5		108.2
Lys	111.2 – 180.9		146.0	103.3 – 161.0		129.4	97.3 – 119.4		110.4
His	11.1 – 28.2		19.6	16.4 – 21.1		19.0	13.7 – 30.9		19.8
Arg	108.0 – 222.6		165.3	121.5 – 199.5		148.5	128.6 – 169.5		149.2
Cys	4.8 – 7.2		5.9	5.2 – 7.1		6.1	5.4 – 7.7		6.4
Taurine	483.5 – 657.7		570.6	530.3 – 620.0		573.2	501.9 – 636.7		564.4
GABA	242.1 – 651.6		446.9	345.1 – 573.6		436.1	389.7 – 629.3		536.1

a. Values represent the range and average of amino acid content from five mice (ng/mg wet tissue)
b. Data from previous reports were included for this amino acid [163],[174], & [175]

Table 5-2 D-Amino Acid Levels in Mice Whole Brain[a] (ng/mg wet tissue)

	ddY/DAO^{+/+}				ddY/DAO^{+/-}				ddY/DAO^{-/-}			
	Range		Average	% D[c]	Range		Average	% D[c]	Range		Average	% D[c]
Asn	0.07 - 0.15		0.11	0.21	0.10 - 0.16		0.12	0.27	0.10 - 0.15		0.13	0.35
Asp[b]	2.56 - 17.50		6.32	0.77	1.35 - 18.90		6.25	0.82	2.75 - 17.59		6.58	0.88
Glu	0.08 - 0.11		0.10	0.01	0.07 - 0.14		0.09	0.01	0.09 - 0.16		0.11	0.01
Gln	0.62 - 0.77		0.70	0.12	0.52 - 0.62		0.59	0.10	0.59 - 0.65		0.62	0.11
Leu[b]	0.03 - 0.09		0.05	0.46	0.34 - 0.65		0.51	5.29	0.49 - 0.74		0.59	5.56
Ile	0.17 - 0.39		0.28	1.36	0.32 - 0.60		0.45	2.33	0.40 - 0.61		0.51	2.62
Met	0.14 - 0.24		0.19	1.67	0.18 - 0.25		0.21	1.43	0.20 - 0.26		0.23	1.54
Phe	0.17 - 0.26		0.22	0.32	0.20 - 0.31		0.24	0.32	0.20 - 0.23		0.22	0.30
Pro[b]	0.003 - 0.08		0.02	0.21	0.01 - 0.05		0.02	0.22	0.02 - 0.05		0.03	0.33
Thr	0.16 - 0.27		0.22	0.14	0.20 - 0.28		0.23	0.17	0.21 - 0.29		0.24	0.19
Trp[b]	0.25 - 0.34		0.29	7.20	0.26 - 0.35		0.31	1.48	0.29 - 0.31		0.30	1.33
Val	0.04 - 0.06		0.05	0.18	0.04 - 0.06		0.05	0.22	0.04 - 0.07		0.06	0.21
Tyr	0.02 - 0.03		0.03	0.18	0.02 - 0.04		0.03	0.17	0.02 - 0.02		0.02	0.16
Ser[b]	21.54 - 30.77		22.11	20.06	18.09 - 34.88		27.41	22.98	24.17 - 38.83		29.90	24.72
Ala[b]	0.41 - 1.77		0.81	0.71	3.05 - 7.30		5.07	4.54	4.21 - 8.01		5.40	4.76
Lys	0.13 - 0.32		0.22	0.15	0.21 - 0.30		0.26	0.20	0.21 - 0.36		0.27	0.25
His[d]	- - -		-	-	- - -		-	-	- - -		-	-
Arg	5.63 - 7.15		6.39	3.72	9.10 - 10.25		9.77	6.41	9.20 - 10.91		9.86	6.24
Cys	0.11 - 0.27		0.18	2.88	0.12 - 0.23		0.18	2.93	0.11 - 0.23		0.15	2.28

a. Values represent the range and average of amino acid content from five mice (ng/mg wet tissue)

b. Data from previous reports were included for this amino acid [163],[174], & [175]

c. % D = 100*D/(D+L)

d. Not detected, below LOD

5.3 Results and discussion

The concentration and enantiomeric composition of all free proteinogenic amino acids, as well as two achiral neurotransmitters, were investigated in mouse whole brain. HPLC-MS/MS MRM chromatograms of the separation of AQC amino acids are shown in **Figure 5-1** and **5-2**. Results are shown in **Tables 1** and **2** and summarized in **Figure 5-3** and **5-4**.
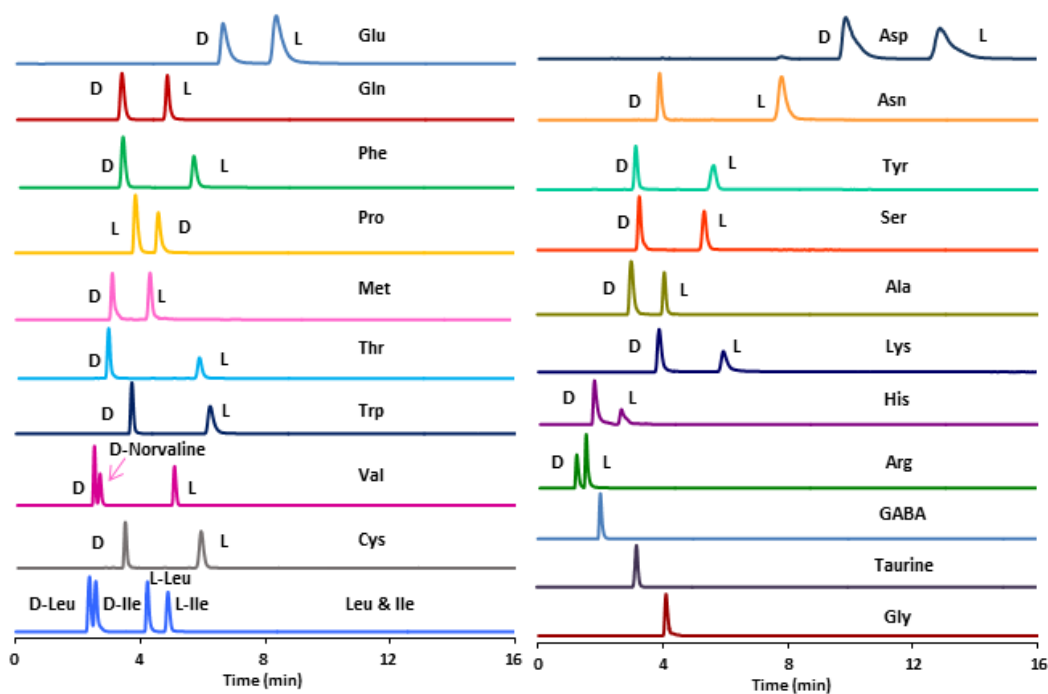
Figure 5-1 HPLC-MS/MS chromatogram of the separation of AQC-amino acid standards on the quinine SPP chiral stationary phase (see Materials and methods for exact conditions). Note the opposite enantioselectivity to that shown in Figure 5-2.
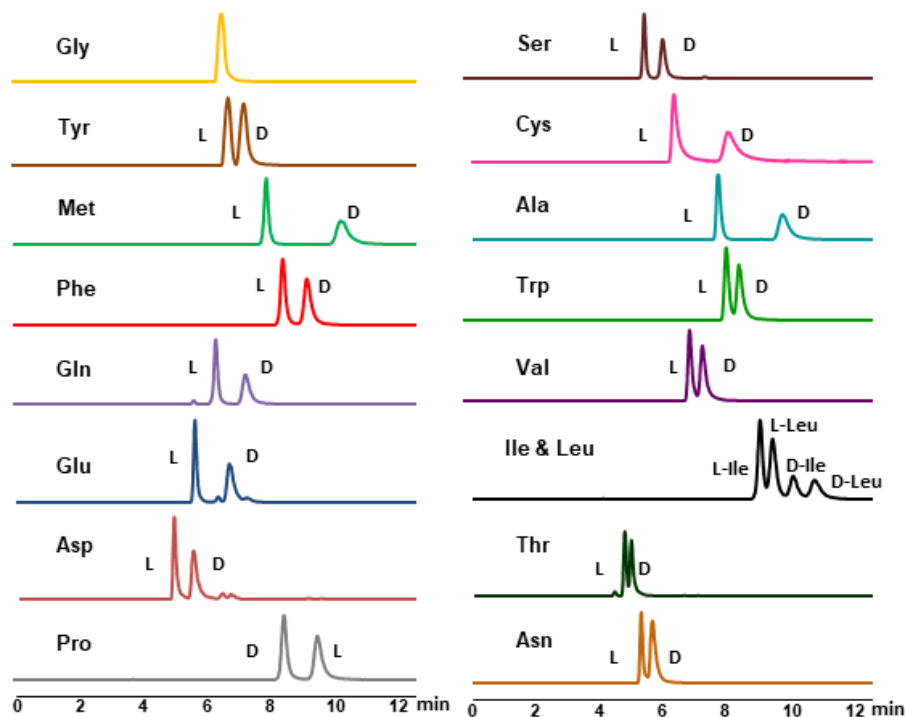
Figure 5-2 HPLC-MS/MS chromatogram of the separation of AQC-amino acid standards on TeicoShell chiral stationary phase (see Materials and methods for exact conditions). Note the opposite enantioselectivity to that shown in Figure 5-1.

5.3.1 L-Amino Acid Levels in Mouse Whole Brain

The L-amino acid with the highest concentration was L-Glu in all three strains of ddY mice, followed by L-Asp then L-Gln (**Figure 5-3**). These results are consistent with the literature, in which Glu, Gln, and Asp showed the highest L-amino acid levels in the cortex and hippocampus regions of NIH Swiss mice [156]. The group of L-amino acids with the highest levels (> 400 ng/mg) included L-Glu, L-Asp, L-Gln, taurine, and GABA, all of which play essential roles in the CNS. L-Glu and L-Asp function as excitatory neurotransmitters, while GABA and taurine function as inhibitory neurotransmitters in

mature mice [176-178]. Gln is a precursor of the neurotransmitter amino acids mentioned above [176]. Considering their important functions in neurotransmission, high levels of these amino acids in the brain are not unexpected. Among the ddY/DAO$^{+/-}$ and ddY/DAO$^{-/-}$ mice, L-Cys (~6.3 ng/mg), L-Pro (~9.3 ng/mg), and L-Leu (~9.6 ng/mg) had the three lowest L-amino acid levels. In the ddY/DAO$^{+/+}$ control group, L-Trp had the lowest level (3.8 ng/mg), followed by L-Cys (5.9 ng/mg) and L-Leu (10.5 ng/mg). No significant difference was observed in L-amino acid levels in ddY/DAO$^{+/+}$, ddY/DAO$^{+/-}$, and ddY/DAO$^{-/-}$ mice except for L-Trp (**Figure 5-3**).
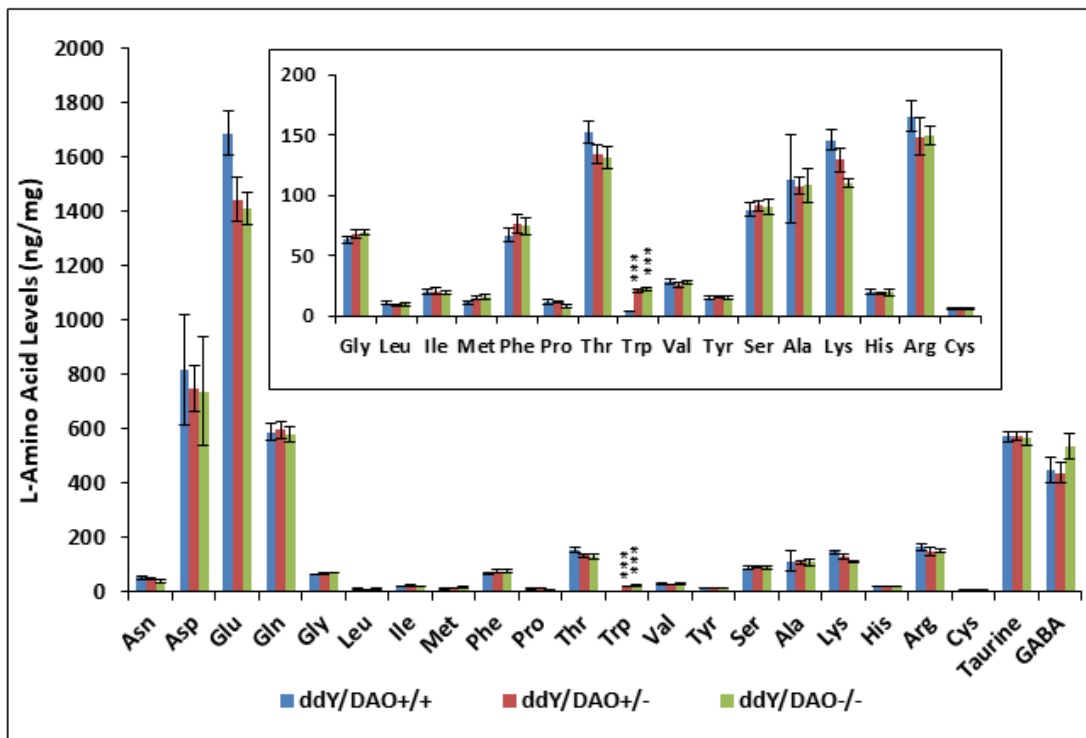
Figure 5-3 L-Amino acid levels in mice whole brain. Values represent mean ± SEM (ng/mg) from five mice. *** $P < 0.001$, significant increase from the values of ddY/DAO+/+ mice.

This study is the first report of elevated L-Trp levels in ddY/DAO$^{+/-}$ and ddY/DAO$^{-/-}$ mice compared to ddY/DAO$^{+/+}$ control group. Higher L-Trp levels in the mutant mouse brains may result from either inhibited L-Trp metabolism or enhanced L-Trp transport into the brain. The two major pathways for L-Trp are the kynurenine pathway and serotonin pathway [179]. Mutation of a gene can lead to changes in other systems, and, in this case, mutation of DAO gene may affect the activities of enzymes that convert L-Trp to kynurenine and serotonin, causing the accumulation of L-Trp in mutant mouse brains. Thus, kynurenine and serotonin levels should be investigated in the brain of ddY/DAO$^{+/-}$, ddY/DAO$^{-/-}$, and ddY/DAO$^{+/+}$ mice. It could be hypothesized that non-detectable or very low levels of kynurenine and serotonin in the mutant mice brain could indicate abnormal metabolism of L-Trp in DAO mutant mice. Another explanation for the higher L-Trp levels may be the elevated uptake of L-Trp from plasma in mutant mice. L-Trp is transported across the blood-brain barrier via the large neutral amino acid transporters [180]. However, the brain L-Trp level does not solely depend on plasma L-Trp level, but also the ratio of L-Trp to other plasma neutral amino acids sharing the same amino acid transporter [181]. Thus plasma L-Trp levels together with other neutral amino acids, *i.e.,* Tyr, Phe, Leu, Ile, and Val should be investigated in the ddY/DAO$^{+/-}$, ddY/DAO$^{-/-}$, and ddY/DAO$^{+/+}$ mice.

Higher L-Trp levels in the brains of mutant mice, if from the elevated uptake of L-Trp, may also lead to higher levels of serotonin. The rate-limiting enzyme on the serotonin pathway, tryptophan hydroxylase, is normally not saturated at brain Trp concentrations [182]. Therefore, serotonin synthesis is dependent on the availability/levels of its precursor, L-Trp, in the brain [180]. If this is true, it may explain the elevated anxiety observed in mice lacking DAO activity [183], since high levels of serotonin have been found to contribute to anxiety [184]. Investigation of kynurenine and serotonin levels in the blood and brain as well as the common amino acid levels in the blood of the wild-type and

mutant ddY mice would be an interesting study and may provide evidence to support these hypotheses. However, the underlying mechanisms through which inactivation of DAO influences other systems remains to be resolved.

5.3.2 D-amino acid levels in mouse whole brain

D-amino acids with high concentrations (> 6 ng/mg) are D-Ser, D-Asp, and D-Arg in all three strains (Figure 5-4). Given their essential roles in the CNS and the presence of racemases in mammals, it is not unexpected that high amounts of D-Ser (~ 26 ng/mg) and D-Asp (~ 6 ng/mg) are found in the brain of both wild-type and mutant mice. D-Arg in the CNS can serve as a stimulant or a depressant at different levels, as demonstrated in a previous study, although the exact mechanism remains unclear [185]. Concentrations of D-Tyr, D-Val, D-Pro, and D-Glu are among the lowest in all three strains (< 0.2 ng/mg). In a previous study, the concentration of D-Glu was below detection limits in the cortex and hippocampus of NIH Swiss mice [156]. In this study, D-Glu in ddY mice whole brain is determined using the sensitive HPLC-MS/MS method (See Materials and methods). It was detected, but only at very low levels (~ 0.1 ng/mg) despite the fact that L-Glu is, by far, the most prevalent amino acid in these brain samples. Further, the % D-Glu was 1 to 3 orders of magnitude lower than any other D-amino acid in this study for all three strains (~ 0.01%). Results from this study further support the hypothesis that D-Glu metabolism may be a unidirectional process and not a cycle, like the L-glutamate-glutamine cycle, considering the high abundance of D-Gln and trace amount of D-Glu [156].

Clear differences were observed for some specific D-amino acids levels in ddY/DAO^{+/-} and ddY/DAO^{-/-} mice compared to ddY/DAO^{+/+} mice, see **Figure 5-4**. D-Leu levels in the brain of ddY/DAO^{+/-} and ddY/DAO^{-/-} mice were twelve times higher than that in ddY/DAO^{+/+} mice ($P < 0.001$). D-Ala levels were increased approximately sevenfold in ddY/DAO^{+/-} and ddY/DAO^{-/-} mice ($P < 0.001$). Significant increases of D-Ser, D-Ile, and D-

Arg levels were also observed in the brain of ddY/DAO^{+/-} and ddY/DAO^{-/-} mice. Results are in accordance with the kinetic studies of DAO, in which DAO shows high substrate affinity and catalytic efficiency for the D-amino acids mentioned above [161]. DAO has been reported to be active for D-Pro as well [162], however, no significant differences of D-Pro levels were observed in the whole brain of the three mouse strains. These results can be explained by the previous report from Hamase *et al.* [163]. D-Pro levels increased significantly only in cerebellum and pituitary gland of mice lacking DAO activity, while the majority of the brain regions did not show much difference [163]. Due to the regional distribution of D-Pro in mouse brain, the increase of D-Pro levels in the whole brain of ddY/DAO^{+/-} and ddY/DAO^{-/-} mice are too low to be noticeable. Acidic D-amino acids, D-Asp and D-Glu, are oxidized by D-aspartate oxidase (DDO), but not DAO [186]. Therefore, given the absence of DAO, no difference in the levels of D-Asp and D-Glu among ddY/DAO^{+/+}, ddY/DAO^{+/-}, and ddY/DAO^{-/-} mice were found or expected. Results obtained from the present study are in good agreement with previously reported values for D-Leu, D-Pro, D-Ser, D-Ala, and D-Asp [163,164,174].
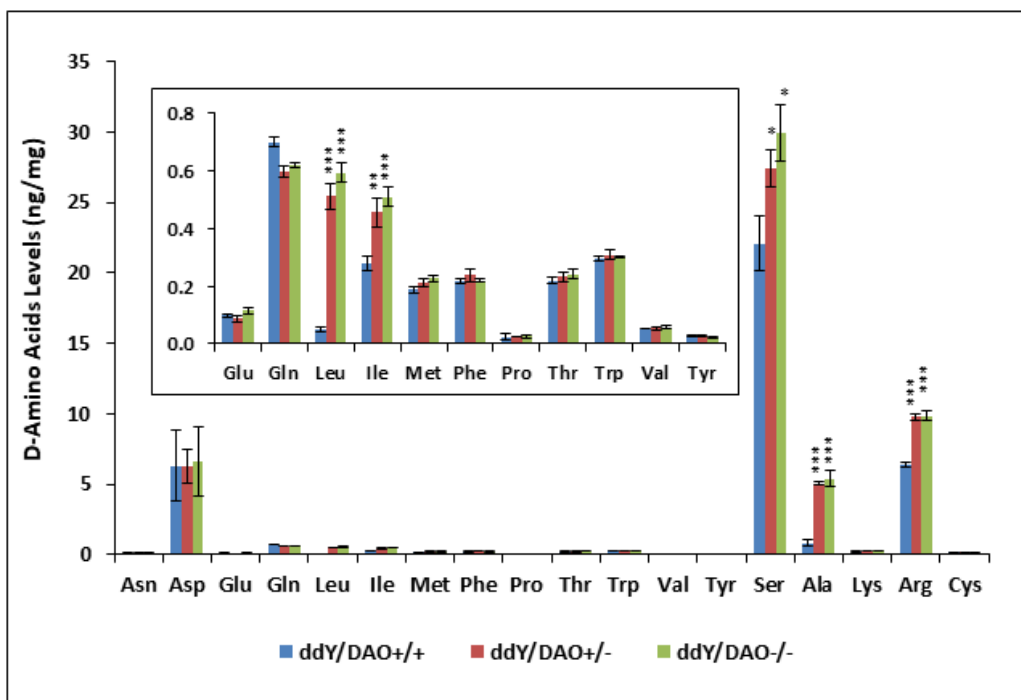
Figure 5-4 D-Amino acid levels in mice whole brain. Values represent mean ± SEM (ng/mg) from five mice. * $P < 0.05$, significant increase from the values of ddY/DAO^{+/+} mice; ** $P < 0.01$, significant increase from the values of ddY/DAO^{+/+} mice; *** $P < 0.001$, significant increase from the values of ddY/DAO^{+/+} mice

5.4 Conclusions

In the present investigation, a rapid and sensitive method was established for the simultaneous analysis of amino acid contents and their enantiomeric compositions in mouse brains. This study provides the most complete analysis of L- and D-amino acids in the whole brain of wild-type mice as well as mice lacking DAO activity. There is no difference observed for L-amino acid levels among wild-type and mutant mice except L-Trp. The elevated levels of L-Trp in DAO deficient mice have not been reported

previously and may be a secondary effect of DAO inactivation. DAO did appear to affect a few D-amino acid levels in the brain of mutant mice in this study, including D-Leu, D-Ala, D-Ser, D-Ile, and D-Arg, but not all the D-amino acids.

Altered D-amino acids levels have been reported in varying diseases, suggesting that D-amino acids may be potential biomarkers and have diagnostic values. Furthermore, regulation of D-amino acid levels via DAO may be a promising approach in the treatment of various diseases. As shown in this study, some D-amino acid levels were affected significantly by altering DAO activity. Inhibition of DAO activity though DAO inhibitors, *e.g.,* 3-methylpyrazole-5-carboxylic acid [187], or application of D-amino acids may improve the conditions caused by insufficient D-amino acids.

Chapter 6

Altered Profiles and Metabolism of L- and D-Amino Acids in Cultured Human Breast

Cancer Cells vs. Non-tumorigenic Human Breast Epithelial Cells

Abstract

Herein we describe for the first time the endogenous levels of free L- and D-amino acids in cultured human breast cancer cells (MCF-7) and non-tumorigenic human breast epithelial cells (MCF-10A). D-Asp and D-Ser, which are co-agonists of the N-methyl- D-aspartate (NMDA) receptors, showed significantly elevated levels in MCF-7 cancer cells compared to MCF-10A cells. This may result from upregulated enzymatic racemases. Possible roles of these D-amino acids in promoting breast cancer proliferation by regulating NMDA receptors were indicated. D-Asn may also be able to serve as exchange currency, like specific L-amino acids, for the required uptake of essential amino acids and other low abundance nonessential amino acids which were elevated nearly 60 fold in cancer cells. The relative levels of specific L- and D-amino acids can be used as malignancy indicators (MIs) for the breast cancer cell line in this study. High MIs (>50) result from the increased demands of specific essential amino acids. Very low MIs (<1) result from the increased demands of specific D-amino acids (i.e., D-Ser, D-Asp) or the cellular release of amino acid exchange currency (i.e., L- and D-Asn) used in the upregulated amino acid antiporters to promote cancer cell proliferation.

6.1 Introduction

Cancer is not a single disease, but a group of related diseases and the most fundamental feature of all cancers is uncontrolled proliferation [188]. More than 90 years ago, German physiologist Otto Warburg observed that cancer cells consumed large amounts of glucose compared to normal cells even in the presence of oxygen, which is now known as the Warburg effect [189]. Besides glucose, another principle nutrient supporting the optimal growth of cancer cells is L-glutamine, as first described by Eagle in the 1950s [190]. While many studies have focused on the metabolism of glucose and L-glutamine in cancer, amino acids besides glutamine also are utilized by cancer cells and may play essential roles in cancer cell proliferation. Recently it has been found that N-methyl-D-aspartate (NMDA) receptors that are widely present in the central nervous system (CNS) are not only expressed but functional in a variety of cancer cell lines and tumors, *e.g.*, lung cancer, breast cancer, and esophageal cancer, with functions in regulating cancer cell growth and division [191]. It is known that D-Ser, as well as D-Asp and D-Ala, act as co-agonists of NMDA receptors [145,149,150]. This means D-amino acids, which were once thought to be unnatural and superfluous in mammalian systems [105,139,156,192], may play important roles in the metabolism and proliferation of cancer cells. Also, it has been noted in a recent report that non-glutamine amino acids provide abundant nitrogen and carbon for biosynthesis to proliferating cells, while most glucose is converted into lactate and exported from cancer cells [193]. The metabolism and essential roles of many amino acids during cancer cell proliferation may be underestimated or have yet to be considered. Cancer patients are always in a hypermetabolic state, thus enhanced protein synthesis and degradation can result in the altered amino acid concentrations [194]. Indeed, it is well established that specific amino acid transporters are upregulated in cancer cells [195]. Free plasma amino acid profiles in patients with different types of cancer have been

found to differ significantly from those of healthy controls, and the altered amino acid profiles may have great potential for the early detection of cancer [196]. For example, patients with breast cancer, in both early and advanced stages, showed high levels of amino acids in their saliva compared to a healthy control group [194]. The accumulation of specific amino acids in cancer cells, particularly specific D-amino acids, could be potential oncometabolites, which are defined as the metabolites whose abundance increases markedly and are involved in the development of malignancy [197]

To date, almost all the cancer studies regarding amino acids focused only on L-amino acids. Questions about D-amino acids and cancer cells have not been asked or answered. One is whether there is cellular uptake or release of D-amino acids during cancer cell proliferation? Second, do D-amino acids exhibit altered profiles in cancer cells as do L-amino acids, and if so, why? This study is the first report of endogenous levels of free L- and D-amino acids in human breast cancer cells (MCF-7) and non-tumorigenic human breast epithelial cells (MCF-10A). Altered profiles and metabolism of free L- and D-amino acids were determined in cultured MCF-7 cells compared to MCF-10A cells. Also, effects of glucose concentration were studied for MCF-7 cell proliferation and their endogenous L- and D-amino acid levels. Further, a simple test using specific D- and L-amino acid relative levels has been derived and used to produce malignancy indicators (MIs) of cancer cells.

6.2 Materials and methods

6.2.1 Chemicals and reagents

Amino acid standards, perchloric acid, and ammonium formate were obtained from Sigma-Aldrich (St. Louis, MO,USA). The AccQ·Tag Ultra derivatization kit (AccQ·Tag Ultra reagent powder [6-aminoquinolyl-*N*-hydroxysuccinimide carbamate (AQC)], AccQ·Tag Ultra borate buffer, and AccQ·Tag Ultra reagent diluent) was

purchased from Waters Corporation (Milford, MA, USA). All the cell medium and
additives were purchased from Sigma-Aldrich. HPLC-MS grade methanol and water were
purchased from Sigma-Aldrich, and ultrapure water was obtained from a Milli-Q water
system (Millipore, Bedford, MA, USA).

6.2.2 Cell Lines and Culture Conditions

Human breast cancer cell line (MCF-7) and non-tumorigenic human breast
epithelial cells (MCF-10A) were purchased from American Type Culture Collection
(ATCC). MCF-7 cells were grown and maintained in normal, or high glucose Dulbecco's
Modified Eagle Medium (DMEM) supplemented with 10% fetal bovine serum (FBS), 1%
L-glutamine, and 1% penicillin-streptomycin. MCF-10 cells were grown and maintained in
Mammary Epithelial Cell Growth Medium (MEGM) that was supplemented with 10% FBS,
100 ng/mL cholera toxin and MEGM kit. All the cells were incubated at 37 °C in a
humidified atmosphere of 5% CO_2.

6.2.3 Cell Counting

Cells were seeded into 150 x 25 mm cell culture dish grown until 80 to 90%
confluency and then split into 9 of 100 x 20 mm cell culture dishes. Triplicate plates were
seeded for each experimental condition. Cells were trypsinized and centrifuged at 1000 g
for 5 min. The cell pellet was washed twice with phosphate buffer saline (PBS). Cells
were counted at the specified time points, *i.e.,* 24 hours, 48 hours, and 72 hours, by
conducting the Trypan blue assay using a hemacytometer (Sigma-Aldrich, St. Louis,
MO).

6.2.4 Intracellular and Extracellular Amino Acids Extraction and Analysis

Amino acids were extracted from the cells or cell media with 0.3 M perchloric
acid and 100 µM norvaline (internal standard) on ice for 30 s (three 10 s pulses) with a Q-
Sonica CL-18 probe (Newtown, CT, USA). After vigorous vortexing, the samples were

centrifuged at 4 °C for 20 min at 13,000 rpm. The supernatant was collected, filtered, and derivatized as previously detailed [198]. In brief, 10 μL of the extract solution was mixed with 70 μL of borate buffer and 20 μL of AQC reagent. The sample was vortexed followed by incubation at 55 °C for 10 min.

High performance liquid chromatography-tandem mass spectrometry (HPLC-MS/MS) analysis was performed on a LCMS-8040 (Shimadzu Scientific Instruments, Columbia, MD, USA), triple quadrupole spectrometer with electrospray ionization (ESI). Two different chiral stationary phases with opposite enantioselectivity were used for all analyses. A Q-Shell column (4.6 x 50 mm), quinine based chiral stationary phase, was prepared in-house and utilized for the separation and quantification of amino acids . A gradient method was used for the chiral separation of amino acids on the Q-Shell column. Mobile phase A was ammonium formate (100 mM)-methanol (10:90, v/v) (pH* 6), and mobile phase B was ammonium formate (50 mM)-methanol (10:90, v/v) (pH* 5). The following gradient was applied: 0 - 4 min, 0 to 100% B; 4 - 15 min, 100% B; 15 - 16 min, 100 - 0% B; 16 - 25 min 100 B%. The second chiral stationary phase was TeicoShell column (4.6 x 150 mm, AZYP, LLC, USA), which was based on macrocyclic glycopeptides. TeicoShell column was used to confirm amino acids peak identity due to its opposite enantioselectivity. For a complex matrix, there is still a chance that an impurity with the same m/z and a similar structure is co-eluting with the analyte of interest on one column. Having a second column with different selectivity can separate the impurity that is co-eluting with the analyte on the first column. Indeed this was the case with these samples where L-Hyp overlapped with L-Ile on the Q-Shell column initially but was resolved on the TeicoShell column. Mobile phase A was ammonium formate (5 mM, pH 4), and mobile phase B was acetonitrile. A gradient method for TeicoShell column was applied as following: 0-2 min, 30% to 40% B; 2-15 min, 40% to 50% B; 15-16 min,

50% to 30% B; 16-30 min, 30% B. The flow rate was 0.65 mL/min for both columns, and a splitter was used before the MS. HPLC-MS/MS was operated in multiple reaction monitoring (MRM) mode using positive ESI source. Collision energies and MRM transitions were optimized for each amino acid. Shimadzu LabSolutions software was used for data acquisition.

Representative chromatograms of the AQC-amino acids in cultured cells are shown in Figure 6-1. Internal standard calibration curve was constructed for each amino acid. The method was evaluated for linearity, sensitivity, precision, accuracy, and matrix effect according to US Food and Drug Administration document for bioanalytical method validation. Detailed procedures for method optimization and validation were described previously [198], and results were shown in. The method developed here is a rapid and sensitive separation method that can complete the analysis of 39 amino acids including L- and D-enantiomers within 15 min with LODs in the sub-pg level. Also, D-enantiomers elute before their corresponding L-enantiomers on Q-Shell column, which is favorable for the quantification of D-amino acids in biological samples due to the lack of interference from the corresponding L-amino acids.
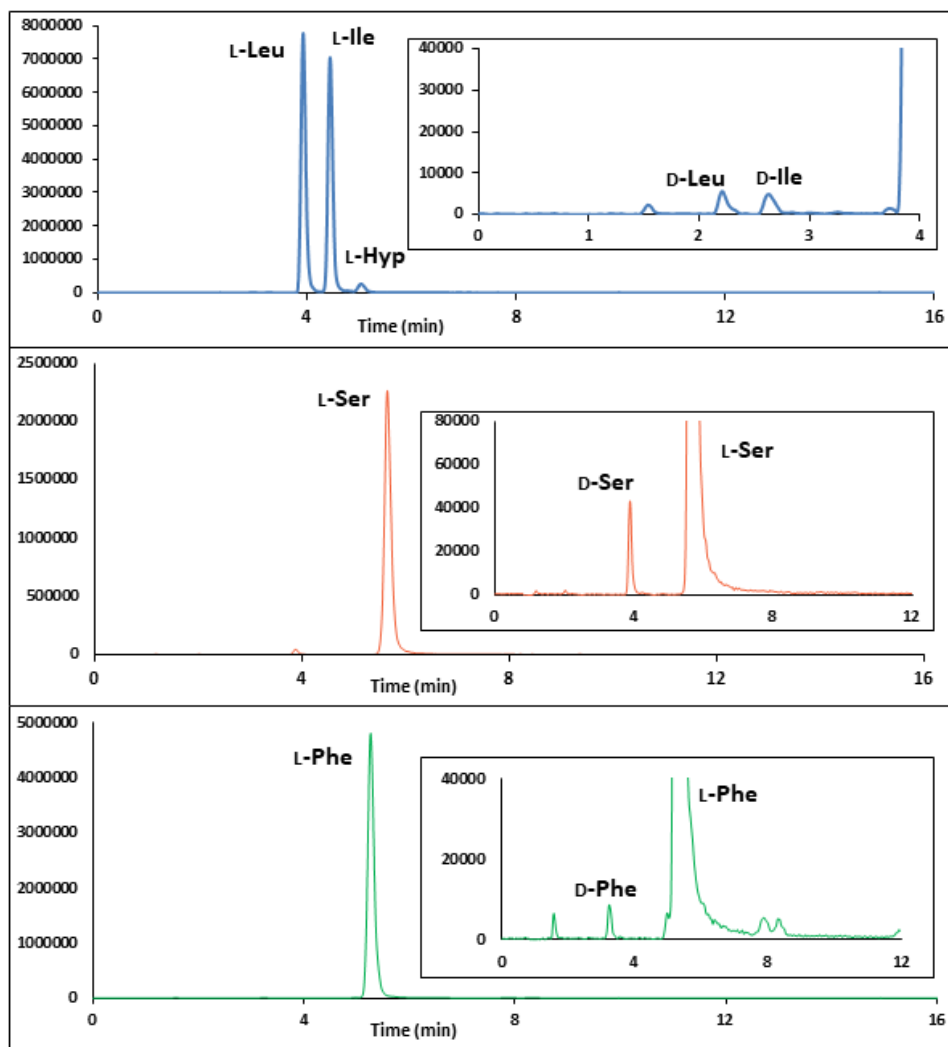
Figure 6-1 Representative chromatograms of AQC derivatized amino acids in MCF-7 cancer cells after 48-hour growth in high glucose medium

The starting amino acid levels of uncultured media (prior to any cell growth) were determined after serum supplementation. To determine changes in extracellular amino acid levels over time, uncultured medium was included in the analysis. Data were plotted as percent change from the uncultured medium, which was calculated by the following equation:

$$\frac{Amino\ acid\ level\ in\ the\ cultured\ medium - amino\ acid\ level\ in\ the\ uncultured\ medium}{Amino\ acid\ level\ in\ the\ uncultured\ medium} x\ 100\%$$

Malignancy indicators (MIs) in were calculated by the following equations:

a. L-amino acids = $\frac{Intracellular\ L-amino\ acid\ levels\ in\ MCF-7\ cells}{Intracellular\ L-amino\ acid\ levels\ in\ MCF-10A\ cells}$

b. D-amino acids = $\frac{Intracellular\ D-amino\ acid\ levels\ in\ MCF-7\ cells}{Intracellular\ D-amino\ acid\ levels\ in\ MCF-10A\ cells}$

c. MIs = $\frac{L-amino\ acids}{D-amino\ acids}$

Each experimental condition was performed in triplicate. Average and standard deviations for intracellular and extracellular amino acid levels were calculated from parallel triplicate experiments.

6.3 Results and Discussion

6.3.1 Free L-Amino Acid Profiles in MCF-7 and MCF-10A Cells

6.3.1.1 Intracellular and extracellular free L-amino acid levels

Intracellular free L-amino acid levels were determined for MCF-7 and MCF-10A cells after 24-hours, 48-hours, and 72-hours incubation, results are shown in Figure 6-2. The general trends in MCF-7 cells from both high and low glucose media were that L-Gln, Gly, L-Glu, and L-Thr had the highest levels after 72-hour growth, ranging from 418 to 866 nmol/10^6 cells. L-Hyp, L-Cys, and GABA had the lowest levels, ranging from 2.3 to 12.5 nmol/10^6 cells. However, different trends of intracellular L-amino acid levels were observed for the non-tumorigenic MCF-10A cells. L-Glu, L-Asp, and L-Asn showed the highest levels in MCF-10A cells after 72-hour growth, ranging from 37 to 73 nmol/10^6 cells. L-Met, GABA, and L-Lys showed the lowest levels which ranged from 1.2 to 4.0 nmol/10^6 cells. L-Asn had the third highest level in MCF-10A cells (~65 nmol/10^6 cells), but it was one of the lowest levels of amino acids in MCF-7 cells (~23 nmol/10^6 cells). Compared to MCF-10A cells, MCF-7 cells with the same incubation time had up to 56

96

fold higher levels of free L-amino acids except for L-Asn. For example, L-Met levels were around 67 nmol/10^6 cells in MCF-7 cells and 1.2 nmol/10^6 cells in MCF-10A cells after a 72-hour growth period (**Fig 6-2C**).

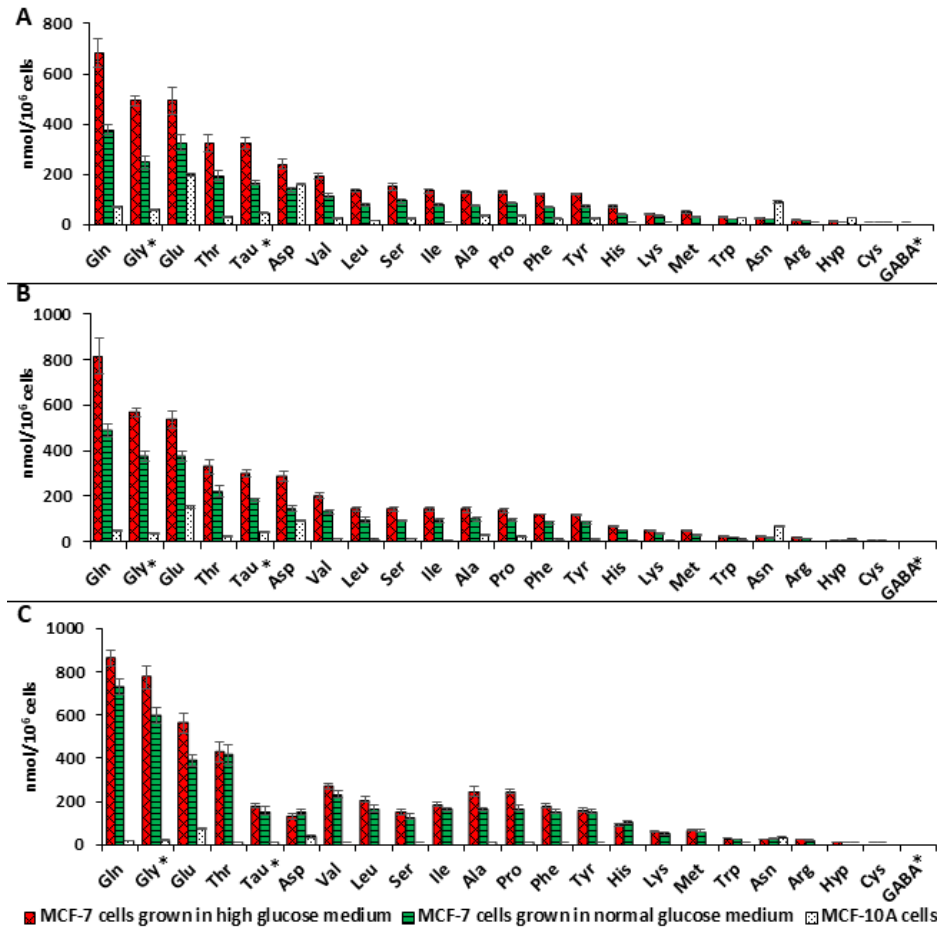Figure 6-2 Intracellular L-Amino Acid Profiles. L-Amino acid levels in MCF-7 and MCF-10 cells after (A) 24-hours, (B) 48-hours, and (C) 72-hours growth in the associated medium. Red bars represent MCF-7 cells grown in high glucose medium, green bars represent MCF-7 cells grown in normal glucose medium, and white bars represent MCF-10A cells grown in the MEGM. * indicates non-chiral amino acids.

Extracellular L-amino acid profiles were expressed as percent changes of the amino acid from the uncultured medium (calculated by the equation shown in Materials and methods) and are shown in Figure 6-3. Extracellular profiles of L-amino acids were divided into two categories: essential and nonessential amino acids, due to the general trends observed in each category. The percent change of the nine essential amino acids from uncultured media showed negative values for both MCF-7 and MCF-10A cells, indicating the uptake of these amino acids from the growth media (Figure 6-3A). Regarding nonessential amino acids, as shown in Figure 6-3B, cellular uptake (net removal from the growth media) of L-Ser, L-Gln, L-Arg, L-Tyr, and L-Cys was observed for MCF-7 and MCF-10A cells. Cellular release of L-Ala, L-Pro, and L-Glu was observed in both cells lines. Cellular uptake of L-Asp and Gly were observed for MCF-7 cells, but cellular release of L-Asp and Gly was shown for MCF-10A cells. On the other hand, the release of L-Asn was detected for MCF-7 cells, but the uptake of L-Asn was detected for MCF-10A cells.
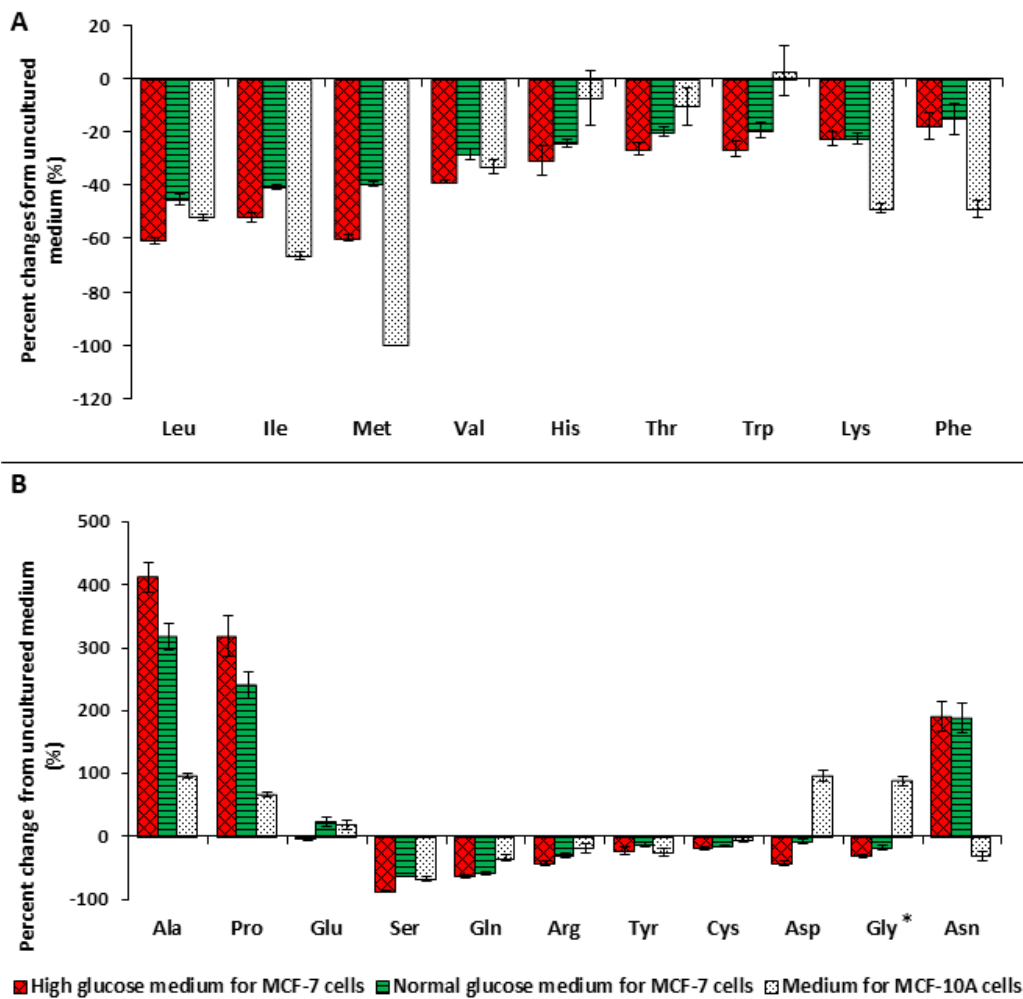
Figure 6-3 Extracellular L-amino acid profiles. Changes of (A) essential amino acid, (B)

non-essential amino acid levels in the media with MCF-7 cells (red: high glucose

medium; green: normal glucose medium) and MCF-10A cells (white: MEGM). Values are

shown as percent change of L-amino acid in the medium after 72-hours incubation from

the uncultured medium, with negative bars indicating cellular consumption and positive

bars indicating production. * indicates non-chiral amino acids.

6.3.1.2 Altered L-amino acid profiles and metabolism for MCF-7 breast cancer cells

Cancer cells require higher amounts of amino acids and glucose to fulfill the metabolic demands associated with proliferation [188]. Significant increases of Pro, Thr, Glu, Phe, Trp, Met, Asp, Ser, Gln, Leu, His, Val, and Lys have been reported in the saliva from breast cancer patients compared to healthy controls [194]. In our study, L-amino acid concentrations were found to be up to 56 times higher in MCF-7 breast cancer cells compared to non-tumorigenic MCF-10A cells in both high and normal glucose media (Figure 6-2). Intracellular high levels of L-amino acids could be one of the reasons that elevated levels of L-amino acids are observed in the saliva and plasma of breast cancer patients.

Cellular uptake of all essential amino acids was anticipated, as essential amino acids cannot be synthesized in mammalian cells and must be acquired from the growth media (Figure 6-3). On the other hand, the net flux of nonessential amino acids was unknown. Although they can be produced in mammalian cells from glycolysis, glutaminolysis, or the TCA cycle, extracellular nonessential amino acids can be readily utilized by the cells to reduce the biosynthetic burden on the cells [199]. In this study, cellular uptake of Gly and L-Asp, two nonessential amino acids, was detected for MCF-7 cells. In contrast, release of Gly and L-Asp were observed for MCF-10A cells, suggesting metabolic differences between MCF-7 and MCF-10A cells. Gly can be synthesized from L-Ser, and both are involved in one-carbon metabolism providing methyl groups for the biosynthesis of nucleotides and cofactors [200]. Although the uptake of L-Ser was seen in both MCF-7 and MCF-10A cell lines, recent evidence suggested that cancer cells were more reliant upon the uptake of extracellular Ser. It has been reported that depletion of exogenous L-Ser reduced cancer cell proliferation by affecting nucleotide synthesis [201]. Additionally, cancer cells have shown upregulated activity of the enzymes involved in L-

Ser and Gly synthesis [202]. Downregulation of argininosuccinate synthase 1 (ASS1), using L-Asp as a substrate, has been reported in cancer cells [203]. Decreased ASS1 activity leads to the elevated L-Asp levels in cancer cells, allowing L-Asp to be used for nucleotide biosynthesis and to support cancerous proliferation [203]. Nonessential amino acids, specifically Gly, L-Ser, and L-Asp could be promising targets in cancer therapy, as they become necessary for cancer cell proliferation [204].

6.3.2 Free D-Amino Acid Profiles in MCF-7 and MCF-10A Cells

6.3.2.1 Intracellular and extracellular free D-amino acid levels

Intracellular free D-amino acid profiles were determined in both MCF-7 and MCF-10A cells (Figure 6-4). D-Asp, D-Ser, and D-Glu had the highest levels in both cell lines, although they were 2 to 22 fold higher in MCF-7 breast cancer cells. Unlike the trend of L-amino acid levels observed between the two cell lines, MCF-7 did not always exhibit higher levels of D-amino acids compared with MCF-10A cells. Some D-amino acid levels were higher in MCF-7 cells, *i.e.,* D-Asp, D-Ser, D-Asn, D-Ala, D-Thr, and D-Tyr. Others showed higher levels in MCF-10A cells, *i.e.,* D-Val, D-Leu, D-Pro, D-Lys, and D-Trp, while a few had similar levels in both cell lines (Figure 6-4). It is noteworthy that D-Pro, D-Lys, and D-Trp were found only in MCF-10A cells and only after 72-hour growth. MCF-10A cells showed higher percentages of D-enantiomers for almost all the amino acids, except D-Asp and D-Asn (Figure 6-5).
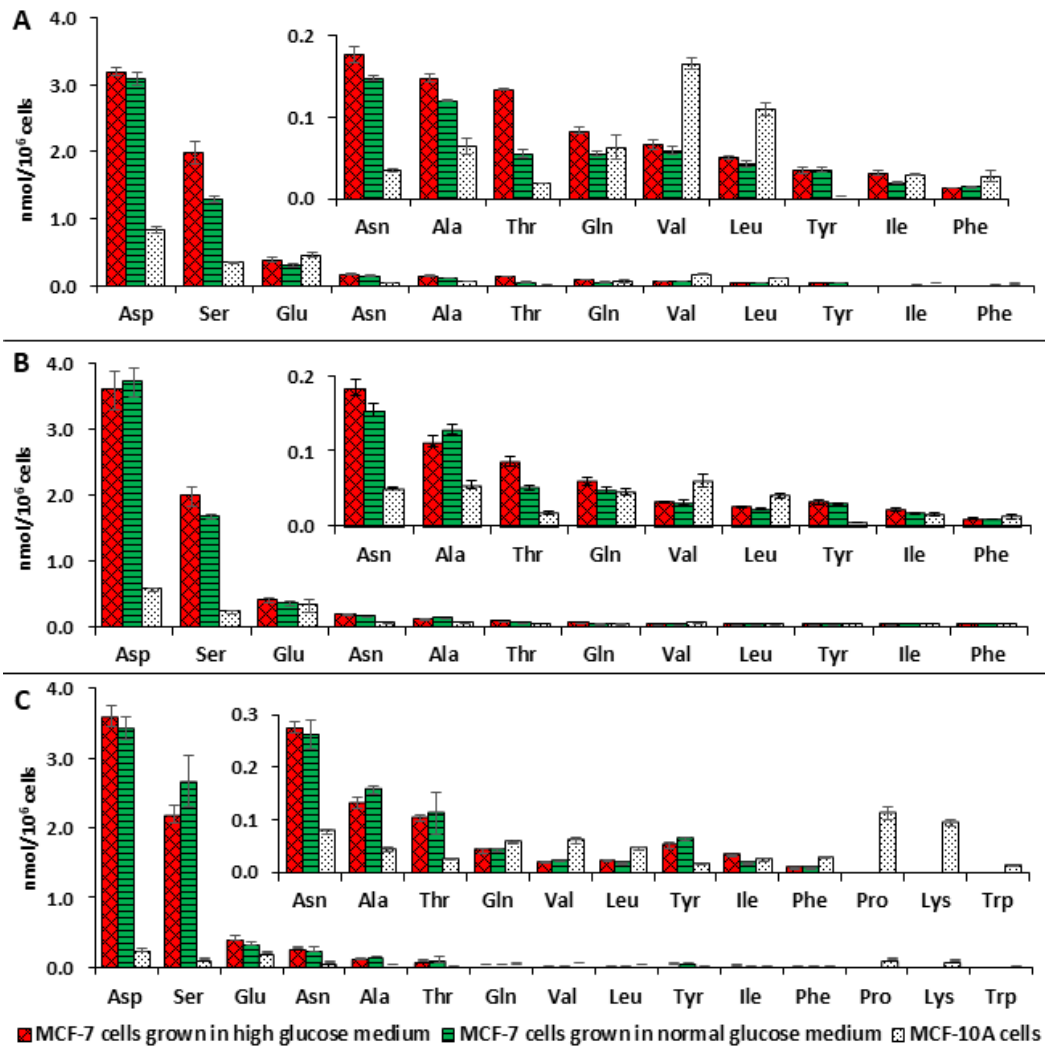
Figure 6-4 Intracellular D-amino acid profiles. D-Amino acid levels in MCF-7 and MCF-10 cells after (A) 24-hours, (B) 48-hours, and (C) 72-hours growth in the associated medium. Red bars represent MCF-7 cells grown in high glucose medium, green bars represent MCF-7 cells grown in normal glucose medium, and white bars represent MCF-10A cells grown in the MEGM.

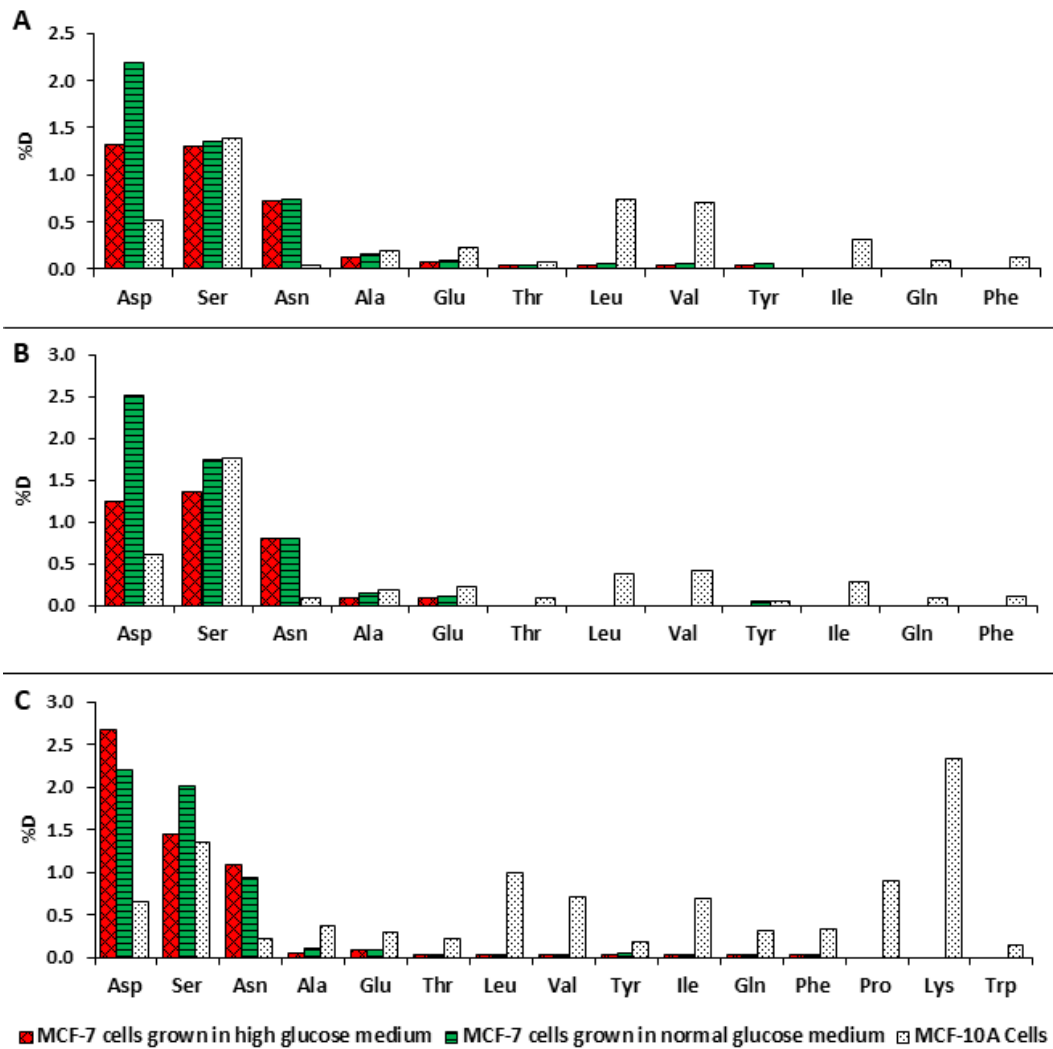Figure 6-5 Intracellular percent D-amino acid levels. Intracellular % D-Amino acids in MCF-7 and MCF-10 cells after (A) 24-hours, (B) 48-hours, and (C) 72-hours growth in their associated medium. Red bars represent MCF-7 cells grown in high glucose medium, green bars represent MCF-7 cells grown in normal glucose medium, and white bars represent MCF-10A cells grown in the MEGM.

Extracellular (*i.e.*, growth media) free D-amino acid profiles were determined for
MCF-7 and MCF-10A cells as shown in Figure 6-6. Cellular uptake of all D-amino acids
was found in MCF-10A cells except for D-Ser and D-Lys. Concerning MCF-7 breast
cancer cells, cellular uptake was observed for D-Leu, D-Asp, D-Gln, D-Ala, D-Tyr, and D-
Val, while cellular release was observed for D-Asn, D-Arg, D-Thr, and D-Ser. Surprisingly,
MCF-7 cells exhibited net uptake of D-Ile, D-Glu, D-Phe, and D-Lys when grown at high
glucose condition, but these amino acids were released from the MCF-7 cells at the
normal glucose condition.

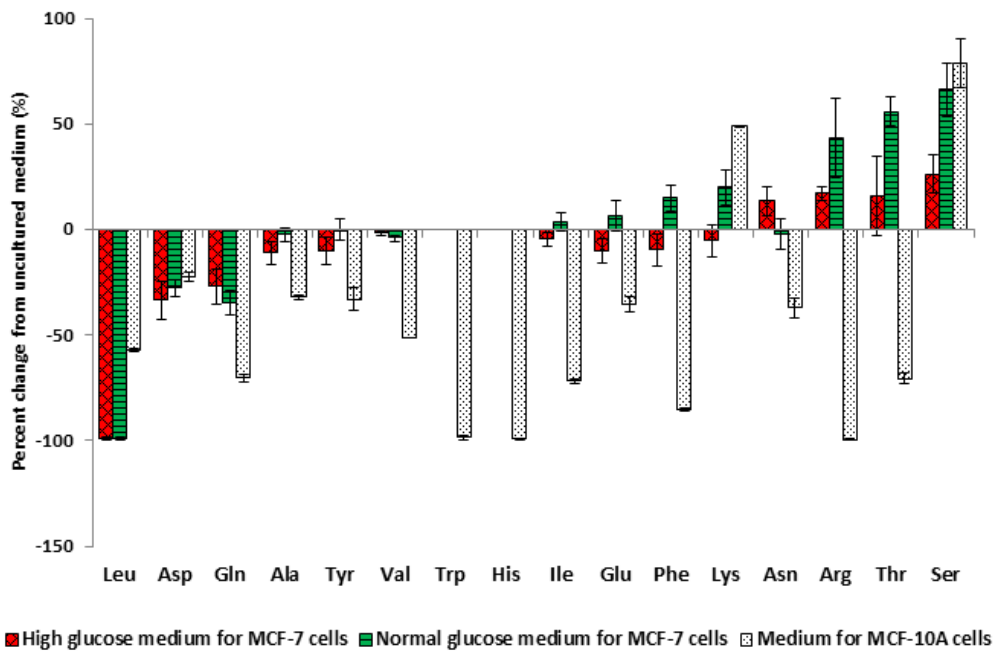Figure 6-6 Extracellular D-amino acid profiles. Percent changes of D-amino acids in the
media with MCF-7 cells (red: high glucose medium; green: normal glucose medium) and
MCF-10A cells (white: MEGM). Values are shown as percent change of L-amino acid in
the medium after 72-hours incubation from the uncultured medium, with negative bars
indicating cellular consumption and positive bars indicating production.

6.3.2.2 Altered D-amino acid profiles and metabolism for MCF-7 breast cancer cells

Low percentages of most D-amino acids were observed in MCF-7 compared to MCF-10A cells. It was mostly due to the high levels of L-amino acids in MCF-7 cells, as the corresponding D-amino acid levels were not much different between these two cell lines (Figures 6-4 and 6-5). However, significantly high amounts of D-Asp and D-Ser were determined in MCF-7 breast cancer cells, *i.e.,* 3 to 22 times higher than in MCF-10A cells. High levels of intracellular D-Asp may be caused by the absorption of D-Asp from extracellular sources (*i.e.*, uptake of D-Asp was observed, Figure 6-6) or the biosynthesis of D-Asp by aspartate racemase or a combination of both [205]. Given the fact that D-Ser levels were increased in the growth media after cell incubation (Figure 6-6), biosynthesis of D-Ser by serine racemase may occur in the cultured cells and then released into the growth medium [206].

Questions arise as to whether the higher intracellular levels indicate an important or unique function of D-Asp and D-Ser for MCF-7 breast cancer cells. Besides the essential roles in the CNS, NMDA receptors have been implicated in regulating cancer cell growth and division [191]. It has been demonstrated that MCF-7 breast cancer cells expressed functional NMDA receptors with NR1 and NR2 subunits, and blockage of NMDA receptors with antagonists inhibited proliferation and reduced viability of cultured MCF-7 cells [207]. Interestingly, it has been determined that D-Ser binds to NMDA receptor NR1 subunits at the glycine binding site, and D-Asp binds to NMDA receptor NR2 subunits at the glutamate binding site [145,149,150]. As co-agonists of NMDA receptors, high levels of D-Asp and D-Ser as shown in our work may be required or at least beneficial for MCF-7 breast cancer cell proliferation since activation of NMDA receptors in breast cancer cells is important for maintaining cell growth and viability. As they have shown increased availability and have selectively accumulated in MCF-7 breast cancer cells, D-

Asp and D-Ala could be potential oncometabolites for breast cancer. Further, accumulation of specific D-amino acids in cancer cells may be the consequences of upregulated racemases, as the presence of Ser racemase and Asp racemase has been reported in mammals [205,206]. Although further investigation and validation are needed for the proposed potential oncometabolites and the possible upregulated racemases for breast cancer, this study provides a new approach for breast cancer diagnosis.

D-Amino acids were found in MCF-7 and MCF-10A cells as well as in the cultured and uncultured media. Changes in extracellular D-amino acid levels were detected, indicating the release or uptake of D-amino acids by MCF-7 and MCF-10A cells (Figure 6-6). Our results demonstrated that the transfer of D-amino acids occurred between cells and growth media. Amino acids are hydrophilic molecules and cannot cross the cell membrane without the aid of amino acid transporters. It has been reported that most of the transporters show high stereoselectivity, and only a few transporters have been shown to transport D-amino acids, *e.g.,* LAT1, ASCT1, ASCT2, ATB$^{0,+}$, and EAAT [208-210]. They have shown selectivity to D-Leu, D-Ser, D-Met, D-Phe, and D-Asp. Cellular release of D-Ser (observed in our study) through the less stereoselective amino acid transporters is likely to be important in regulating extracellular levels of D-Ser, which activate NMDA receptors and further affects breast cancer cell proliferation. It has been determined that cancer cells express some amino acid transporters at high levels to satisfy their increased demand for amino acids [195]. Interestingly, all the transporters mentioned above have been shown to be upregulated in cancer cells. This further supports the possibility that altered D-amino acid profiles may be a metabolic adaptation to breast cancer cell proliferation. Thus, reducing the availability of the potential oncometabolites, D-Asp and D-Ser, to breast cancer cells could be a possible anticancer strategy. Future studies could explore more on the inhibition of the enzymes/pathways that produce D-Asp and D-

Ser, and interference with the upregulated amino acid transporters in cancer cells that show selectivity for these D-amino acids. Another notable result was that D-Thr, D-Tyr, and D-Ala also were elevated in MCF-7 cells. Although it has been reported that D-Ala can also bind to NMDA receptor, the presence of Ala racemases have not been confirmed in mammals. Concerning D-Thr and D-Tyr, there are no studies concerning their presence and functions for breast cancer cells to our knowledge. Our results suggest that it may be worthy of exploring the roles of D-Thr, D-Tyr, and D-Ala during cancer cell proliferation.

6.3.3 L-Asn and D-Asn May Both Serve as Exchange Currency During Breast Cancer Cell Proliferation

Amino acid transporters carry out not only net transport of amino acids (*i.e.*, symporters, substrates travel in the same direction), but also obligatory amino acid exchange (*i.e.*, antiporters), which means uptake of one amino acid via this transporter is obligatorily coupled to the export of another amino acid [210]. A recent study indicated that depletion of intracellular and/or extracellular L-Asn in breast cancer cells impaired the uptake of extracellular amino acids, especially L-Ser, L-Arg, and L-His, and reduced cancer cell proliferation [211]. However, the function of D-Asn for cancer cell proliferation was not investigated. In the present study, cellular uptake of L-Ser, L-Arg, and L-His was observed for MCF-7 breast cancer cells (Figure 6-3). In addition, cellular release of both L-Asn and D-Asn was observed for MCF-7 breast cancer cells, but not for MCF-10A cells (Figures 6-3 and 6-6). Our results support and further suggest that intracellular L-Asn, together with D-Asn, exchanges with extracellular amino acids, especially L-Ser, L-Arg, and L-His, to promote cancer cell proliferation [211]. Asn, L- and D-enantiomers, may serve as exchange currency for the uptake of essential amino acids and/or low abundance nonessential amino acids that are required by cancer cells during proliferation.

6.3.4 Malignancy Indicators May Be Used to Indicate The Presence of Cancer

The question arises, as to whether the substantially altered levels of D- and L-amino acids in cancer cells can be used to provide a sensitive and reliable index to identify malignancy? A relatively simple malignancy indicator (MI) comparing the ratio of each L-amino acid in cancer vs. noncancerous cell line and divided by the analogous ratio of D-amino acid, are given in Table 6-1 (see Materials and methods for calculations). Clearly, there are three notable features which are: 1) increased demands of specific L-amino acids contribute to a high MI; 2) increased demands of specific D-amino acids contributes to low MIs, and 3) designated cellular release of specific L- and D-amino acids contribute to low MI. Gln, Phe, Ile, Val, and Leu show high MI due the significant elevated levels of L-enantiomers but decreased levels of D-enantiomers in MCF-7 breast cancer cells. Low MI values are determined for Asn, Asp, and Ser, and how these elevated D-amino acids contribute to low MIs were discussed above.

Table 6-1 Malignancy indicators for breast cancer

	L-amino acids[a]	D-amino acids[b]	Malignancy Indicator (MI)[c]
Asn	0.8	3.4	*0.2*
Asp	4.0	14.0	*0.3*
Ser	15.0	22.0	*0.7*
Glu	5.4	1.6	3.4
Ala	13.7	3.6	3.8
Tyr	16.8	4.2	4.0
Thr	35.9	4.4	8.2
Trp[d]	2.7	0.07	> 39[d]
Gln	41.0	0.8	*51*
Phe	18.0	0.3	*60*
Ile	46.0	0.7	*66*
Val	27.0	0.4	*68*
Leu	36.0	0.4	*90*

| Pro[d] | 13.6 | 0.03[d] | > 450[d] |
| Lys[d] | 12.9 | 0.01[d] | > 1300[d] |

Results in this table were obtained from MCF-7 breast cancer cells grown in normal glucose condition vs. MCF-10A cells after 72-hours incubation. Calculations for: L-amino acids [a], d-amino acids[b], and Malignancy Indicator[c] are given in the Materials and methods. [d] indicates that this D-amino acid was detected only in MCF-10A cells, but not in MCF-7 breast cancer cells. In these cases, the limit of detection (LOD) for these D-amino acids was used to estimate a MI value.

6.3.5 Effect of glucose concentration on MCF-7 cell proliferation and amino acid levels

Cell media with different glucose concentrations (i.e., 5 mM and 25 mM) were examined for the effect of glucose level on cancer cell proliferation. Cell number and free amino acid levels were measured for MCF-7 cells with different growth times, i.e., 24-hours, 48-hours, and 72-hours (S4, S5, S7, S8, S10, S11, and S25 Tables). As expected, the proliferation of MCF-7 cells increased when the glucose concentration in the medium was increased from 5.5 mM to 25mM at 72 hours (Fig S3). MCF-7 cells grown in high glucose medium showed higher levels of free l-amino acids compared to those grown in normal glucose medium (Fig 6-2). For instance, l-Gln levels in MCF-7 cells grown in high glucose and normal glucose condition were 681 nmol/10^6 cells and 377 nmol/10^6 cells, respectively, after 24-hour incubation (**Fig 6-2A**). However, the trends of intracellular l-amino acid levels for MCF-7 cells were similar despite the glucose concentration in the medium (Fig 6). l-Gln, Gly, and l-Glu were the three amino acids with the highest levels, and the three l-amino acids with the lowest levels were always GABA, l-Cys, and l-Hyp in MCF-7 cells regardless of the growth media. Concerning d-amino acids, most of them did not show significant changes in MCF-7 cells when the glucose levels were changed in

the medium (Fig 6-4). The exceptions were d-Thr and d-Ser, which were higher in MCF-7 cells grown in high glucose conditions, especially after 24-hour growth.

6.4 Conclusions

The altered intracellular and extracellular free L-amino acid profiles determined in MCF-7 breast cancer cells, demonstrate the metabolic differences between the breast cancer cells and non-tumorigenic breast cells. Significantly high intracellular L-amino acids levels may contribute to the elevated levels of L-amino acids that are observed in the saliva and plasma of breast cancer patients. Our data indicate that cellular uptake and release of specific D-amino acids occur during cancer cell proliferation. It is clear that D-amino acids also have altered profiles in cancer cells. Specific D-amino acids showed significantly altered levels in cancer cells compared to non-tumorigenic cells. In particular, two D-amino acids, D-Ser and D-Asp, had elevated levels and could be potential oncometabolites for breast cancer via selective accumulation in MCF-7 breast cancer cells. Elevated levels of D-Ser and D-Asp in MCF-7 breast cancer cells may result from upregulated enzymatic racemases. Like specific L-amino acids, D-amino acids may also be able to serve as exchange currency to drive the uptake of essential and/or low abundance nonessential amino acids required by the cancer cells. A simple index using specific L- and D-amino acid relative levels has been derived and used to produce malignancy indicator (MI) of cancer. High MIs (>60) result from the increased demands of specific essential amino acids (*i.e.*, L-Leu, L-Ile, L-Val, and L-Phe) and L-Gln that functions like "essential" amino acids for cancer cells during proliferation. Very low MIs (<1) result from the increased demands of specific D-amino acids (*i.e.*, D-Ser, D-Asp) or the cellular release of amino acid exchange currency (*i.e.*, L- and D-Asn) to promote cancer cell proliferation. Such a simple and fast technique based on both high and low MI values

may be used to predict/estimate the development of malignancy and perhaps in the future, early diagnosis of breast cancer. Though we have yet to explore this, it is conceivable that different cancers will each have a unique combination of MIs for a specific set of AAs, something akin to a fingerprint, which could be used for broad range cancer detection.

Chapter 7

General Summary

7.1 Part one (Chapter 2)

Chapter 2 of this dissertation described the synthesis and development of a

hydrolytically stable HILIC stationary phase- carboxylated cyclofructan 6. This novel

stationary phase showed unique selectivity compared to all other commercially available

HILIC stationary phases. This was demonstrated with a stationary phase selectivity plot.

The new bonding chemistry provided a stationary phase of great hydrolytically stability.

By continuously running the column with a high pH mobile phase for 30 hours, the

carboxylated CF6 stationary phase showed superior stability to a "bare" silica column.

The superficially porous silica gel particles enable high efficiency and faster separations

for highly polar pharmaceuticals. Salicylic acid analogues, β-blockers as well as nucleic

acids and their bases were well separated with this exceptional HILIC stationary phase.

7.2 Part two (Chapter 3-6)

The application of HPLC-MS/MS analysis of challenging biological compounds

was demonstrated in Chapters 3-6. Sensitive, selective and rapid bioanalysis for

glycosaminoglycan disaccharides and amino acids were achieved by using novel

methodologies. The currently developed LC-MS/MS methods show much better

chromatographic performance, faster analysis times, and lower detection limits than the

other reported methodologies. Chapter 3 described the sensitive and rapid analysis of

glycosaminoglycan disaccharides with HPLC-MS/MS. The traditional analysis of these

disaccharides faces the challenge of incomplete structural isomer separation and long

analysis times. By using two hydrolytically stable HILIC stationary phases, which were

developed in house, separations of isomeric as well as structurally similar disaccharides

were well resolved. Lower detection limits were achieved when using the CF6 stationary phase as compared to the teicoplanin stationary phase. The methods showed good linearity and precision. Disaccharide compositions of glycosaminoglycan from different animal sources were determined. For disaccharides that were above the detection limits, comparable results were obtained using the two methods.

Chapter 4 outlined a novel application of paired ion electrospray ionization (PIESI) for the sensitive detection of FMOC derivatized amino acids. The PIESI approach showed advantage in terms of selectivity and sensitivity. Symmetrical and unsymmetrical ion pairing reagents were tested and $C_5(bpyr)_2$ gave the lowest detection limit. The approach was able to improve the detection limits for these FMOC amino acids by 5 to 100 fold as compared to those obtained in negative mode ESI-MS. LODs obtained with the optimal ion-pairing reagents ranged from 0.5 to 20 pg.

A mass spectrometry compatible chiral separation of D and L-amino acids was developed by using quinine and teicoplanin stationary phases with detection by triple quadrupole MS. Quinine and teicoplanin CSP showed opposite selectivity for the two enantiomers of the amino acids, which helped in confirming peak identity, especially for trace amounts of D-amino acids. Compared with the previous 2-D HPLC method, the current one dimensional LC-MS/MS method shortened total sample analysis time by ~60 times. The method was implemented for quantitation of free D and L-amino acid concentrations in mouse brain tissue as well as human breast cell lines. These results were presented in Chapter 5 and 6 respectively. In Chapter 5, levels of D- and L-amino acids were determined in the whole brain of wild-type ddY mice (ddY/DAO$^{+/+}$), mutant mice lacking DAO activity (ddY/DAO$^{-/-}$), and the heterozygous mice (ddY/DAO$^{+/-}$). It was found that only L-Trp was markedly elevated in the DAO+/- and DAO-/- mice while L-enantiomer levels for other amino acid remained similar among the three strains. The

highest concentration of D-amino acid was found to be D-Ser (~30%), whereas D-Glu had the lowest % D value (~0.1%) in all three strains. Significant differences of specific amino acids, such as D-Leu, D-Ala, D-Ser, D-Arg, and D-Ile were observed in ddY/DAO$^{+/-}$ and ddY/DAO$^{-/-}$ mice compared to ddY/DAO+/+ mice. In Chapter 6, intracellular and extracellular D- and L- amino acid concentrations were investigated for the first time. Differences in the concentrations suggested metabolic process might be different for the breast cancer cells and non-tumorigenic breast cells. Higher L-amino acids levels were detected in the MCF-7 cancer cells and the different profiles for D-amino acids were also demonstrated in this study.

Appendix A

Publication Information and Contributing Authors

Chapter 2. A manuscript published in Analytical Methods and reproduced with permission from The Royal Society of Chemistry. Yadi Wang, M. Farooq Wahab, Zachary S. Breitbach, Daniel W. Armstrong, 2016,8, 6038-6045. DOI:10.1039/C6AY01246A.

Chapter 3. A manuscript in preparation.

Chapter 4. A manuscript published in Analytical and Bioanalytical Chemistry. Yadi Wang, Siqi Du, Daniel W. Armstrong, 2018, 410: 4725. DOI: 10.1007/s00216-018-0901-5.

Chapter 5. A manuscript published in Analytical and Bioanalytical Chemistry Siqi Du, Yadi Wang, Choyce A. Weatherly, Kylie Holden, Daniel W. Armstrong, 2018, 410: 2971. DOI: 10.1007/s00216-018-0979-9

Chpater 6. A manuscript published in Journal of Pharmaceutical and Biomedical Analysis Siqi Du, Yadi Wang, Nagham Alatrash, Choyce A.Weatherly, Daipayan Roy, Frederick M.MacDonnell, Daniel W. Armstrong 2019, 164, 421-429. DOI: 10.1016/j.jpba.2018.10.047.

Appendix B

Copyright and Permissions

This Agreement between Yadi Wang ("You") and Springer Nature ("Springer Nature") consists of your license details and the terms and conditions provided by Springer Nature and Copyright Clearance Center.

License Number	4572000854995
License date	Apr 18, 2019
Licensed Content Publisher	Springer Nature
Licensed Content Publication	Analytical and Bioanalytical Chemistry
Licensed Content Title	Sensitive analysis of N-blocked amino acids using high-performance liquid chromatography with paired ion electrospray ionization mass spectrometry
Licensed Content Author	Yadi Wang, Siqi Du, Daniel W. Armstrong
Licensed Content Date	Jan 1, 2018
Licensed Content Volume	410
Licensed Content Issue	19
Type of Use	Thesis/Dissertation
Requestor type	academic/university or research institute
Format	print and electronic
Portion	full article/chapter
Will you be translating?	no
Circulation/distribution	<501
Author of this Springer Nature content	yes
Title	ADVANCES IN LIQUID CHROMATOGRAPHY AND LIQUID CHROMATOGRAPHY MASS SPECTROMETRY FOR THE ANALYSIS OF BIOLOGICALLY IMPORTANT PHARMACEUTICALS, GLYCOSAMINOGLYCANS AND AMINO ACIDS
Institution name	University of Texas at Arlington
Expected presentation date	May 2019
Requestor Location	Chemistry & Physics Building (CPB) 700 Planetarium Place ARLINGTON, TX 76019 United States Attn: Yadi Wang
Total	0.00 USD

Terms and Conditions

119

References

(1) Alpert, A. J. *Journal of Chromatography A* **1990**, *499*, 177-196.

(2) Cubbon, S.; Bradbury, T.; Wilson, J.; Thomas-Oates, J. *Analytical Chemistry* **2007**, *79*, 8911-8918.

(3) Buszewski, B.; Krupczyńska, K.; Gadzała-Kopciuch, R. M.; Rychlicki, G.; Kaliszan, R. *Journal of Separation Science* **2003**, *26*, 313-321.

(4) Bocian, S.; Buszewski, B. *Journal of Separation Science* **2010**, *33*, 3033-3042.

(5) Dinh, N. P.; Jonsson, T.; Irgum, K. *Journal of Chromatography A* **2011**, *1218*, 5880-5891.

(6) Ibrahim, M. E. A.; Liu, Y.; Lucy, C. A. *Journal of Chromatography A* **2012**, *1260*, 126-131.

(7) Jandera, P. *Analytica Chimica Acta* **2011**, *692*, 1-25.

(8) Knox, J. H.; Kaur, B.; Millward, G. R. *Journal of Chromatography A* **1986**, *352*, 3-25.

(9) Iverson, C. D.; Lucy, C. A. *Journal of Chromatography A* **2014**, *1373*, 17-24.

(10) Wahab, M. F.; Ibrahim, M. E. A.; Lucy, C. A. *Analytical Chemistry* **2013**, *85*, 5684-5691.

(11) Linda, R.; Lim, L. W.; Takeuchi, T. *Analytical Sciences* **2013**, *29*, 631-635.

(12) Wimalasinghe, R. M.; Weatherly, C. A.; Wahab, M. F.; Thakur, N.; Armstrong, D. W. *Analytical Chemistry* **2018**, *90*, 8139-8146.

(13) Capila, I.; Linhardt, R. J. *Angewandte Chemie International Edition* **2002**, *41*, 390-412.

(14) Fuster, M. M.; Esko, J. D. *Nature Reviews Cancer* **2005**, *5*, 526.

(15) Sasisekharan, R.; Shriver, Z.; Venkataraman, G.; Narayanasami, U. *Nature Reviews Cancer* **2002**, *2*, 521.

(16) Ulf Lindahl, J. C., Koji Kimata, Jeffrey D. Esko. In *Essentials of Glycobiology [Internet]. 3rd edition.*, Varki A, C. R., Esko JD, Ed.; Cold Spring Harbor (NY): Cold Spring Harbor Laboratory Press, 2015-2017.

(17) Ly, M.; Laremore, T. N.; Linhardt, R. J. *OMICS: A Journal of Integrative Biology* **2010**, *14*, 389-399.

(18) Yang, B.; Chang, Y.; Weyers, A. M.; Sterner, E.; Linhardt, R. J. *Journal of Chromatography A* **2012**, *1225*, 91-98.

(19) Kinoshita, A.; Sugahara, K. *Analytical Biochemistry* **1999**, *269*, 367-378.

(20) Skidmore, M. A.; Guimond, S. E.; Dumax-Vorzet, A. F.; Yates, E. A.; Turnbull, J. E. *Nature Protocols* **2010**, *5*, 1983.

(21) Osago, H.; Shibata, T.; Hara, N.; Kuwata, S.; Kono, M.; Uchio, Y.; Tsuchiya, M. *Analytical Biochemistry* **2014**, *467*, 62-74.

(22) Gill, V. L.; Aich, U.; Rao, S.; Pohl, C.; Zaia, J. *Analytical Chemistry* **2013**, *85*, 1138-1145.

(23) Turiák, L.; Tóth, G.; Ozohanics, O.; Révész, Á.; Ács, A.; Vékey, K.; Zaia, J.; Drahos, L. *Journal of Chromatography A* **2018**, *1544*, 41-48.

(24) Sharer, J. D.; De Biase, I.; Matern, D.; Young, S.; Bennett, M. J.; Tolun, A. A.; on behalf of the, A. L. Q. A. C. *Genetics in Medicine* **2018**, *20*, 1499-1507.

(25) Simpson, R. J.; Neuberger, M. R.; Liu, T. Y. *Journal of Biological Chemistry* **1976**, *251*, 1936-1940.

(26) Einarsson, S.; Josefsson, B.; Lagerkvist, S. *Journal of Chromatography A* **1983**, *282*, 609-618.

(27) Lindroth, P.; Mopper, K. *Analytical Chemistry* **1979**, *51*, 1667-1674.

(28) Graser, T. A.; Godel, H. G.; Albers, S.; Földi, P.; Fürst, P. *Analytical Biochemistry* **1985**, *151*, 142-152.

(29) Watanabe, Y.; Imai, K. *Journal of Chromatography A* **1982**, *239*, 723-732.

(30) Imai, K.; Watanabe, Y. *Analytica Chimica Acta* **1981**, *130*, 377-383.

(31) Buck, K.; Voehringer, P.; Ferger, B. *Journal of Neuroscience Methods* **2009**, *182*, 78-84.

(32) Bathena, S. P.; Huang, J.; Epstein, A. A.; Gendelman, H. E.; Boska, M. D.; Alnouti, Y. *Journal of Chromatography B* **2012**, *893-894*, 15-20.

(33) Prinsen, H. C. M. T.; Schiebergen-Bronkhorst, B. G. M.; Roeleveld, M. W.; Jans, J. J. M.; de Sain-van der Velden, M. G. M.; Visser, G.; van Hasselt, P. M.; Verhoeven-Duif, N. M. *Journal of Inherited Metabolic Disease* **2016**, *39*, 651-660.

(34) Weatherly, C. A.; Du, S.; Parpia, C.; Santos, P. T.; Hartman, A. L.; Armstrong, D. W. *ACS Chemical Neuroscience* **2017**, *8*, 1251-1261.

(35) Armstrong, D. W.; Liu, Y.; Ekborgott, K. H. *Chirality* **1995**, *7*, 474-497.

(36) Buszewski, B.; Noga, S. *Analytical and Bioanalytical Chemistry* **2012**, *402*, 231-247.

(37) Jin, H. L.; Stalcup, A. M.; Armstrong, D. W. *Journal of Liquid Chromatography* **1988**, *11*, 3295-3304.

(38) Armstrong, D. W.; Jin, H. L. *J Chromatogr* **1989**, *462*, 219-232.

(39) Armstrong, D. W.; Jin, H. L. *Chirality* **1989**, *1*, 27-37.

(40) Wang, C.; Jiang, C.; Armstrong, D. W. *Journal of Separation Science* **2008**, *31*, 1980-1990.

(41) Liu, M.; Chen, E. X.; Ji, R.; Semin, D. *Journal of Chromatography A* **2008**, *1188*, 255-263.

(42) Olsen, B. A. *Journal of Chromatography A* **2001**, *913*, 113-122.

(43) Guo, Y.; Gaiki, S. *Journal of Chromatography A* **2005**, *1074*, 71-80.

(44) Guo, Y.; Huang, A. *Journal of Pharmaceutical and Biomedical Analysis* **2003**, *31*, 1191-1201.

(45) Strege, M. A. *Analytical Chemistry* **1998**, *70*, 2439-2445.

(46) Naidong, W. *Journal of Chromatography B* **2003**, *796*, 209-224.

(47) Houbenová, A.; Claessens, H. A.; de Haan, J. W.; Cramers, C. A.; Stulík, K. *Journal of Liquid Chromatography* **1994**, *17*, 49-68.

(48) Hetem, M. J. J.; De Haan, J. W.; Claessens, H. A.; Van de Ven, L. J. M.; Cramers, C. A.; Kinkel, J. N. *Analytical Chemistry* **1990**, *62*, 2288-2296.

(49) O'Gara, J. E.; Alden, B. A.; Gendreau, C. A.; Iraneta, P. C.; Walter, T. H. *Journal of Chromatography A* **2000**, *893*, 245-251.

(50) Kirkland, J. J.; Henderson, J. W. *Journal of Chromatographic Science* **1994**, *32*, 473-480.

(51) Kirkland, J. J.; van Straten, M. A.; Claessens, H. A. *Journal of Chromatography A* **1995**, *691*, 3-19.

(52) Claessens, H. A.; van Straten, M. A.; Kirkland, J. J. *Journal of Chromatography A* **1996**, *728*, 259-270.

(53) Kirkland, J. J.; Henderson, J. W.; DeStefano, J. J.; van Straten, M. A.; Claessens, H. A. *Journal of Chromatography A* **1997**, *762*, 97-112.

(54) Kirkland, J. J.; van Straten, M. A.; Claessens, H. A. *Journal of Chromatography A* **1998**, *797*, 111-120.

(55) Snyder, L. R.; Kirkland, J. J. *Introduction to modern liquid chromatography*; Wiley, 1979.

(56) Jiang, C.; Tong, M.-Y.; Breitbach, Z. S.; Armstrong, D. W. *ELECTROPHORESIS* **2009**, *30*, 3897-3909.

(57) Zhang, Y.; Breitbach, Z. S.; Wang, C.; Armstrong, D. W. *Analyst* **2010**, *135*, 1076-1083.

(58) Sun, P.; Wang, C.; Breitbach, Z. S.; Zhang, Y.; Armstrong, D. W. *Analytical Chemistry* **2009**, *81*, 10215-10226.

(59) Sun, P.; Armstrong, D. W. *Journal of Chromatography A* **2010**, *1217*, 4904-4918.

(60) Sun, P.; Wang, C.; Padivitage, N. L. T.; Nanayakkara, Y. S.; Perera, S.; Qiu, H.; Zhang, Y.; Armstrong, D. W. *Analyst* **2011**, *136*, 787-800.

(61) Qiu, H.; Loukotková, L.; Sun, P.; Tesařová, E.; Bosáková, Z.; Armstrong, D. W. *Journal of Chromatography A* **2011**, *1218*, 270-279.

(62) Shu, Y.; Lang, J. C.; Breitbach, Z. S.; Qiu, H.; Smuts, J. P.; Kiyono-Shimobe, M.; Yasuda, M.; Armstrong, D. W. *Journal of Chromatography A* **2015**, *1390*, 50-61.

(63) Dinh, N. P.; Jonsson, T.; Irgum, K. *Journal of Chromatography A* **2013**, *1320*, 33-47.

(64) Alexander, G. B.; Heston, W. M.; Iler, R. K. *The Journal of Physical Chemistry* **1954**, *58*, 453-455.

(65) Trammell, B. C.; Ma, L.; Luo, H.; Jin, D.; Hillmyer, M. A.; Carr, P. W. *Analytical Chemistry* **2002**, *74*, 4634-4639.

(66) Di Palma, S.; Boersema, P. J.; Heck, A. J. R.; Mohammed, S. *Analytical Chemistry* **2011**, *83*, 3440-3447.

(67) Kotoni, D.; D'Acquarica, I.; Ciogli, A.; Villani, C.; Capitani, D.; Gasparrini, F. *Journal of Chromatography A* **2012**, *1232*, 196-211.

(68) Kirkland, J. J.; Adams, J. B.; van Straten, M. A.; Claessens, H. A. *Analytical Chemistry* **1998**, *70*, 4344-4352.

(69) Zhou, T.; Lucy, C. A. *Journal of Chromatography A* **2010**, *1217*, 82-88.

(70) Kawahara, M.; Nakamura, H.; Nakajima, T. *Journal of Chromatography A* **1990**, *515*, 149-158.

(71) Arkles, B. In *Silane Coupling Agents: Connecting Across Boundaries*, Gelest, I., Ed.: Morrisville, 2004, p 157.

(72) Liu, X.; Pohl, C. *Journal of Chromatography A* **2008**, *1191*, 83-89.

(73) Ibrahim, M. E. A.; Wahab, M. F.; Lucy, C. A. *Analytica Chimica Acta* **2014**, *820*, 187-194.

(74) Padivitage, N. L. T.; Armstrong, D. W. *Journal of Separation Science* **2011**, *34*, 1636-1647.

(75) Guo, Y.; Gaiki, S. *Journal of Chromatography A* **2011**, *1218*, 5920-5938.

(76) Yamada, S.; Sugahara, K.; Ozbek, S. *Communicative & Integrative Biology* **2011**, *4*, 150-158.

(77) Bougatef, H.; Krichen, F.; Capitani, F.; Amor, I. B.; Maccari, F.; Mantovani, V.; Galeotti, F.; Volpi, N.; Bougatef, A.; Sila, A. *Carbohydrate Polymers* **2018**, *196*, 272-278.

(78) Krichen, F.; Volpi, N.; Sila, A.; Maccari, F.; Mantovani, V.; Galeotti, F.; Ellouz-Chaabouni, S.; Bougatef, A. *International Journal of Biological Macromolecules* **2017**, *95*, 32-39.

(79) Nandini, C. D.; Sugahara, K. In *Advances in Pharmacology*; Academic Press, 2006, pp 253-279.

(80) Gill, S.; Wight, T. N.; Frevert, C. W. *The Anatomical Record* **2010**, *293*, 968-981.

(81) Mourão, P. A. S.; Pereira, M. S.; Pavão, M. S. G.; Mulloy, B.; Tollefsen, D. M.; Mowinckel, M.-C.; Abildgaard, U. *Journal of Biological Chemistry* **1996**, *271*, 23973-23984.

(82) Krichen, F.; Bougatef, H.; Capitani, F.; Ben Amor, I.; Koubaa, I.; Gargouri, J.; Maccari, F.; Mantovani, V.; Galeotti, F.; Volpi, N.; Bougatef, A. *RSC Advances* **2018**, *8*, 37965-37975.

(83) Weyers, A.; Yang, B.; Yoon, D. S.; Park, J.-H.; Zhang, F.; Lee, K. B.; Linhardt, R. J. *OMICS: A Journal of Integrative Biology* **2012**, *16*, 79-89.

125

(84) Binder, M. J.; McCoombe, S.; Williams, E. D.; McCulloch, D. R.; Ward, A. C. *Cancer Letters* **2017**, *385*, 55-64.

(85) Purushothaman, A.; Fukuda, J.; Mizumoto, S.; ten Dam, G. B.; van Kuppevelt, T. H.; Kitagawa, H.; Mikami, T.; Sugahara, K. *Journal of Biological Chemistry* **2007**, *282*, 19442-19452.

(86) Sugahara, K.; Mikami, T. *Current Opinion in Structural Biology* **2007**, *17*, 536-545.

(87) Berretta, S. *Neuropharmacology* **2012**, *62*, 1584-1597.

(88) Ariga, T.; Miyatake, T.; Yu, R. K. *Journal of Neuroscience Research* **2010**, *88*, 2303-2315.

(89) Ernst, S.; Langer, R.; Cooney, C. L.; Sasisekharan, R. *Critical Reviews in Biochemistry and Molecular Biology* **1995**, *30*, 387-444.

(90) Yang, B.; Weyers, A.; Baik, J. Y.; Sterner, E.; Sharfstein, S.; Mousa, S. A.; Zhang, F.; Dordick, J. S.; Linhardt, R. J. *Analytical Biochemistry* **2011**, *415*, 59-66.

(91) Zhang, F.; Sun, P.; Muñoz, E.; Chi, L.; Sakai, S.; Toida, T.; Zhang, H.; Mousa, S.; Linhardt, R. J. *Analytical Biochemistry* **2006**, *353*, 284-286.

(92) Wahab, M. F.; Wimalasinghe, R. M.; Wang, Y.; Barhate, C. L.; Patel, D. C.; Armstrong, D. W. *Analytical Chemistry* **2016**, *88*, 8821-8826.

(93) Dolzan, M. D.; Spudeit, D. A.; Breitbach, Z. S.; Barber, W. E.; Micke, G. A.; Armstrong, D. W. *Journal of Chromatography A* **2014**, *1365*, 124-130.

(94) Kang, P.; Mechref, Y.; Klouckova, I.; Novotny, M. V. *Rapid communications in mass spectrometry : RCM* **2005**, *19*, 3421-3428.

(95) Wang, Y.; Wahab, M. F.; Breitbach, Z. S.; Armstrong, D. W. *Analytical Methods* **2016**, *8*, 6038-6045.

(96) Desai, M. J.; Armstrong, D. W. *Journal of Mass Spectrometry* **2004**, *39*, 177-187.

(97) Hellinghausen, G.; Readel, E. R.; Wahab, M. F.; Lee, J. T.; Lopez, D. A.; Weatherly, C. A.; Armstrong, D. W. *Chromatographia* **2019**, *82*, 221-233.

(98) Berthod, A.; Liu, Y.; Bagwill, C.; Armstrong, D. W. *Journal of Chromatography A* **1996**, *731*, 123-137.

(99) Volpi, N. *Analytical Biochemistry* **2010**, *397*, 12-23.

(100) Berg, J. M.; Tymoczko, J. L.; L., S. *Biochemistry*; W H Freeman: New York, 2002.

(101) Wu, G. *Amino Acids* **2009**, *37*, 1-17.

(102) Poncet, N.; Taylor, P. M. *Current Opinion in Clinical Nutrition and Metabolic Care* **2013**, *16*, 57-65.

(103) Schwartz, J. H. In *Encyclopedia of the Human Brain*; Academic Press: New York, 2002, pp 601-611.

(104) Armstrong, D. W.; Gasper, M.; Lee, S. H.; Zukowski, J.; Ercal, N. *Chirality* **1993**, *5*, 375-378.

(105) Armstrong, D. W.; Duncan, J. D.; Lee, S. H. *Amino Acids* **1991**, *1*, 97-106.

(106) Brückner, H.; Haasmann, S.; Friedrich, A. *Amino Acids* **1994**, *6*, 205-211.

(107) Armstrong, D. W.; Zukowski, J.; Ercal, N.; Gasper, M. *Journal of Pharmaceutical and Biomedical Analysis* **1993**, *11*, 881-886.

(108) Armstrong, D. W.; Gasper, M. P.; Lee, S. H.; Ercal, N.; Zukowski, J. *Amino Acids* **1993**, *5*, 299-315.

(109) Armstrong, D. W.; Rundlett, K. L.; Chen, J.-R. *Chirality* **1994**, *6*, 496-509.

(110) Molnár-Perl, I. *Journal of Chromatography A* **2003**, *987*, 291-309.

(111) Desai, M. J.; Armstrong, D. W. *Rapid Communications in Mass Spectrometry* **2004**, *18*, 251-256.

(112) Uutela, P.; Ketola, R. A.; Piepponen, P.; Kostiainen, R. *Analytica Chimica Acta* **2009**, *633*, 223-231.

(113) Bank, R. A.; Jansen, E. J.; Beekman, B.; te Koppele, J. M. *Analytical Biochemistry* **1996**, *240*, 167-176.

(114) Gartenmann, K.; Kochhar, S. *Journal of Agricultural and Food Chemistry* **1999**, *47*, 5068-5071.

(115) Soukup-Hein, R. J.; Remsburg, J. W.; Dasgupta, P. K.; Armstrong, D. W. *Analytical Chemistry* **2007**, *79*, 7346-7352.

(116) Soukup-Hein, R. J.; Remsburg, J. W.; Breitbach, Z. S.; Sharma, P. S.; Payagala, T.; Wanigasekara, E.; Huang, J.; Armstrong, D. W. *Analytical Chemistry* **2008**, *80*, 2612-2616.

(117) Dodbiba, E.; Breitbach, Z. S.; Wanigasekara, E.; Payagala, T.; Zhang, X.; Armstrong, D. W. *Analytical and Bioanalytical Chemistry* **2010**, *398*, 367-376.

(118) Dodbiba, E.; Xu, C.; Payagala, T.; Wanigasekara, E.; Moon, M. H.; Armstrong, D. W. *Analyst* **2011**, *136*, 1586-1593.

(119) Zhang, X.; Wanigasekara, E.; Breitbach, Z. S.; Dodbiba, E.; Armstrong, D. W. *Rapid Communications in Mass Spectrometry* **2010**, *24*, 1113-1123.

(120) Warnke, M. M.; Breitbach, Z. S.; Dodbiba, E.; Wanigasekara, E.; Zhang, X.; Sharma, P.; Armstrong, D. W. *Journal of the American Society for Mass Spectrometry* **2009**, *20*, 529-538.

(121) Breitbach, Z. S.; Berthod, A.; Huang, K.; Armstrong, D. W. *Mass Spectrometry Reviews* **2016**, *35*, 201-218.

(122) Breitbach, Z. S.; Warnke, M. M.; Wanigasekara, E.; Zhang, X.; Armstrong, D. W. *Analytical Chemistry* **2008**, *80*, 8828-8834.

(123) Guo, H.; Dolzan, M. D.; Spudeit, D. A.; Xu, C.; Breitbach, Z. S.; Sreenivasan, U.; Armstrong, D. W. *International Journal of Mass Spectrometry* **2015**, *389*, 14-25.

(124) Guo, H.; Riter, L. S.; Wujcik, C. E.; Armstrong, D. W. *Talanta* **2016**, *149*, 103-109.

(125) Breitbach, Z. S.; Wanigasekara, E.; Dodbiba, E.; Schug, K. A.; Armstrong, D. W. *Analytical Chemistry* **2010**, *82*, 9066-9073.

(126) Xu, C.; Guo, H.; Breitbach, Z. S.; Armstrong, D. W. *Analytical Chemistry* **2014**, *86*, 2665-2672.

(127) Lopes, N. P.; Stark, C. B. W.; Gates, P. J.; Staunton, J. *Analyst* **2002**, *127*, 503-506.

(128) Grimalt, S.; Pozo, Ó. J.; Marín, J. M.; Sancho, J. V.; Hernández, F. *Journal of the American Society for Mass Spectrometry* **2005**, *16*, 1619-1630.

(129) Guo, H.; Breitbach, Z. S.; Armstrong, D. W. *Analytica Chimica Acta* **2016**, *912*, 74-84.

(130) Remsburg, J. W.; Soukup-Hein, R. J.; Crank, J. A.; Breitbach, Z. S.; Payagala, T.; Armstrong, D. W. *Journal of the American Society for Mass Spectrometry* **2008**, *19*, 261-269.

(131) Xu, C.; Pinto, E. C.; Armstrong, D. W. *Analyst* **2014**, *139*, 4169-4175.

(132) Vatansever, B.; Lahrichi, S. L.; Thiocone, A.; Salluce, N.; Mathieu, M.; Grouzmann, E.; Rochat, B. *Journal of Separation Science* **2010**, *33*, 2478-2488.

(133) Macchi, F. D.; Shen, F. J.; Keck, R. G.; Harris, R. J. In *Amino Acid Analysis Protocols*, Cooper, C.; Packer, N.; Williams, K., Eds.; Humana Press: Totowa, NJ, 2000, pp 9-30.

(134) Glew, R. H.; Melah, G.; El-Nafaty, A. I.; Brandt, Y.; Morris, D.; VanderJagt, D. J. *Clinica Chimica Acta* **2004**, *342*, 179-185.

(135) Auclair, J. L.; Patton, R. L. *Rev Can Biol* **1950**, *9*, 3-8.

(136) Stevens, C. M.; Halpern, P. E.; Gigger, R. P. *Journal of Biological Chemistry* **1951**, *190*, 705-710.

(137) Corrigan, J. J. *Science* **1969**, *164*, 142-149.

(138) Robinson, T. *Life Sciences* **1976**, *19*, 1097-1102.

(139) Armstrong, D. W.; Gasper, M.; Lee, S. H.; Zukowski, J.; Ercal, N. *Chirality* **1993**, *5*, 375-378.

(140) Kullman, J. P.; Chen, X.; Armstrong, D. W. *Chirality* **1999**, *11*, 669-673.

(141) Kreil, G. *Annual Review of Biochemistry* **1997**, *66*, 337-345.

(142) Ollivaux, C.; Soyez, D.; Toullec, J.-Y. *Journal of Peptide Science* **2014**, *20*, 595-612.

(143) Armstrong, D. W.; Zukowski, J.; Ercal, N.; Gasper, M. *Journal of Pharmaceutical and Biomedical Analysis* **1993**, *11*, 881-886.

(144) Schell, M. J.; Brady, R. O., Jr.; Molliver, M. E.; Snyder, S. H. *Journal of Neuroscience* **1997**, *17*, 1604-1615.

(145) Mothet, J. P.; Parent, A. T.; Wolosker, H.; Brady, R. O., Jr.; Linden, D. J.; Ferris, C. D.; Rogawski, M. A.; Snyder, S. H. *Proc Natl Acad Sci U S A* **2000**, *97*, 4926-4931.

(146) Bendikov, I.; Nadri, C.; Amar, S.; Panizzutti, R.; De Miranda, J.; Wolosker, H.; Agam, G. *Schizophr Res* **2007**, *90*, 41-51.

(147) Madeira, C.; Freitas, M. E.; Vargas-Lopes, C.; Wolosker, H.; Panizzutti, R. *Schizophrenia Research* **2008**, *101*, 76-83.

(148) Hashimoto, K.; Fukushima, T.; Shimizu, E.; Komatsu, N.; Watanabe, H.; Shinoda, N.; Nakazato, M.; Kumakiri, C.; Okada, S.; Hasegawa, H.; Imai, K.; Iyo, M. *Arch Gen Psychiatry* **2003**, *60*, 572-576.

(149) Tsai, G. E.; Yang, P.; Chang, Y.-C.; Chong, M.-Y. *Biological Psychiatry* **2006**, *59*, 230-234.

(150) Errico, F.; Nistico, R.; Napolitano, F.; Mazzola, C.; Astone, D.; Pisapia, T.; Giustizieri, M.; D'Aniello, A.; Mercuri, N. B.; Usiello, A. *Neurobiology of Aging* **2011**, *32*, 2229-2243.

(151) D'Aniello, A.; Lee, J. M.; Petrucelli, L.; Di Fiore, M. M. *Neuroscience Letters* **1998**, *250*, 131-134.

(152) Newcomer, J. W.; Farber, N. B.; Olney, J. W. *Dialogues in Clinical Neuroscience* **2000**, *2*, 219-232.

(153) Moaddel, R.; Luckenbaugh, D. A.; Xie, Y.; Villasenor, A.; Brutsche, N. E.; Machado-Vieira, R.; Ramamoorthy, A.; Lorenzo, M. P.; Garcia, A.; Bernier, M.; Torjman, M. C.; Barbas, C.; Zarate, C. A., Jr.; Wainer, I. W. *Psychopharmacology (Berl)* **2015**, *232*, 399-409.

(154) Hartman, A. L.; Santos, P.; O'Riordan, K. J.; Stafstrom, C. E.; Hardwick, J. M. *Neurobiology Disease* **2015**, *82*, 46-53.

(155) Holden, K.; Hartman, A. L. *Epilepsy & Behavior* **2018**, *78*, 202-209.

(156) Weatherly, C. A.; Du, S.; Parpia, C.; Santos, P. T.; Hartman, A. L.; Armstrong, D. W. *ACS Chem. Neurosci.* **2017**, *8*, 1251-1261.

(157) Yoshimura, T.; Esak, N. *Journal of Bioscience and Bioengineering* **2003**, *96*, 103-109.

(158) Wolosker, H.; Sheth, K. N.; Takahashi, M.; Mothet, J. P.; Brady, R. O., Jr.; Ferris, C. D.; Snyder, S. H. *Proc Natl Acad Sci U S A* **1999**, *96*, 721-725.

(159) Kim, P. M.; Duan, X.; Huang, A. S.; Liu, C. Y.; Ming, G. L.; Song, H.; Snyder, S. H. *Proc Natl Acad Sci U S A* **2010**, *107*, 3175-3179.

(160) Krebs, H. A. *Biochemical Journal* **1935**, *29*, 1620-1644.

(161) Pollegioni, L.; Piubelli, L.; Sacchi, S.; Pilone, M. S.; Molla, G. *Cellular and Molecular Life Sciences* **2007**, *64*, 1373-1394.

(162) Sacchi, S.; Caldinelli, L.; Cappelletti, P.; Pollegioni, L.; Molla, G. *Amino Acids* **2012**, *43*, 1833-1850.

(163) Hamase, K.; Inoue, T.; Morikawa, A.; Konno, R.; Zaitsu, K. *Analytical Biochemistry* **2001**, *298*, 253-258.

(164) Morikawa, A.; Hamase, K.; Inoue, T.; Konno, R.; Niwa, A.; Zaitsu, K. *Journal of Chromatography B* **2001**, *757*, 119-125.

(165) Sasaki, M.; Konno, R.; Nihio, M.; Niwa, A.; Yasumura, Y.; Enami, J. *Biochimica et Biophysica Acta (BBA) - Molecular Basis of Disease* **1992**, *1139*, 315-318.

(166) Huxtable, R. J. *Physiological Reviews* **1992**, *72*, 101-163.

(167) Kontro, P.; Marnela, K. M.; Oja, S. S. *Acta Physiol Scand Suppl* **1984**, *537*, 71-74.

(168) Petroff, O. A. *The Neuroscientist* **2002**, *8*, 562-573.

(169) Pawlowska, M.; Chen, S.; Armstrong, D. W. *Journal of Chromatography A* **1993**, *641*, 257-265.

(170) Patel, D. C.; Breitbach, Z. S.; Yu, J.; Nguyen, K. A.; Armstrong, D. W. *Analytica Chimica Acta* **2017**, *963*, 164-174.

(171) Karlsson, C.; Karlsson, L.; Armstrong, D. W.; Owens, P. K. *Analytical Chemistry* **2000**, *72*, 4394-4401.

(172) Péter, A.; Vékes, E.; Armstrong, D. W. *Journal of Chromatography A* **2002**, *958*, 89-107.

(173) US-FDA. **2001**.

(174) Miyoshi, Y.; Hamase, K.; Tojo, Y.; Mita, M.; Konno, R.; Zaitsu, K. *Journal of Chromatography B* **2009**, *877*, 2506-2512.

(175) Suzuki, S.; Mori, A. *Neurochemical Research* **1992**, *17*, 693-698.

(176) Albrecht, J.; Sidoryk-Wegrzynowicz, M.; Zielinska, M.; Aschner, M. *Neuron Glia Biology* **2010**, *6*, 263-276.

(177) Wu, J.-Y.; Prentice, H. *Journal of Biomedical Science* **2010**, *17*, S1-S1.

(178) Okamoto, K.; Kimura, H.; Sakai, Y. *Brain Research* **1983**, *259*, 319-323.

(179) Le Floc'h, N.; Otten, W.; Merlot, E. *Amino Acids* **2011**, *41*, 1195-1205.

(180) Pardridge, W. M. *Neurochemical Research* **1998**, *23*, 635-644.

(181) Fernstrom, J. D.; Wurtman, R. J. *Science* **1972**, *178*, 414-416.

(182) Silber, B. Y.; Schmitt, J. A. J. *Neuroscience & Biobehavioral Reviews* **2010**, *34*, 387-407.

(183) Pritchett, D.; Hasan, S.; Tam, S. K.; Engle, S. J.; Brandon, N. J.; Sharp, T.; Foster, R. G.; Harrison, P. J.; Bannerman, D. M.; Peirson, S. N. *European Journal of Neuroscience* **2015**, *41*, 1167-1179.

(184) Frick, A.; Åhs, F.; Engman, J.; et al. *JAMA Psychiatry* **2015**, *72*, 794-802.

(185) Navarro, E.; Alonso, S. J.; Martin, F. A.; Castellano, M. A. *Basic & Clinical Pharmacology & Toxicology* **2005**, *97*, 149-154.

(186) D'Aniello, A.; D'Onofrio, G.; Pischetola, M.; D'Aniello, G.; Vetere, A.; Petrucelli, L.; Fisher, G. H. *Journal of Biological Chemistry* **1993**, *268*, 26941-26949.

(187) Adage, T.; Trillat, A.-C.; Quattropani, A.; Perrin, D.; Cavarec, L.; Shaw, J.; Guerassimenko, O.; Giachetti, C.; Gréco, B.; Chumakov, I.; Halazy, S.; Roach, A.; Zaratin, P. *European Neuropsychopharmacology* **2008**, *18*, 200-214.

(188) Hanahan, D.; Weinberg, Robert A. *Cell* **2011**, *144*, 646-674.

(189) Warburg, O.; Wind, F.; Negelein, E. *The Journal of General Physiology* **1927**, *8*, 519-530.

(190) Eagle, H.; Oyama, V. I.; Levy, M.; Horton, C. L.; Fleischman, R. *Journal of Biological Chemistry* **1956**, *218*, 607-616.

(191) Deutsch, S. I.; Tang, A. H.; Burket, J. A.; Benson, A. D. *Biomedicine & pharmacotherapy = Biomedecine & pharmacotherapie* **2014**, *68*, 493-496.

(192) Di Fiore, M. M.; Santillo, A.; Chieffi Baccari, G. *Amino Acids* **2014**, *46*, 1805-1818.

(193) Hosios, A. M.; Hecht, V. C.; Danai, L. V.; Johnson, M. O.; Rathmell, J. C.; Steinhauser, M. L.; Manalis, S. R.; Vander Heiden, M. G. *Developmental Cell* **2016**, *36*, 540-549.

(194) Cheng, F.; Wang, Z.; Huang, Y.; Duan, Y.; Wang, X. *Clinica Chimica Acta* **2015**, *447*, 23-31.

(195) Bhutia, Y. D.; Babu, E.; Ramachandran, S.; Ganapathy, V. *Cancer Research* **2015**, *75*, 1782-1788.

(196) Bi, X.; Henry, C. J. *Nutrition Diabetes* **2017**, *7*, e249.

(197) DeBerardinis, R. J.; Chandel, N. S. *Science Advance* **2016**, *2*, e1600200.

(198) Du, S.; Wang, Y.; Weatherly, C. A.; Holden, K.; Armstrong, D. W. *Analytical and Bioanalytical Chemistry* **2018**, *410*, 2971-2979.

(199) Vinci, V.; Parekh, S. R. *Handbook of industrial cell culture: mammalian, microbial, and plant cells*; Humana Press: Totowa, N.J, 2003.

(200) Labuschagne, C. F.; van den Broek, N. J.; Mackay, G. M.; Vousden, K. H.; Maddocks, O. D. *Cell Rep* **2014**, *7*, 1248-1258.

(201) Maddocks, Oliver D.; Labuschagne, Christiaan F.; Adams, Peter D.; Vousden, Karen H. *Molecular Cell* **2016**, *61*, 210-221.

(202) Snell, K.; Natsumeda, Y.; Weber, G. *Biochemical Journal* **1987**, *245*, 609-612.

(203) Rabinovich, S.; Adler, L.; Yizhak, K.; Sarver, A.; Silberman, A.; Agron, S.; Stettner, N.; Sun, Q.; Brandis, A.; Helbling, D.; Korman, S.; Itzkovitz, S.; Dimmock, D.; Ulitsky, I.; Nagamani, S. C. S.; Ruppin, E.; Erez, A. *Nature* **2015**, *527*, 379-383.

(204) Geck, R. C.; Toker, A. *Adv Biol Regul* **2016**, *62*, 11-17.

(205) Wolosker, H.; D'Aniello, A.; Snyder, S. H. *Neuroscience* **2000**, *100*, 183-189.

(206) De Miranda, J.; Santoro, A.; Engelender, S.; Wolosker, H. *Gene* **2000**, *256*, 183-188.

(207) North, W. G.; Gao, G.; Memoli, V.; Pang, R. H. L.; Lynch, L. *Breast cancer research and treatment* **2010**, *122*, 307-314.

(208) Hatanaka, T.; Huang, W.; Nakanishi, T.; Bridges, C. C.; Smith, S. B.; Prasad, P. D.; Ganapathy, M. E.; Ganapathy, V. *Biochemical and Biophysical Research Communications* **2002**, *291*, 291-295.

(209) Foster, A. C.; Farnsworth, J.; Lind, G. E.; Li, Y. X.; Yang, J. Y.; Dang, V.; Penjwini, M.; Viswanath, V.; Staubli, U.; Kavanaugh, M. P. *PLoS ONE* **2016**, *11*, e0156551.

(210) Hyde, R.; Taylor, P. M.; Hundal, H. S. *Biochemical Journal* **2003**, *373*, 1-18.

(211) Krall, A. S.; Xu, S.; Graeber, T. G.; Braas, D.; Christofk, H. R. *Nat Commun* **2016**, *7*, 11457.

Biographical Information

Yadi Wang received her B.S. degree in Pharmaceutical Science in 2012 from Tianjin University in China. Her undergraduate research area focused on isolation and identification of bioactive compounds from Traditional Chinese Medicine. She obtained her Ph.D in Analytical Chemistry at The University of Texas at Arlington under the supervision of Prof. Daniel W. Armstrong. Her research focuses on different chromatography and mass spectrometry methodologies for rapid, sensitive and robust analysis of pharmaceutical and biological important compounds by using HPLC and LC-MS.